

**GRADIENT AGEING OF Ni-RICH NiTi SHAPE MEMORY
ALLOY**

by

MUHAMMAD FAUZINIZAM BIN RAZALI

**Thesis submitted in fulfillment of the
requirements for the degree of
Master of Science**

September 2013

ACKNOWLEDGEMENT

First and foremost, I would like to express my greatest thanks to Dr. Abdus Samad for serving as a successful supervisor of this research project and for providing me with the insights and guidance. His understanding, valuable suggestion, wide knowledge and writing guidance have provided a good basis for the present thesis.

I would like to thank Universiti Sains Malaysia for all the scholarship and research grant I have received. Sincere thanks to all technical staff of School of Mechanical Engineering for their invaluable technical assistance. I would like to also thank all NFM members for sharing jokes, knowledge, advices and guidelines throughout the whole project.

Last but not least, I would like to express deepest gratitude to my beloved parents and wife, for their continuous love, support and encouragement. For those who have directly and indirectly contributed to the accomplishment of this project, thank you so much.

Muhammad Fauzinizam bin Razali

September 2013

TABLE OF CONTENTS

ACKNOWLEDGEMENT	ii
TABLE OF CONTENTS.....	iii
LIST OF TABLES	vii
LIST OF FIGURES	viii
LIST OF ABBREVIATIONS	xi
LIST OF SYMBOLS	xii
ABSTRAK	xiii
ABSTRACT	xv
CHAPTER 1 SHAPE MEMORY ALLOYS	1
1.1 Shape memory unique behaviour	1
1.1.1 Thermodynamics of the phase transformation	5
1.1.2 Deformation behaviour of shape memory alloy.....	7
1.2 NiTi shape memory alloys	10
1.2.1 Phase diagram	10
1.2.2 Crystal structures of the austenite and the martensite phases	11
1.2.3 Thermal transformation temperature.....	12
1.3 Isothermal deformation behaviour	14
1.4 Application of shape memory alloys.....	15
1.5 Problem Statement	18
1.6 Objectives.....	19
1.7 Scope of work	20

CHAPTER 2 SHAPE MEMORY BEHAVIOUR ALTERATION BY AGEING	
TREATMENT	21
2.1 Factors influence shape memory behaviour.....	21
2.1.1 Effect of operating temperature	21
2.1.2 Effect of strain rate.....	22
2.1.3 Cyclic deformation.....	22
2.1.4 Thermomechanical treatment.....	23
2.2 Precipitation process of NiTi alloys.....	24
2.2.1 Ageing temperature and duration.....	26
2.2.2 Effect of ageing on thermal transformation	27
2.2.3 Effect of ageing on mechanical behaviour.....	29
2.3 Multiple-stage transformations	31
2.4 Complex effect of precipitation	32
2.4.1 Precipitate distribution	32
2.4.2 Precipitate coherency	33
2.5 Shape memory behaviour modification	35
CHAPTER 3 EXPERIMENTAL DESIGN	37
3.1 Procedures overview	37
3.2 Isothermal ageing treatment.....	38
3.2.1 Thermal martensitic transformation analysis	39
3.2.2 Deformation behaviour analysis	39
3.3 Gradient temperature ageing	41
3.3.1 Furnace fabrication.....	41
3.3.2 Furnace parts	44
3.3.3 Gradient ageing	47

3.3.4 Thermal and deformation analysis	48
CHAPTER 4 RESULT AND DISCUSSION	50
4.1 Effect of ageing on thermal transformation behaviour	50
4.1.1 Complex multiple peak transformation.....	50
4.1.2 Effect of ageing duration towards transformation temperature	52
4.1.3 Effect of ageing temperature towards transformation temperature.....	55
4.2 Effect of ageing temperature on deformation behaviour	61
4.2.1 Isothermal ageing for 10 minutes.....	61
4.2.2 Isothermal ageing for 20 minutes.....	64
4.2.3 Isothermal ageing for 30 minutes.....	66
4.2.4 Isothermal ageing for 60 minutes.....	69
4.3 Effect of ageing duration on deformation behaviour	71
4.4 Gradient ageing treatment	72
4.4.1 Gradient deformation behaviour	72
4.4.2 Gradient transformation behaviour	76
CHAPTER 5 CONCLUSION AND FUTURE WORKS.....	80
5.1 Isothermal ageing treatment.....	80
5.1.1 Effect of ageing on thermal behaviour.....	80
5.1.2 Effect of ageing on deformation behaviour	80
5.2 Gradient ageing treatment	81
5.3 Future development.....	81

LIST OF TABLES

Table 1.1. Temperature-actuated switch	17
Table 2.1. Precipitate size with respect to alloy composition and heat treatment condition.....	34
Table 3.1. Properties defined for pseudoelastic deformation behaviour.....	41
Table 3.2. Gauge length of gradient ageing specimen at different duration	49
Table 4.1. Forward and reverse stress interval of isothermal ageing specimen.....	71
Table 4.2. Forward and reverse stress interval of gradient ageing specimen	75

LIST OF FIGURES

Figure 1.1. Typical DSC curve of shape memory alloy.....	3
Figure 1.2. Schematic diagram of crystalline structure of shape memory alloy during martensitic phase transformation (a to b) and slip deformation (c)	4
Figure 1.3. Schematic diagram of crystalline structure of shape memory alloys under thermal and mechanical influence.....	5
Figure 1.4. Schematic of alloy system with martensitic transformation induced by an external force.....	6
Figure 1.5. Stress-strain-temperature curve of shape memory effect of shape memory alloys	8
Figure 1.6. Stress-strain curve of pseudoelastic behaviour of shape memory alloys ..	9
Figure 1.7. Phase diagram of NiTi alloys	11
Figure 1.8. (a) Austenite and (b) martensite lattice structure.....	12
Figure 1.9. Schematic of transformation behaviour of NiTi shape memory alloys ...	13
Figure 1.10. Change of M_s temperature as a function of nickel fraction of NiTi alloy.....	14
Figure 1.11. Stress-strain curve of NiTi alloy at different operating temperature.....	15
Figure 1.12. Change of (a) pseudoelastic curve and (b) critical stress of martensitic transformation at different operating temperature	21
Figure 1.13. Tensile stress-strain curves of pseudoelastic cycling of Ti-50.8at%Ni	22
Figure 1.14. Load versus deflection curve of arch wire made by pseudoelastic NiTi alloy and stainless steel	18
Figure 2.1. Phase digram of Ni-rich NiTi alloy	24
Figure 2.2. Time-temperature-transformation diagram of Ti-52at%Ni alloy	26

Figure 2.3. Effect of ageing temperature and duration on A_f temperature of Ti-50.7at%Ni alloy	28
Figure 2.4. Variation of R_s and M_s temperature of Ti-51.0at%Ni and Ti-52.6at%Ni against ageing duration	29
Figure 2.5. Effect of ageing treatment on forward and reverse plateau of Ti-50.7at%Ni stent wire	30
Figure 2.6. Multi-stage transformation of NiTi shape memory alloys	32
Figure 2.7. Precipitation preferences at low and high Ni supersaturation	33
Figure 2.8. TEM micrographs of the 50.7NiTi shape memory alloy after ageing at 400°C, 450°C and 500°C for 1hour and 10 hours	35
Figure 2.9. Stress-strain curve for pseudoelastic shape memory alloy(a) homogeneous microstructure and (b) gradient microstructure	19
Figure 2.10. Stress-strain curve of gradient-annealed Ti-50.5at%Ni alloy as deformed in tension at 40°C	36
Figure 3.1. Tensile test setup with the thermal chamber.....	40
Figure 3.2. Illustration of properties defined for pseudoelastic stress-strain curve ...	41
Figure 3.3. Gradient temperature furnace setup.....	42
Figure 3.4. Schematic diagram of heating element loop on the ceramic tube	42
Figure 3.5. Schematic diagram of thermocouples and NiTi wire inside the gradient temperature tube furnace	44
Figure 3.6. Circuit diagram of temperature controller	46
Figure 3.7. Real time plot of temperature recorded by eight thermocouples for 60 minutes of gradient ageing treatment	47
Figure 3.8. Temperature profile recorded by the thermocouples.....	48

Figure 3.9. Sectioning of DSC and tensile specimen from the total length of gradient aged NiTi wire.....	49
Figure 4.1. Complex multiple-peak transformation of aged Ti-50.8at%Ni alloy.....	51
Figure 4.2. Thermal transformation behaviour of Ti-50.8at%Ni alloy after ageing at 430°C for different duration.....	53
Figure 4.3. Partial cooling measurement of specimen aged at 430°C for 60 minutes	54
Figure 4.4. Schematic illustration to demonstrate the nucleation of Ti_3Ni_4 precipitate within NiTi specimen matrix: (a) after 10 minutes ageing, (b) after 60 minutes ageing	55
Figure 4.6. Thermal transformation behaviour of Ti-50.8at%Ni alloy after ageing at different temperature for 20 minutes.....	57
Figure 4.7. Thermal transformation behaviour of Ti-50.8at%Ni alloy after ageing at different temperature for 30 minutes.....	58
Figure 4.8. Thermal transformation behaviour of Ti-50.8at%Ni alloy after ageing at different temperature for 60 minutes.....	59
Figure 4.9. Effect of ageing temperature and duration on A_f temperature of Ti-50.8at%Ni alloy.....	61
Figure 4.10. Pseudoelastic behaviour of Ti-50.8at%Ni alloy after ageing at different temperature for 10 minutes	62
Figure 4.11. Effect of ageing temperature on stress-induced deformation behaviour of Ti-50.8at%Ni alloy aged for 10 minutes	63
Figure 4.12. Effect of ageing temperature on plateau and residual strain of Ti-50.8at%Ni alloy aged for 10 minutes.....	64
Figure 4.13. Effect of ageing temperature on stress-induced deformation behaviour of Ti-50.8at%Ni alloy aged for 20 minutes	65

Figure 4.14. Effect of ageing temperature on plateau and residual strain of Ti-50.8at%Ni alloy aged for 20 minutes.....	65
Figure 4.15. Pseudoelastic behaviour of Ti-50.8at%Ni alloy after ageing at different temperature for 30 minutes	66
Figure 4.16. Effect of ageing temperature on stress-induced deformation behaviour of Ti-50.8at%Ni alloy aged for 30 minutes	68
Figure 4.17. Effect of ageing temperature on plateau and residual strain of Ti-50.8at%Ni alloy aged for 30 minutes.....	68
Figure 4.18. Effect of ageing temperature on stress-induced deformation behaviour of Ti-50.8at%Ni alloy aged for 60 minutes	70
Figure 4.19. Effect of ageing temperature on plateau and residual strain of Ti-50.8at%Ni alloy aged for 60 minutes.....	70
Figure 4.20. Effect of ageing duration on pseudoelastic behaviour of Ti-50.8at%Ni alloy ageing at 430°C	72
Figure 4.21. Gradient deformation behaviour of specimen ageing within gradient temperature furnace.....	74
Figure 4.22. Thermal transformation behaviour along the length of 10 minutes gradient ageing specimen.....	77
Figure 4.23. Thermal transformation behaviour along the length of 30 minutes gradient ageing specimen.....	78
Figure 4.24. Thermal transformation behaviour along the length of 60 minutes gradient ageing specimen.....	79

LIST OF ABBREVIATIONS

DSC	Differential Scanning Calorimeter
ASTM	American Society for Testing and Materials
NiTi	Nickel Titanium

LIST OF SYMBOLS

M_s	Martensite start temperature
M_f	Martensite finish temperature
A_s	Austenite start temperature
A_f	Austenite finish temperature
A	Austenite phase
M	Martensite phase
R	R-phase

PENYEPUHLINDAPAN BERCERUN ALOI INGATAN BENTUK

NiTi

ABSTRAK

Sehingga kini, penggunaan sifat ingatan aloi NiTi adalah terhad kepada aplikasi yang memerlukan tindakan refleks sahaja dan tidak bersesuaian bagi aplikasi yang memerlukan tindakan boleh kawal. Bagi mengatasi limitasi ini, penghasilan NiTi aloi dengan sifat tingkah laku ubah bentuk bercerun melalui pengubahsuaian mikrostruktur menerusi proses rawatan haba adalah perlu. Tujuan kajian ini adalah untuk menghasilkan wayar NiTi dengan sifat tingkah laku ubah bentuk bercerun melalui proses penyepuhlindapan bercerun. Pendekatan ini adalah berdasarkan kebergantungan sifat termomekanikal NiTi aloi terhadap perubahan suhu dan tempoh proses penyepuhlindapan.

Kerja eksperimen dibahagikan kepada dua peringkat. Peringkat pertama melibatkan kajian kesan suhu dan tempoh penyepuhlindapan terhadap tingkah laku terma dan tingkah laku ubah bentuk. Berdasarkan pembentukan mendakan yang tidak sekata, tempoh penyepuhlindapan yang lama menyebabkan tingkah laku ubah bentuk bagi spesimen isoterma berlaku dalam keadaan bercerun. Hasilnya, tekanan transformasi hadapan mempamerkan kecerunan positif dengan nilai 3.4 GPa.

Peringkat kedua mengkaji tingkah laku ubah bentuk NiTi aloi setelah di penyepuhlindap dalam profil suhu yang bercerun. Spesimen yang dipenyepuhlindap selama 60 minit antara suhu 430°C hingga 460°C mempamerkan kecerunan optimum dengan kecerunan tekanan hadapan sebanyak 5.0 GPa, kecerunan tekanan membalik sebanyak 5.2 GPa dan sisa terikan sebanyak 0.5%, . Pendekatan penyepuhlindapan

bercerun didapati berdaya maju dalam menghasilkan sifat tingkah laku ubah bentuk
bercerun bagi NiTi aloi.

GRADIENT AGEING OF Ni-RICH NiTi SHAPE MEMORY

ALLOY

ABSTRACT

To date, the shape memory behaviour are limited only for discrete action application leaving no option for any progressive or intermediate state of control. The creation of gradient plateau is one of the best solutions and it is possible by many ways, and one of it is by microstructure modification via heat treatment that includes annealing and ageing. The purpose of this study is to create a functionally graded NiTi wire with an optimum pseudoelastic behaviour through a gradient ageing treatment. This approach is based on the sensitivity of the alloys' thermomechanical properties with respect to temperature and duration of ageing treatment.

The experimental works are divided into two stages. The first stage involved the study of the effect of temperature and duration of isothermal ageing on thermal and deformation behaviour of NiTi shape memory alloys. Due to the heterogeneous precipitate distribution, prolonged ageing led to the gradient deformation on the isothermal aged specimen with respect to gradual variation of Ni composition within the alloy matrix. The result shows that the stress plateau of the phase transformation exhibits positive stress gradient with a value of 3.4 GPa.

The second stage studied the deformation behaviour of specimen aged in a gradient temperature profile. It was found that the optimum gradient deformation behaviour was occurred on the specimen aged between 430°C to 460°C for 60 minutes. During deformation, the specimen exhibited forward stress gradient of 5.0 GPa, reverse stress gradient of 5.2 GPa and small residual strain of 0.5%. This novel heat treatment approach indicates that the gradient ageing treatment approach is viable in creating a functionally gradient behaviour of Ni-rich NiTi alloys.

CHAPTER 1

SHAPE MEMORY ALLOYS

1.1 Shape memory unique behaviour

Shape memory alloy is named after an alloy which has an ability to remember its original shape after huge inelastic deformation strain. This shape recovery can be achieved instantaneously upon the release of the load or heated to above its specific temperature. This type of alloys promotes magnificent deformation recovery, where it is capable to regain original length of ten times longer elongation than any conventional alloys [1]. This huge strain recovery is achieved from the alloy's ability to undergo reversible martensitic phase transformation upon the application of external stress or heat. In some shape memory alloys, the transformation can also be stimulated by magnetic [2, 3] and electrical [4, 5]. Nevertheless, thermomechanical types of shape memory alloys are more widely utilized in many engineering applications for their superior martensitic transformation strain and shape recovery [6-8].

There are few numbers of alloy systems that exhibit shape memory ability, with few of the famous alloys are Cu-Al-Ni, Cu-Zn-Al, Fe-Mn-Si, Ni-Ti, Ni-Ti-Cu, Fe-Pt, Fe-Pd and Fe-Ni-Co-Ti [9-12]. Even though various of alloys promotes shape memory ability, only those demonstrate great strain recovery and generate huge force upon changing shape are of commercial interest. To date, shape memory alloys have been used in variety of applications such as pipe coupling, earthquake dampeners, orthodontic wire, heat engine, micro-actuator and variety of medical implants [13-17].

The first discovery of thermo-responsive shape memory behaviour was reported in 1932 by Swedish physicist, Arne Ölander in his study of “rubber like effect” in gold–cadmium alloy [18, 19]. Since then, insignificant finding has been reported about this alloy. It is only in 1951 that Chang and Read reported the reversibility of solid phase transformation through electrical resistivity on the same gold-cadmium alloy system [20]. Based on this observation, the term “shape memory alloy” was first used to characterise the unique recovery behaviour of that gold-cadmium bar.

Martensite phase transformation in shape memory alloys involves reversible phase change in between high-temperature phase called austenite and low temperature phase called martensite [21, 22]. The characteristic temperatures of thermal martensitic phase transformation are defined into four critical temperatures. Usually, these critical temperatures of shape memory alloys are determined by Differential Scanning Calorimeter (DSC) instrument. This instrument classifies the critical temperatures by measuring the heat absorbed and released upon the martensitic transformation. Typical shape of DSC curve for shape memory alloy is shown as in Figure 1.1.

Martensite starts temperature (M_s) is at which the alloy starts transforming from austenite to martensite. Martensite finishes temperature (M_f) is temperature at which the alloy is fully in martensitic phase. Austenite starts temperature (A_s) is temperature at which the martensite starts to transform into austenite. Austenite finishes temperature (A_f) is temperature at which the alloy is fully in austenitic phase.

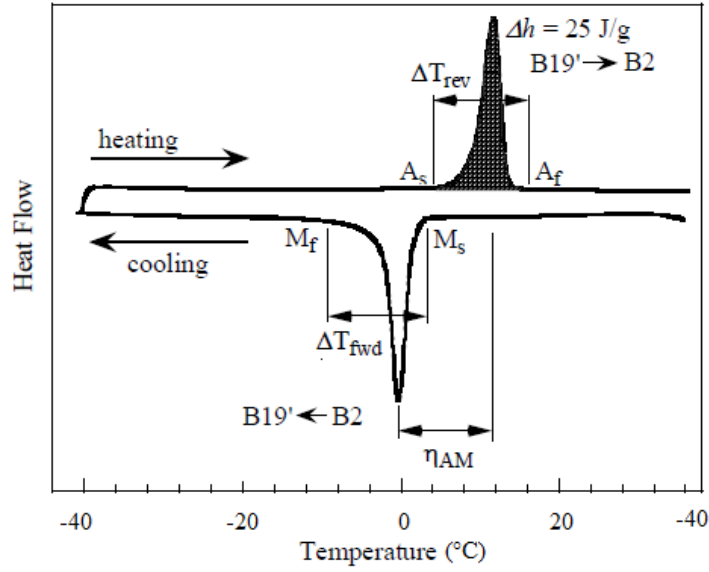


Figure 1.1. Typical DSC curve of shape memory alloy [23]

The transformation of austenite into martensite is an exothermic transformation, whereas the transformation of martensite into austenite is endothermic. The thermal phase transition between austenite and martensite proceeds proportionally to the change of temperature. The phase transformation between austenite and martensite happens over a temperature range, namely hysteresis η_{AM} . As shown in Figure 1.1, shape memory alloys have a small temperature interval, ΔT of 10°C both on forward and reverse transformation, with a latent heat, Δh of $\sim 25\text{J/g}$. Note that the bulk of the phase transition occurring within a narrower range of $\sim 5^{\circ}\text{C}$ [24-26].

The martensite phase transformation in shape memory alloys is a diffusionless transformation attributed by shear-like mechanism [27, 28] as shown schematically in Figure 1.2 (a) and (b). The macro strain obtains during the martensitic transformation is corresponded to the change in the lattice structure of the alloy. Full recovery is allowable as the distorted unit cell return to its original position. Meanwhile, Figure 1.2 (c) shows the lattice structure of the conventional alloy which undergoes slip deformation, thus it is not reversible.

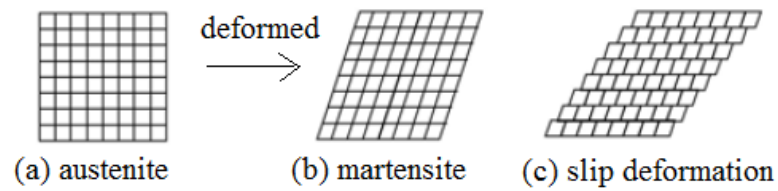


Figure 1.2. Schematic diagram of crystalline structure of shape memory alloy during martensitic phase transformation (a to b) and slip deformation (c) [29]

Figure 1.3 shows the effect of thermal and mechanical input against the change on the crystalline structure of shape memory alloys. The alloy forms into simple cubic B2 austenite structure at high temperature (a) and monoclinic B19' martensite at a low temperature (b). Cooling the austenite phase to below M_f temperature causes the alloy to self-accommodate into twinned lattice structure. The pink and blue monoclinic structure represents the possible martensite variant formed during the twinning process. No macroscopic shape change is produced during the self-accommodation mechanism as the crystal structure accommodates each other within the confined grain boundaries.

The movement of the twin structure in the presence of external load is shown from (b) to (c). The twin structure move and deforms easily to a new single variant in the direction of the applied stress. This emerging phenomenon of many variants into one single variant is called detwinning. The detwinning mechanism causes the most favourably oriented variant with the longest strain yield in the direction of the applied stress. In this case, the pink colour variant grows and dominates the blue colour variant. A macroscopic strain is observable at this moment. The strained alloy will recover to the original shape once subjected to heat particularly above the A_f temperature. This mechanism of shape recovery through heating explains the shape memory effect.

Figure (a) and (c) shows the transformation of austenite to martensite by stress loading at above A_f temperature. This mechanism is called as stress-induced martensitic transformation. The martensite formed above A_f temperature is very unstable in the absence of stress. Upon unloading, the reverse transformation instantly takes place, recovering the martensite structure into austenite structure. This mechanism of shape recovery by unloading explains the pseudoelastic behaviour.

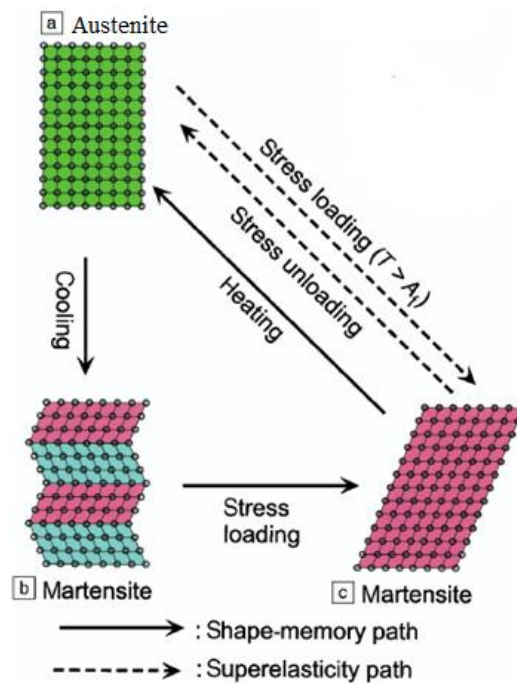


Figure 1.3. Schematic diagram of crystalline structure of shape memory alloys under thermal and mechanical influence [28]

1.1.1 Thermodynamics of the phase transformation

The martensitic transformation is highly dependent on operating temperature and applied stress as both parameters act as a driving force for phase transformation. Wollants *et al.* explained the relation of those parameters on an equilibrium system as illustrated in Figure 1.4.

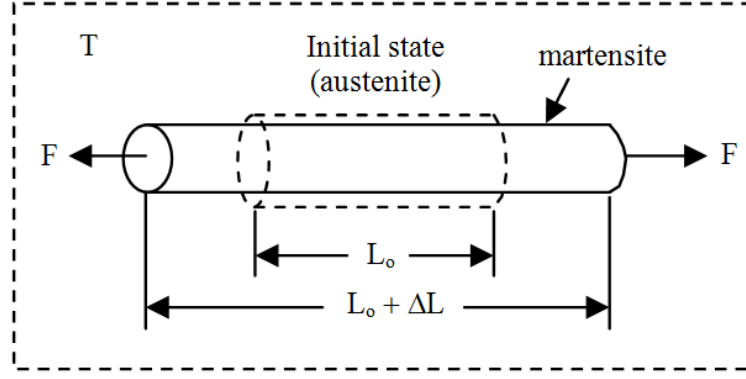


Figure 1.4. Schematic of alloy system with martensitic transformation induced by an external force [30]

Assume shape memory wire is subjected to uniaxial load, F , which resulted in an expansion of ΔL during the martensitic transformation. Under this condition, the free-energy balance, ΔG of the wire can be expressed as;

$$\Delta G = \Delta H - T\Delta S - F\Delta L = \Delta H - T\Delta S - \frac{1}{\rho}\sigma\epsilon_t \quad (1.1)$$

where ΔH is enthalpy energy, ΔT is entropy energy getting from the lattice change during the transformation, $F\Delta L$ is mechanical work done to the alloy, ρ is the density of alloy, σ is applied stress and ϵ is strain produced by the transformation. Differentiating Equation 1.1 under an equilibrium condition at $\Delta G=0$, $T=T_o$, $\sigma = \sigma_o$, yields;

$$\frac{d\sigma_o}{dT_o} = \frac{-\rho\Delta S}{\epsilon_t} = \frac{-\rho\Delta H}{\epsilon_t T_o} \quad (1.2)$$

This relation is called as Clausius–Clapeyron relationship, which is widely used for analysis phenomena involving thermoelastic martensitic transformation. Recently, the relation between critical stress for stress-induced martensitic (SIM) transformation and change in operating temperature has been simplified as in Equation 1.3 [31].

$$\sigma_{SIM} = k (T_{operating} - T_{Ms}) \quad (1.3)$$

where k denotes the linear constant defined by the Clausius–Clapeyron equation for the martensitic transformation.

1.1.2 Deformation behaviour of shape memory alloy

The unique deformation behaviours of shape memory alloys are characterised into three types, namely shape memory effect, two-way shape memory and pseudoelastic. Shape memory effect is the ability of shape memory alloy to gain shape recovery by heating above A_f temperature, after being deformed while in twinned martensitic phase.

Figure 1.5 shows the thermomechanical loading path of shape memory effect on the stress-strain-temperature space. Suppose that the shape memory alloy is in the form of fully twinned martensite at below M_f temperature (b). Once subjected to an external load, the detwinning of martensite is accommodated through a great inelastic strain at a constant stress plateau. When the load is removed at (d), the small elastic portion of detwinned martensite is recovered, leaving a substantial value of residual strain at (e). As the alloy remembers its high-temperature structure, heating up the alloy above A_f temperature at (a) caused the residual strain progressively

reduced. This shape memory effect is one-time application, where the alloy needs to be deformed again to gain next cycle of shape recovery.

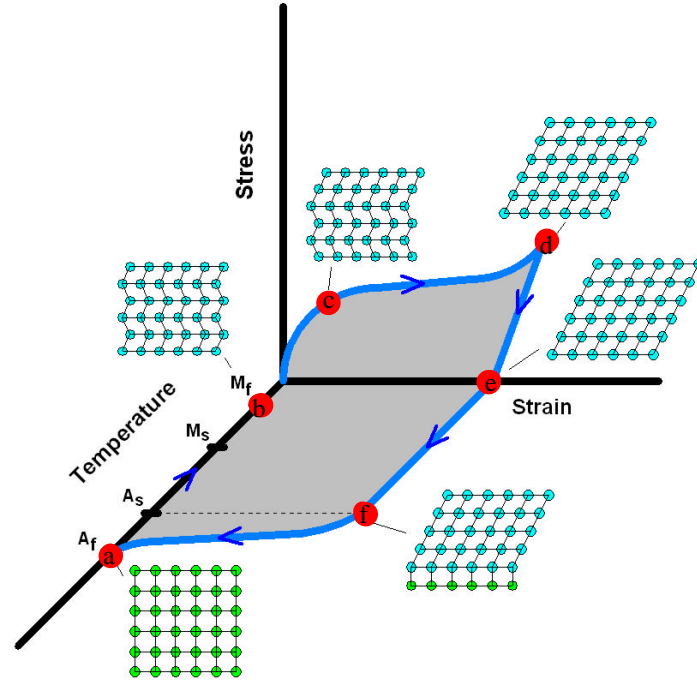


Figure 1.5. Stress-strain-temperature curve of shape memory effect of shape memory alloys [32]

Another unique shape memory behaviour is two-way shape memory effect. Alloys of this behaviour have the ability to exhibit shape change only by cooling or heating and without any help from external stress stimulation. However, this unique behaviour is not a natural behaviour of shape memory alloy since the material needs to be ‘trained’ under special thermomechanical treatment for it to develop the two way shape memory effect [33-35].

The next unique shape memory behaviour is known as pseudoelasticity. Pseudoelasticity is characterised by instant recovery of deformed shape memory alloys upon the removal of applied force. This behaviour is observable only if the shape memory alloy being deformed in between A_f and M_d temperature. M_d

temperature denotes the maximum temperature to observe pseudoelasticity before the alloy naturally deformed in plastic.

Figure 1.6 displays the typical pseudoelastic stress-strain curve obtained during the tensile test of shape memory alloys. The austenite structure yield elastically from (a) to (b) once deformed above A_f . Further loading to (c) involves the formation of stress-induced martensitic transformation at a constant stress plateau. The constant stress plateau corresponds to small transformation temperature intervals of martensitic transformation. Note that the reverse transformation of martensite to austenite also occurs at a constant stress plateau from (e) to (a).

In addition, the constant stress plateau on the stress-strain curve indicates the motion of shear band interfaces of NiTi structures via a localized Lüders-like deformation [36-38]. This Lüders-like deformation mainly observed in tension loading cases, which involved stress-induced martensitic transformation [36].

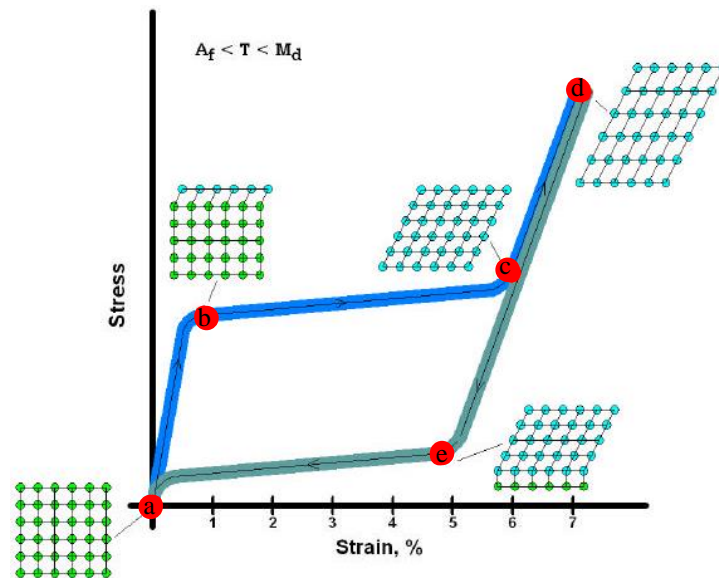


Figure 1.6. Stress-strain curve of pseudoelastic behaviour of shape memory alloys [32]

1.2 NiTi shape memory alloys

Even though there are a number of shape memory alloys available for variety of application, it is only NiTi that captures the most attention. This is due to its promising shape memory behaviour and in addition to corrosion resistance, nonmagnetic nature, low density and high fatigue strength [39]. Additionally, this alloy system promotes valid biocompatibility with human body and exhibit excellent magnetic resonance imaging opacity, which makes its viewable under X-Ray. With regards to these properties, NiTi alloy has been used widely for biomaterial product such as orthodontic arch wires, guide wires, orthopaedic implants and stents [16, 40, 41].

1.2.1 Phase diagram

Commonly, NiTi shape memory alloy always subjected to heat treatment to alter the thermal and deformation behaviour to be in line with the wanted application. For this purpose, the phase diagram has been used extensively in understanding the microstructure properties of NiTi alloy at desired heat treatment temperature. Figure 1.7 shows the most reliable phase diagram of NiTi alloy as proposed by Massalski *et al.*

The region of interest of the phase diagram relies on the near-equiatomic region bounded by Ti_2Ni and TiNi_3 , as this region promotes shape memory behaviour. Note that the boundary of TiNi phase lessens with decreasing temperature on the Ni-rich side and almost unchanged on the vertical Ti-rich side. The wide boundary of TiNi phase on Ni-rich side provided large space to tailor the shape memory effect and pseudoelasticity by thermomechanical treatment.

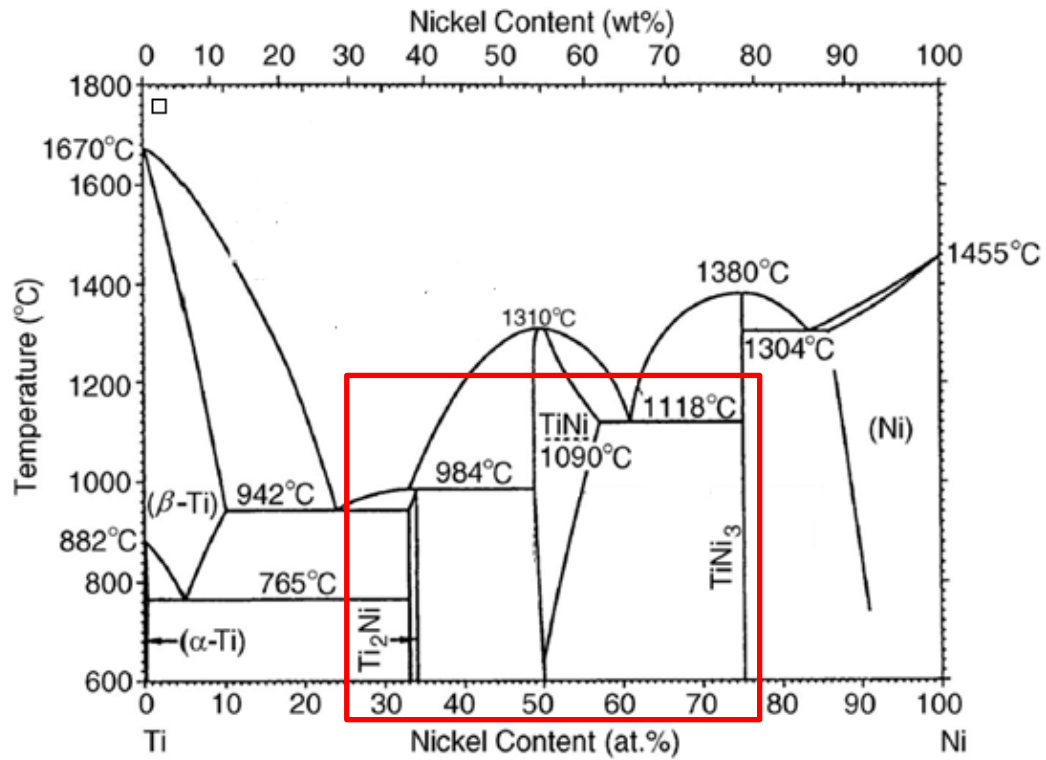


Figure 1.7. Phase diagram of NiTi alloys [42]

1.2.2 Crystal structures of the austenite and the martensite phases

In NiTi shape memory alloy, austenite exists in a form of cubic (B2) crystal structure with a lattice constant of 0.3015 nanometer at room temperature. Austenite has titanium atom located at all corners of the cube structure leaving a single nickel atom at the center (Figure 1.8a). This phase is dominant at high temperature and has a stable crystal structure due to its crystal symmetric. In comparison, martensite exists in the form of monoclinic (B19') crystal structure with different atoms located at each corner of the structure (Figure 1.8b). This monoclinic structure is accommodated at low temperature and less stable due to the low symmetric structure.

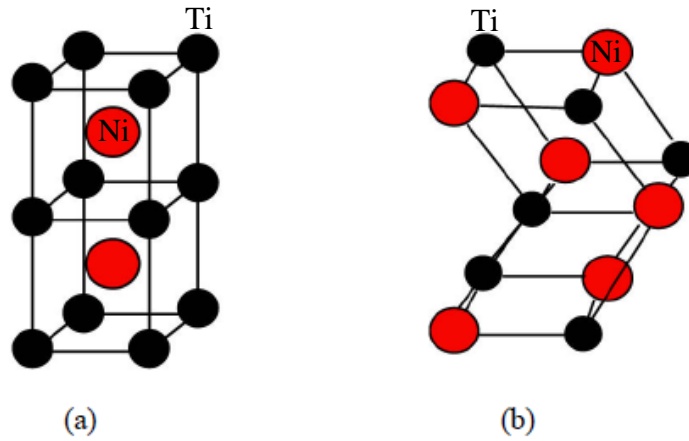


Figure 1.8. (a) Austenite and (b) martensite lattice structure [29]

1.2.3 Thermal transformation temperature

In general, NiTi shape memory alloys in a solution state always demonstrate a single-stage $A \leftrightarrow M$ transformation (Figure 1.9a), with $A \rightarrow M$ and $M \rightarrow A$ known as forward and reverse transformation, respectively. Since this type of alloys is frequently subjected to thermal cycling [43], annealing after cold work [44] and aging for Ni-rich alloys [45], it has been reported that the phase transformation may proceed in two-stage of $A \leftrightarrow R \leftrightarrow M$ transformation (Figure 1.9b).

The rhombohedral phase (R phase) transition occurred as the M_s being depressed below R-phase transformation temperature as a result of created internal stress fields associated with either dislocations or precipitates formation [46-50]. R-phase transition is considered as another martensitic phase transformation as it also exhibits shape memory behaviour [51]. The $A \leftrightarrow R$ transformation exhibits a very small transformation strain of 1% with hysteresis of 2–5°C. In contrast, $A \leftrightarrow M$ and $R \leftrightarrow M$ transformations are characterised by larger transformation strain of 10% and hysteresis of 20–70°C [52].

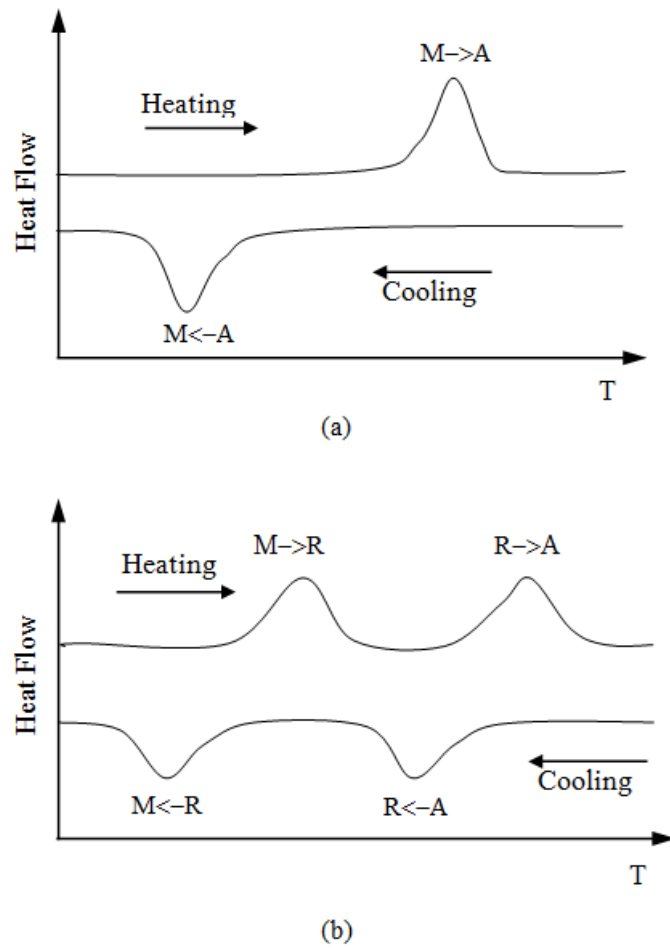


Figure 1.9. Schematic of transformation behaviour of NiTi shape memory alloys [49]

Additionally, the transformation temperature of the particular NiTi alloy system is very sensitive to the mole fraction of Ni. Figure 1.10 shows how the M_s temperature rapidly descended as the Nickel fraction increases along the Ni-rich side. In fact, an increase of one percent of Ni content from 0.50at% to 0.51at% causes a gap of 200°C on the M_s temperature of NiTi alloy.

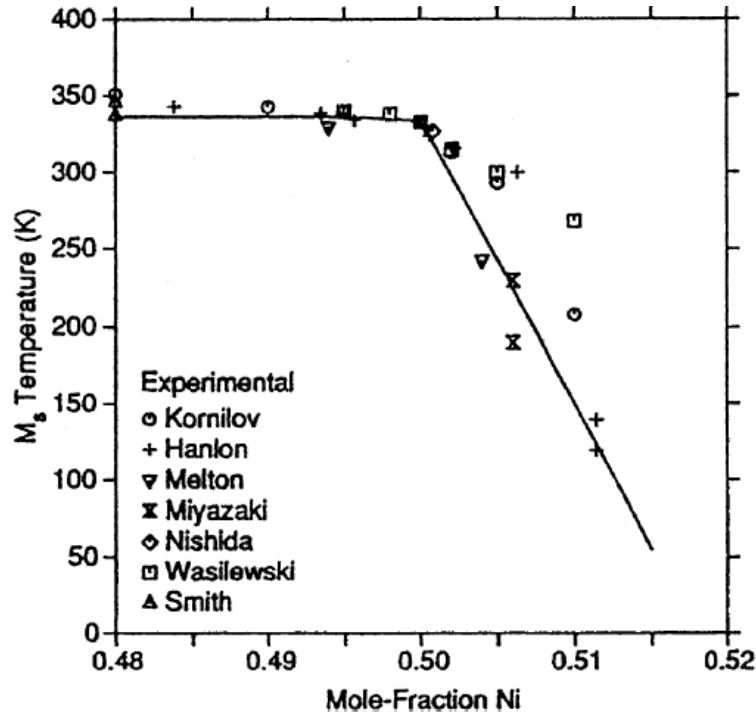


Figure 1.10. Change of M_s temperature as a function of nickel fraction of NiTi alloys [53]

1.3 Isothermal deformation behaviour

The isothermal deformation behaviour of near-equiatomic NiTi alloys varies against operating temperature. Figure 1.11 shows four types of deformation behaviour with respect to the operating temperature. Curve (a) is obtained by deforming NiTi alloy at temperature above M_d temperature. Upon deformation, the stress proceeds to a higher stress level, exceeding the critical stress for slip. Curve (b) illustrates the deformation behaviour that takes place when NiTi alloy is deformed at temperature in between A_f and M_d . As explained before, this behaviour is well known as pseudoelasticity. The alloy recovers the generated strain upon unloading at the end of the stress plateau. If the deformation proceeds over the stress plateau, the martensite hardens and results to alloy fracture. Curve (c) shows the deformation behaviour of NiTi alloy pulled at temperature in between M_s and R_f . As claimed in [24, 54], the R-phase transformation introduced a shoulder form at the initial stage of deformation.

Curve (d) is the stress-strain response obtained when NiTi alloy is pulled below M_f temperature. As discussed before, this behaviour represents the shape memory effect. The alloy recovers the generated strain upon heating above the A_f temperature.

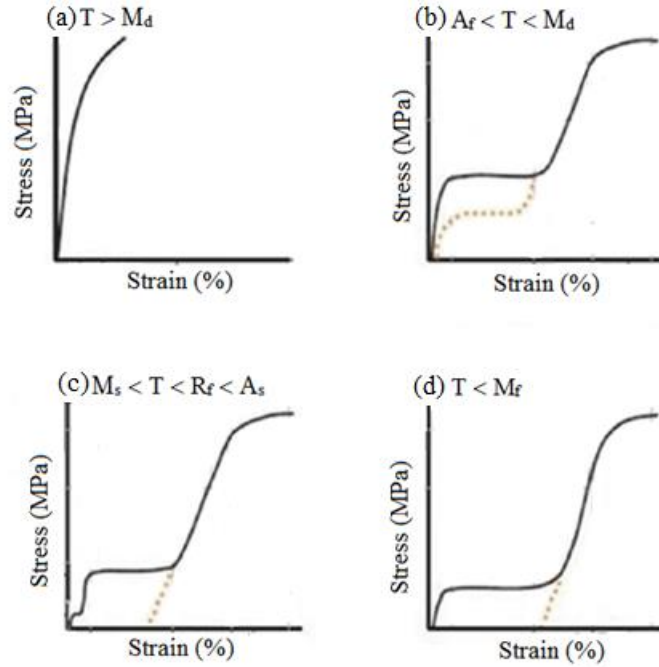


Figure 1.11. Stress-strain curve of NiTi alloy at different operating temperature [55]

1.4 Application of shape memory alloys


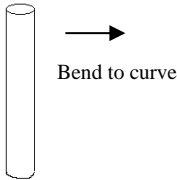
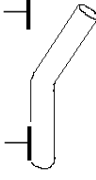
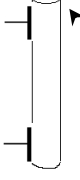

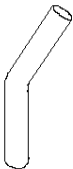
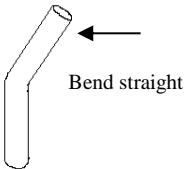

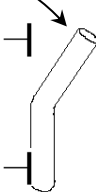
The superior behaviours of shape memory alloy over ordinary metals has lifted this alloy for many applications. To specify, application of shape memory alloy is divided into four categories. The first category is free recovery application. The shape memory alloy is being deformed in martensitic phase, and let to recover to the original shape when subjected to heat. The most successful application so far is a blood-clot filter [56]. The blood-clot filter is made from NiTi wire and placed in outer hearth chambers to trap a blood clot in a vein. Upon the deployment, the blood clot filter is introduced inside the vein in a deformed cylindrical shape. Once exposed

to the body temperature, the deformed filter returns to its original shape and anchors properly to catch passing clots.

The second category is constrained recovery. The shape memory alloy is prevented from recovering to its original shape, thus generating stress on the constraining object. The most commercial application is hydraulic–tube couplings made for F-14 jet fighter [22]. NiTi coupler is machined to have a smaller inner diameter than the outer diameter of the tubes to be joined. Upon installation, the coupler is cooled to below its M_f temperature before deforming to the diameter of the tube. Once warmed to A_f temperature, the coupler was constrained from recovering and so applying larger stress on the tube. To add, the joint strength is more powerful than weld and provides a chance of removing it back for maintenance.

Next category is force actuator application. The shape memory alloy is designed to apply force over a range of motions. One such example is a fire-safety switch, where Cu-Zn-Al actuator is designed to shut off flammable gas or toxic when fire occurs [57] as shown in Table 1.1.

Table 1.1. Temperature-actuated switch [57]

Initial shape	Additional cold or hot shaping	Shape after quenching	Position at room temperature	Remembered position (above A_f)
	No martensite	Now contains martensite	Martensite under stress	No martensite
	None			
				

The last category is pseudoelastic recovery application. The shape memory alloy is designed to store potential energy through large and recoverable deformation. This category has been widely used in various fields, especially in medical industry with respect to high compatibility properties.

The magnificent used of pseudoelasticity of shape memory alloys is reported in orthodontic application [58]. Figure 1.12 shows the mechanical characteristic of pseudoelastic NiTi alloy in comparison to conventional elastic material. Excessive force zone denotes the force, which causes tissue damage, and optimal force zone denotes the effective force for bone remodeling. The effective strain range (ϵ_{eff}) denotes the activation range available while moving the teeth. As illustrated, NiTi alloy demonstrated large effective strain range over the optimal force zone as compared to stainless steel. Thus, NiTi alloy provides a greater range of activation and less adjustment of arch wire is needed to move the teeth to the final position.

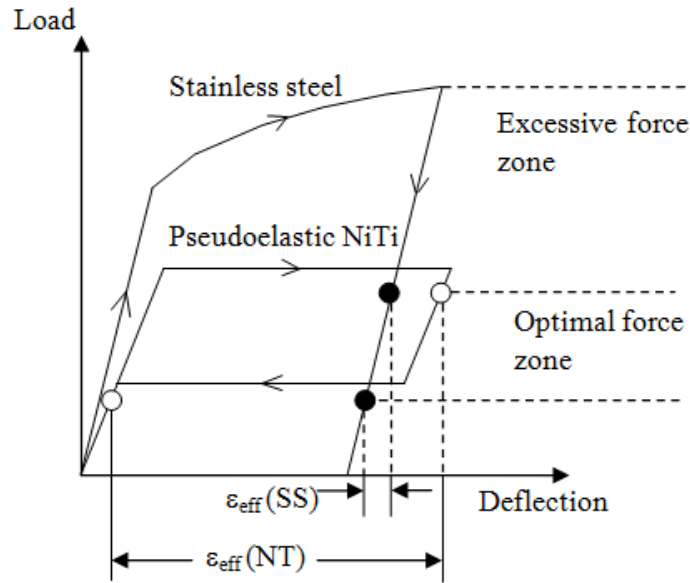


Figure 1.12. Load versus deflection curve of arch wire made by pseudoelastic NiTi alloy and stainless steel [58]

1.5 Problem Statement

Today, successful practical applications of shape memory alloy are restricted only on sudden response mechanism. Due to small transformation temperature window and zero transformation stress intervals, the shape memory application undergoes an abrupt shape change once the thermal or the stress stimulus reached somewhat a threshold value [26, 59].

For better understanding, refer to pseudoelastic stress-strain curve in

Figure 1.13 (a). The pseudoelastic shape memory wire experienced a surprising increase of 5.5% strain once the input stress reached a threshold value of 500 MPa. The same phenomena happen upon unloading, where there is an abrupt retraction of the wire once the input stress lower down to 200 MPa.

The sudden responds during deformation and recovery limits the applicability of shape memory application, especially for a case which requires intermediate or continuous control of the output. Industries found difficulties in controlling the motion of the shape memory apparatus as it requires a precise control in external

input signals, either temperature or stress. Since shape memory behaviour is dependent on thermomechanical treatment, it would be a great advantage if gradient microstructure properties can be programmed along the shape memory alloy in order to create the desired gradient response against the input stimulation.

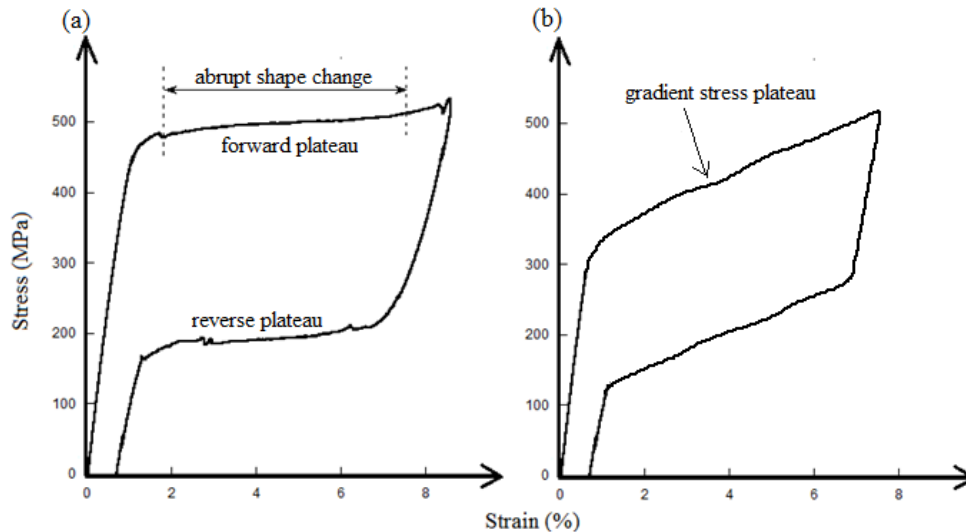


Figure 1.13. Stress-strain curve for pseudoelastic shape memory alloy (a) homogeneous microstructure and (b) gradient microstructure

1.6 Objectives

In order to solve the current controllability issues, the creation of the gradient functionally behaviour of NiTi alloy with a nearly full recovery property is a must.

Two objectives have been proposed in this research project as listed below;

1. To quantify the effects of isothermal ageing treatments on thermal and deformation behaviour of Ti-50.8at%Ni alloy.
2. To create a functionally graded Ti-50.8at%Ni alloy through gradient ageing treatment, and based on the isothermal knowledge, to optimize the gradient deformation behaviour.

1.7 Scope of work

This research deals with material characteristic improvement through heat treatment. The material used is NiTi alloy with a composition of 50.8at%Ni. This alloy composition has been used widely for biomaterial product, since the shape memory application suits with the human body temperature [55].

For the isothermal ageing work, the selection of ageing temperature and duration are restricted from 310°C to 550°C for 60 minutes, where the effect of precipitates can be utilized in altering both major parameters [60].

For the gradient ageing work, the optimization of the gradient deformation behaviour of the gradient aged alloy is carried out by selecting the optimum temperature range available within the effective duration of ageing. The temperature range must promote large and continuous change of forward and reverse transformation stress comply with a good strain recovery.

CHAPTER 2

SHAPE MEMORY BEHAVIOUR ALTERATION BY AGEING TREATMENT

2.1 Factors influence shape memory behaviour

Shape memory behaviour of NiTi shape memory alloy is very sensitive against the processing condition such as operating temperature, strain rate, cyclic deformation and thermomechanical treatment history.

2.1.1 Effect of operating temperature

The critical stress for stress-induced martensitic transformation is temperature dependent. Figure 2.1 shows that the critical stress needed to stress-induced martensitic transformation increases proportionally as the environmental temperature increases. Both forward and reverse critical stresses for the transformation indicate a linear correlation with operating temperature.

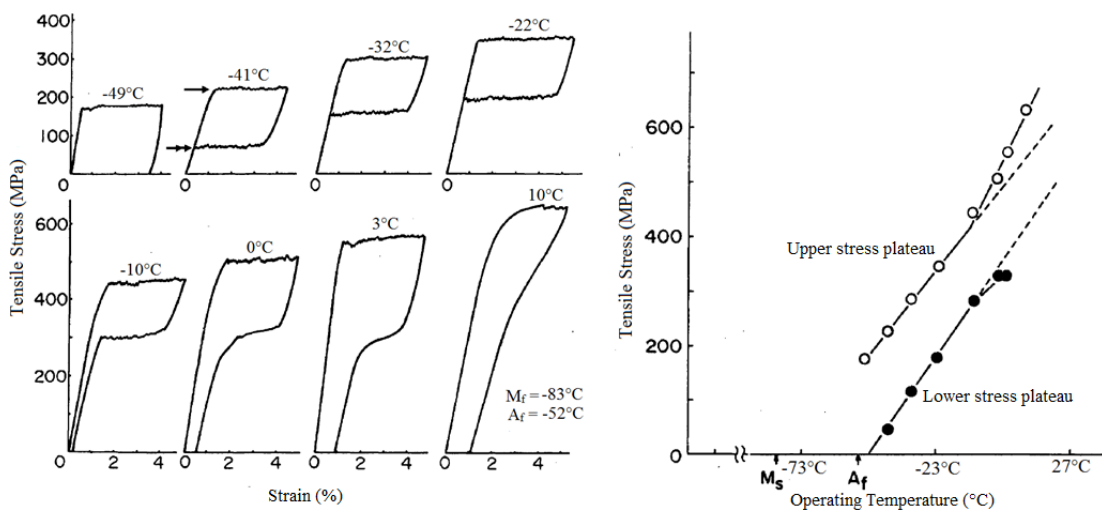


Figure 2.1. Change of (a) pseudoelastic curve and (b) critical stress of martensitic transformation at different operating temperature [36]

2.1.2 Effect of strain rate

The shape memory behaviour is also affected by deformation strain rate. It is found that high strain rate leads to be self-heating the NiTi alloy during the stress-induced transformation. Consequently, this phenomenon raises the temperature of the vicinity region of the untransformed part, thus increases the required critical stress needed to form martensite [61]. Normally, NiTi alloys are deformed at a slower strain rate of 0.0167s^{-1} to eliminate such self-heating effect [54].

2.1.3 Cyclic deformation

NiTi shape memory alloy also exhibits different shape memory behaviour after being deformed for few numbers of cycles. It is reported that the stress hysteresis between forward and reverse plateau is found to be decreased prior to cyclic deformation. As shown in Figure 2.2 the forward stress plateau gradually reduced from the first cycle before it's stabilized at a lower level upon 125th cycles. The stress field generated from cyclic deformation assists the applied stress leading to the decrease in the critical stress needed for inducing martensite [62-64].

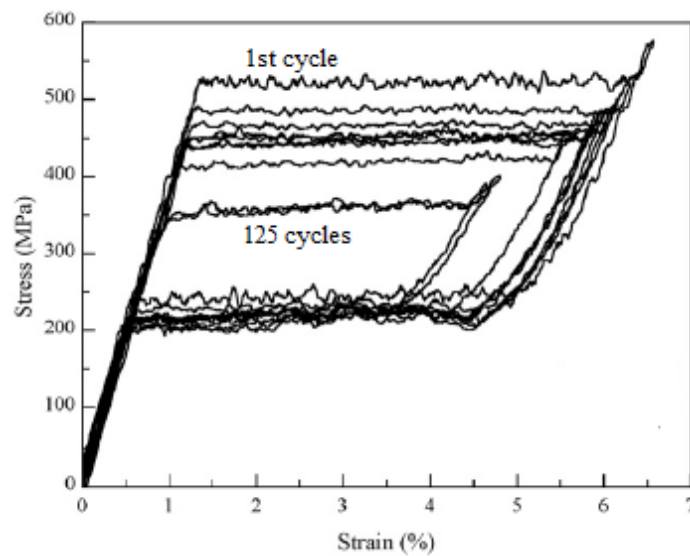


Figure 2.2. Tensile stress-strain curves of pseudoelastic cycling of Ti-50.8at%Ni [65]

2.1.4 Thermomechanical treatment

In the earlier time, the pseudoelastic application of NiTi shape memory alloy always ended up with failure due to its low critical stress for slip [66]. Work hardening and age hardening have been used extensively to delay the critical stress for slip to a higher stress level. Both hardening processes improve pseudoelastic behaviour by increasing the yield strength of martensite, which enables stress-induced martensitic transformation to take place at higher temperatures.

Work hardening commonly used on near-equiatomic NiTi alloy. Near equiatomic NiTi alloy is named after NiTi alloy with Ni content of 49.5at%–50.5at%. The hardening process starts with applying an amount of cold work on the alloy followed by annealing within 300°C–600°C [53]. This process introduced high density of dislocation, which increases the resistance to slip deformation. To date, researchers have manipulated the percentage of cold work and the temperature of annealing in altering the shape memory behaviour of near-equiatomic NiTi alloy.

In contrast, age-hardening is widely used for Ni-rich NiTi alloy, which has Ni content more than 50.5at% [67]. The age hardening process is started by solution treating the alloy followed by ageing at temperature range of 300°C–550°C [45, 68]. Ageing treatment introduces secondary phase particles known as Ni-rich precipitate, which acts as a strong barrier for dislocation motion. The characteristic of the precipitate varies with ageing condition. It is very important to control the characteristic of this precipitates through ageing treatment in optimizing the shape memory behaviour of aged NiTi alloy.

However, it is reported that the critical stress for slip is effectively increased by combining the work hardening and the age hardening on the same alloy [69]. This

type of heat treatment produces good pseudoelastic alloy with zero residual strain upon unloading of the force. Additionally, combining both hardening processes also reported to demonstrate improved pseudoelastic stability on cyclic deformation.

2.2 Precipitation process of NiTi alloys

NiTi alloy with Ni content of 49.8at%–56at% is sensitive to form secondary phase of Ni-rich precipitates during heat treatment. As display in Figure 2.3, the precipitation process is accompanied by three different precipitates namely as Ti_3Ni_4 , Ti_2Ni_3 and TiNi_3 .

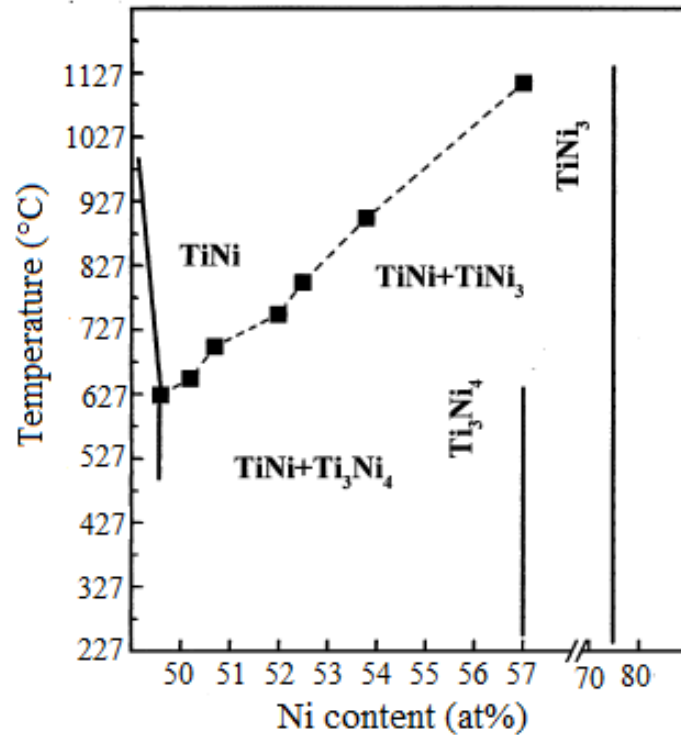


Figure 2.3. Phase diagram of Ni-rich NiTi alloy [53]

Even though there are three types of precipitate available, it is only Ti_3Ni_4 affects the deformation behaviour of NiTi shape memory alloy [70]. The crystal structure of those precipitates is briefly described as below:

- a) Ti_3Ni_4 exists in lenticular shape with a rhombohedral structure. The lattice parameters are $a = 0.6704 \text{ nm}$ and $\alpha = 113.85^\circ$ [71].
- b) Ti_2Ni_3 exists in plate and indefinite block shapes. This precipitate form into an orthorhombic structure at 25°C with lattice parameters of $a = 0.3095 \text{ nm}$, $b = 0.4398 \text{ nm}$, $c = 1.3544 \text{ nm}$. At temperature above 100°C , it forms into a tetragonal structure with lattice parameters of $a = 0.3095$ and $c = 1.3585 \text{ nm}$ [71].
- c) TiNi_3 exists in the form of block shape. It has a hexagonal structure with lattice parameters of $a = 0.51010 \text{ nm}$ and $c = 0.83068 \text{ nm}$ [72].

The Ti_3Ni_4 , Ti_2Ni_3 and TiNi_3 precipitate form in sequence with respect to ageing temperature and duration [53, 73]. Prolonged aging caused the pre-existed Ti_3Ni_4 being dissolved into the matrix, giving a room for the formation of Ti_2Ni_3 to take place. The same goes for prolonged ageing of pre-existed Ti_2Ni_3 which later being replaced by TiNi_3 . However, the duration required for the precipitate to dissolve is highly dependent on the Ni composition of the alloy. Miyazaki found that it only takes one hour for Ti-50.6at%Ni alloy aged at 600°C to experience the dissolution of Ti_3Ni_4 precipitate [55]. In contrast, Nishida reported that Ti-52at%Ni alloy required about 25 hours of ageing at 600°C for the Ti_3Ni_4 to be replaced by Ti_2Ni_3 [67].

The precipitates dissolve gradually as a function of ageing temperature, following the sequence of its nucleation. As seen in Figure 2.4, the TiNi_3 has the highest dissolution temperature followed by Ti_2Ni_3 and Ti_3Ni_4 . In addition, the precipitate dissolution temperature is also dependent on alloy composition, in which the temperature increases with an increase in the Ni content of the alloy. For

example, the dissolution temperature of Ti_3Ni_4 increases from 527°C in Ti-50.6at%Ni alloy to 560°C in Ti-50.8at%Ni alloy [74, 75].

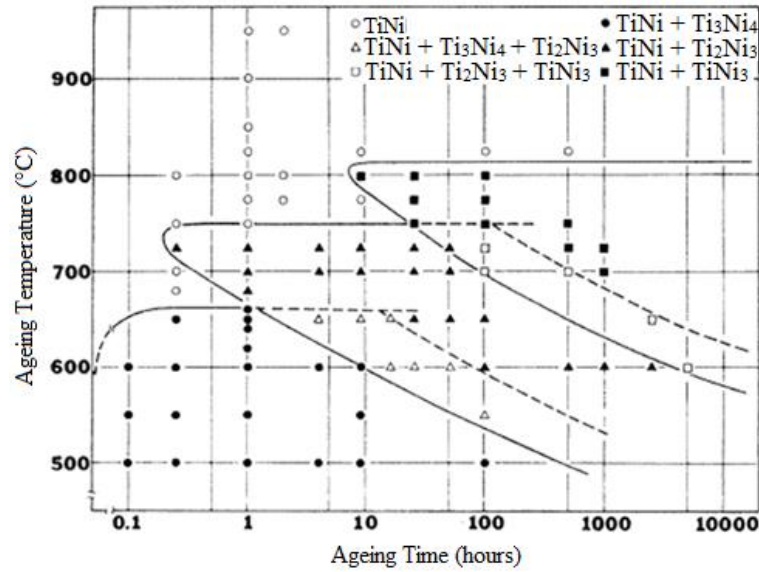


Figure 2.4. Time-temperature-transformation diagram of Ti-52at%Ni alloy [67]

2.2.1 Ageing temperature and duration

As shown in Figure 2.3, the selection of temperature and duration of ageing to improve the pseudoelastic behaviour of NiTi alloys are limited by the region enclosed by the TiNi and Ti_3Ni_4 . For alloy with a higher number of Ni content, larger temperature range and longer duration of ageing are available. In short, Ni-rich NiTi alloys have a larger amount of Ni content ready for participate during the precipitation of Ti_3Ni_4 .

Ageing at different temperature and duration varies the size and density of Ti_3Ni_4 , which later influence the transformation behaviour [76-82] and mechanical properties of NiTi alloy [83]. Even though the ageing effect is present from heat treatment between 300°C and 550°C , not all temperatures would results to a good shape memory behaviour. Ageing at a lower temperature as 300°C and high temperature as 600°C always end up with large residual strain detected at the end of

deformation [54]. The optimum ageing temperature has been proposed by Nishida *et al.* [67] to be 400°C–450°C for good pseudoelastic behaviour on Ti-50.8at%Ni alloy.

2.2.2 Effect of ageing on thermal transformation

Many researchers have studied the effect of ageing temperature and duration on thermal transformation temperature of Ni-rich NiTi alloy. Most of them focus on the variation of A_f and M_s temperature, since both temperature critically determines the modes of deformation of shape memory alloy [45, 53, 60, 84].

K. Gall in his study of single crystal of Ti-50.9at%Ni claimed that the transformation temperature was influenced by the size of Ti_3Ni_4 precipitate [63]. Ageing at 350°C rises the transformation temperature as the 10 nm size precipitate increases the stress field from the lattice mismatch. As the precipitate grew to 500 nm at 550°C, its start to be incoherent, lowering the stress field and reducing the A_f temperature.

Besides the effect of generated stress field, Pelton *et al.* in his study of Ti-50.8at%Ni alloy [60] and Liu *et al.* in his study of Ti-50.7at%Ni [84] explained the rise of transformation temperature in terms of depletion of Ni content. Upon the precipitation process, the Ni atoms congregate in the precipitates whereas the Ti atoms moved into the NiTi matrix. As the matrix becomes lacked of Ni content, the transformation temperature increases as explained from the relationship of composition and transformation temperatures [55].

Liu *et al.* found that the A_f temperature continuously increased only for the first 60 minutes of ageing, with an insignificant change of A_f temperature for the next minutes (Figure 2.5). The saturation of A_f temperature above 60 minutes of ageing is linked to the saturation of the precipitation process as the number of available Ni content for precipitation reduces. In addition, ageing at 400°C promoted maximum

precipitation of Ti_3Ni_4 , concerning to rapid change in the value of A_f temperature. This temperature provides maximum nucleation rate and diffusion rate, which required during the nucleation of the precipitate [67, 84, 85]. Pelton *et al.* [60, 86] reported this optimized temperature in getting maximum nucleation and diffusion rate is shifted to 425°C for Ti-50.8at%Ni alloy

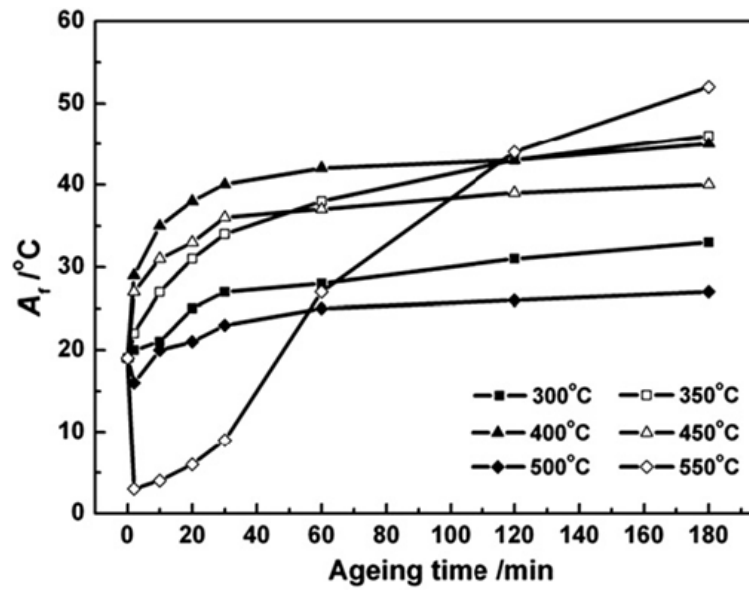


Figure 2.5. Effect of ageing temperature and duration on A_f temperature of Ti-50.7at%Ni alloy [84]

Otsuka visualized the behaviour of R_s and M_s temperature against the ageing duration through Figure 2.6. The R_s temperature constantly maintained regardless of subjected ageing duration. This is due to an insignificance resistance built by the Ti_3Ni_4 precipitate for small deformation as B2–R transformation.

In contrast, the M_s temperature increased proportionally as a function of ageing duration. This is because, the Ti_3Ni_4 particles provide a sturdy resistance for large deformation as R–B19' transformation. As more precipitate nucleated upon prolong ageing, more resistance is built, which lead to higher M_s temperature.

Additionally, longer ageing duration is required by Ti-52.6at%Ni alloy to reach the saturation temperature as compared to Ti-51at%Ni alloy. This is corresponding to the extra amount of Ni content available in Ti-52.6at%Ni alloy for the precipitation process. Note that, the constant value of transformation temperature is independent of initial alloy composition.

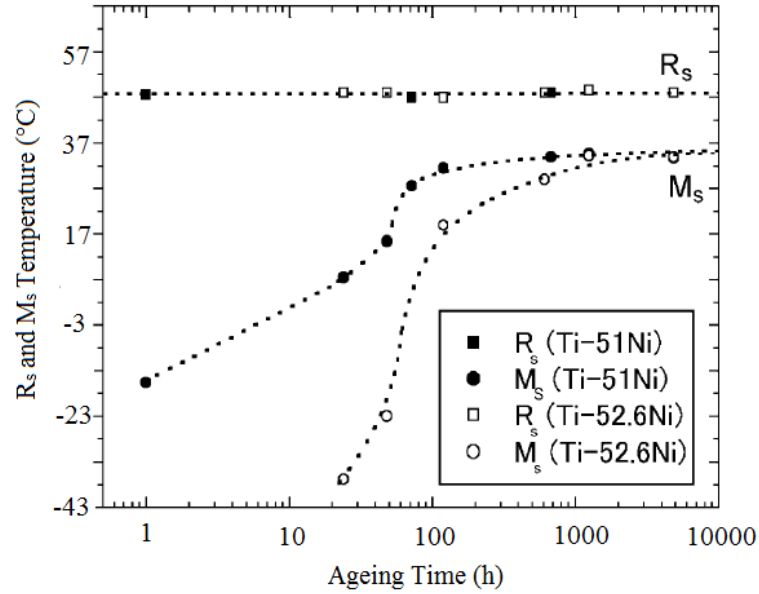


Figure 2.6. Variation of R_s and M_s temperature of Ti-51.0at%Ni and Ti-52.6at%Ni against ageing duration [53]

2.2.3 Effect of ageing on mechanical behaviour

Liu *et al.* demonstrated the effect of ageing temperature and duration on forward and reverse plateau as in Figure 2.7 [84]. At the same ageing temperature, the forward and reverse plateau reduced gradually against the duration of ageing. The decrease of plateau stress is linked to the increment of phase transformation temperature. Thus, lower stress is needed to form martensite as the gap between transformation temperature and testing temperature reduces.

Besides, the plateau stresses only experienced rapid decreased for the first 60 minute of ageing. Prolonged ageing above 60 minutes bring less significance change in the stress level of forward and reverse plateau, supporting the saturation point of

precipitate formation. As explained previously, the insignificant variation of the stress plateau follows the constant pattern of A_f after aged at more than 60 minutes.

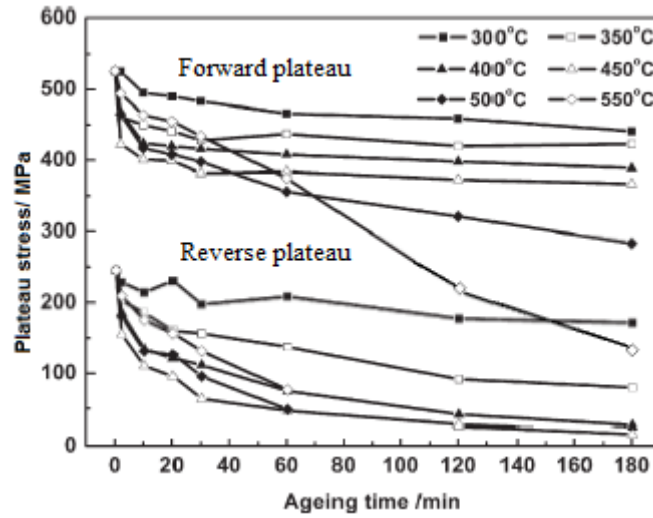


Figure 2.7. Effect of ageing treatment on forward and reverse plateau of Ti-50.7at%Ni stent wire [84]

Furthermore, Gall *et al.* [87] reported a drop in forward plateau as the ageing temperature increases from 300°C to 450°C. At 550°C, the forward plateau starts to experience a rapid increase. The coherent 50 nm precipitate size induced at 450°C is believed to produce nucleation sites for martensitic transformation, which subsequently reducing the stress needed for transformation. As the precipitate grows to 300 nm at 550°C, it loses the coherency with matrix resulting in the increase of the stress needed to induce martensite.

Liu *et al.* [54] revealed the effect of ageing temperature and duration on martensite yield of Ti-50.9at%Ni alloy. He reported that the martensite yield reduced linearly with ageing temperature and shows no dependency on the duration of ageing. The small size precipitates formed during ageing at 400°C is preferable since it is suitable in suppressing the slip motion, thus delay the plastic yield.

Moreover, Liu *et al.* [84] suggested ageing treatment to be done between 300°C and 450°C below 60 minutes for Ti-50.7at%Ni alloy. These ageing

parameters promoted maximal recoverability of the alloy after deformation. Prolong ageing above 60 minutes at 500°C caused the residual strain to increase from 0.3% to 5%.

2.3 Multiple-stage transformations

There are cases where literature reported complex transformation involving two-stage, three-stage or even four-stage of phase transformations [47-49, 88-96]. It is found that the multiple-stage transformation only seen in polycrystalline alloy due to the sensitiveness of precipitate particles to form near to the grain boundary [48]. The large scale of heterogeneous precipitate distribution is believed to be the concept behind the multi-stage transformation as shown in Figure 2.8. The descriptions for each peak (a, b, c, d and e) are simply described as below:

- a) B19'-B2 transformation at the grain interior (precipitate free)
- b) B19'-B2 transformation at the grain boundary (with Ti_3Ni_4 precipitate)
- c) B2-B19' transformation at the grain interior (precipitate free)
- d) R-B19' transformation at the grain boundary (with Ti_3Ni_4 precipitate)
- e) B2-R transformation at the grain boundary (with Ti_3Ni_4 precipitate)

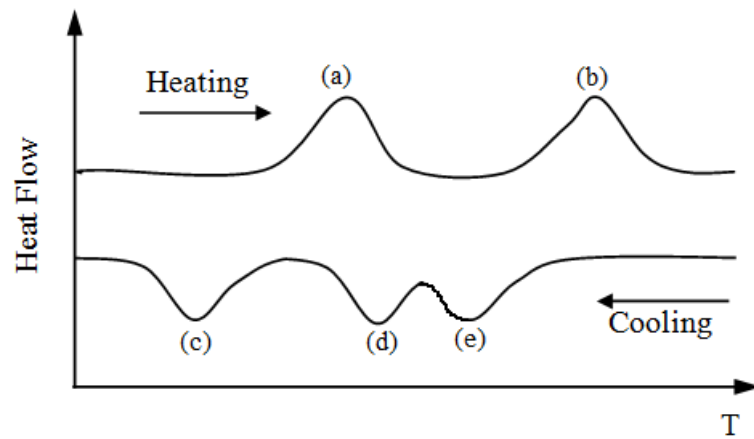


Figure 2.8. Multi-stage transformation of NiTi shape memory alloys [49]

As a result of heterogeneous precipitate formation, Liu *et al.* [45] classified the formed martensite phase into three different classes (M_0 , M_1 and M_2), each formed at a different Ni composition region. Dlouhý *et al.* [97] also reported the overlapping of two different transformation peak within similar transformation temperature due to the heterogeneous distribution of Ti_3Ni_4 precipitate.

2.4 Complex effect of precipitation

2.4.1 Precipitate distribution

The precipitate formation in NiTi alloy is a complex process. It is highly depending on (a) percentage of Ni composition, (b) temperature, (c) time [63, 98-100]. The NiTi alloy having as much as 51%Ni possesses enough amounts of Ni particles to form precipitates and homogeneously nucleates it within the alloy matrix [53]. In contrast, alloy contains lower than 50.9%Ni causes preferential precipitation at only the vicinity of grain boundary [91, 101]. The selective site for precipitation leads to a heterogeneous precipitate distribution.

Ren displayed the effect of heterogeneous precipitate formation on the concentration of Ni content as in Figure 2.9. Since precipitation of Ti_3Ni_4 consuming

Ni content from the alloy matrix, the nucleation of the precipitate continuously depleted the Ni content of the grain boundary region. This phenomenon creates a contra Ni concentration between the grain boundary and the core (a). On the contrary, due to the homogeneous distribution of the precipitate during ageing treatment, the high Ni content alloy experienced a similar Ni concentration across the grain matrix (b).

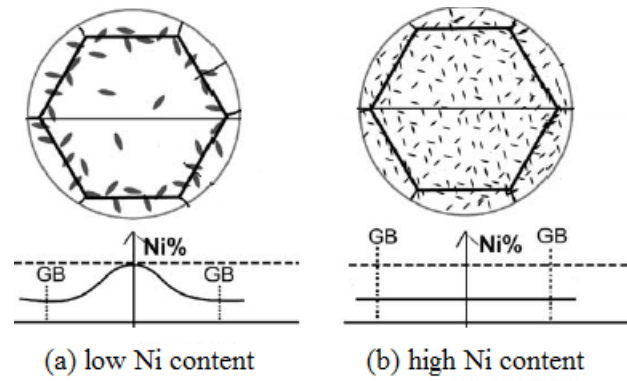


Figure 2.9. Precipitation preferences at low and high Ni supersaturation [48]

2.4.2 Precipitate coherency

Precipitate with good coherency is reported to elevate the transformation temperature [53], lowering the critical stress required to induce martensite phase during deformation [102] and promoting a higher value of martensite yield [87].

Many researchers describe the Ti_3Ni_4 coherency in terms of precipitate size. Ti_3Ni_4 precipitate with the size below than 100 nm is said to be coherent with the main matrix of the NiTi alloy [103]. Upon nucleation, coherent Ti_3Ni_4 precipitate created a strong surrounding local stress field within the austenite matrix of NiTi alloy. These local stress field results to a local resolved shear stress, which reduces the critical stress required for martensitic transformation.

This argument was further supported by Gall *et al.* [104] in their study on the effect of coherent precipitate on the stress-induced martensitic transformation

through the uses of Schmid law and schematic model. They demonstrated that the coherent precipitate resulted to reduction of critical transformation stress level.

Table 2.1 tabulates the size of Ti_3Ni_4 precipitate with respect to their subjected ageing parameters and Ni composition. The precipitate grows in size as the ageing temperature and duration increases. However, for low Ni rich NiTi alloy, ageing for longer than one hour is not suggested as the precipitate tends to increase in the volume and starts to merge and forms a large block shape as shown in Figure 2.10.

Table 2.1. Precipitate size with respect to alloy composition and heat treatment condition

No.	Alloy composition	Prior heat treatment	Ageing temperature and duration	Precipitate size (nm)	Ref.
1	Ti-50.7 at% Ni	Solution treated at 850°C 0.25h	450°C 1h 450°C 10h	230 900	[83]
2	Ti-50.8 at% Ni	Solution treated at 1000°C 24h	450°C 1.5h 500°C 1.0h 550°C 1.5h	50 150 400	[105]
3	Ti-50.9 at% Ni	Solution treated 1000°C 24h	350°C 1.5h 550°C 1.5h	10 500	[63]
4	Ti-50.9 at% Ni	Hot rolled at 995°C	350°C 1.5h 450°C 1.5h 550°C 1.5h 600°C 1.5h	10 50 300 1	[68]
5	Ti-50.9 at% Ni	Solution treated at 1000°C 24 h	350°C 1.5h 400°C 1.5h 450°C 1.5h	100 200 400	[106]

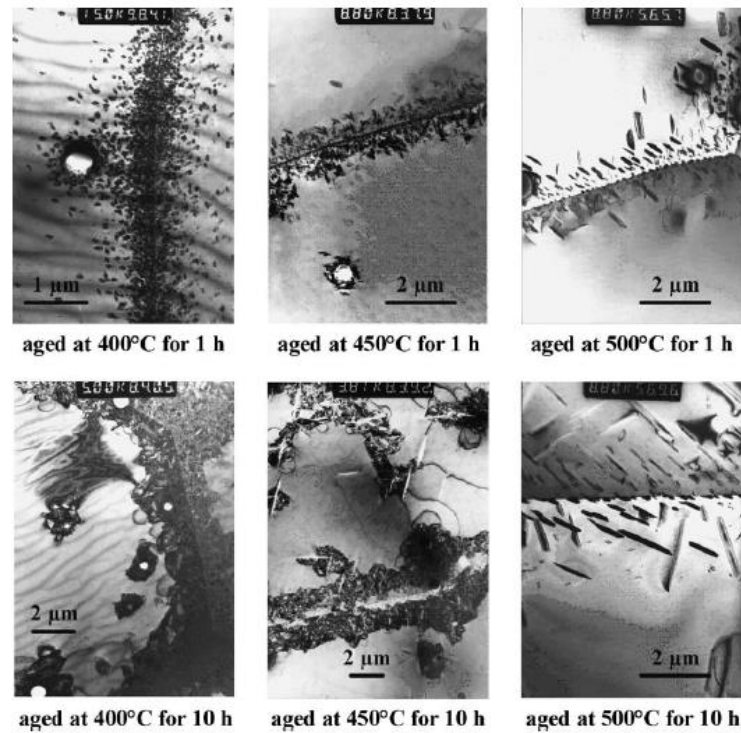


Figure 2.10. TEM micrographs of the 50.7NiTi shape memory alloy after ageing at 400°C, 450°C and 500°C for 1 hour and 10 hours [49]

2.5 Shape memory behaviour modification

The creation of functionally graded NiTi alloy has been conducted before by gradient annealing treatment as in [24, 107-109]. However, the gradient behaviour is not so optimized due to the shortcoming of cold work and annealing process itself, which promoted large residual strain. Besides, the gradient annealing treatment was conducted over large temperature range, without considering the linearity of gradient deformation. As illustrated in Figure 2.11, the gradient deformation proceeded in a nonlinear pattern with a substantial residual strain of 3.7% remaining at the end of the deformation.

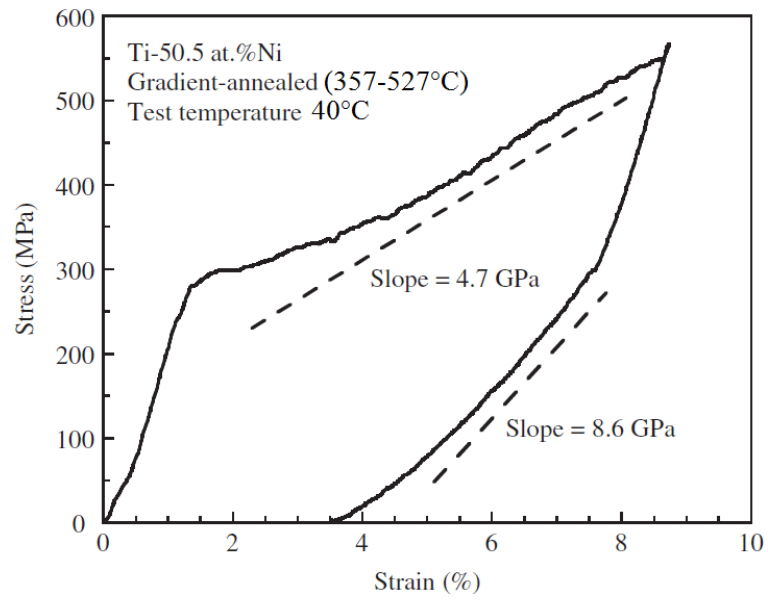


Figure 2.11. Stress-strain curve of gradient-annealed Ti-50.5at%Ni alloy as deformed in tension at 40°C [110]

CHAPTER 3

EXPERIMENTAL DESIGN

3.1 Procedures overview

This chapter explained every task carried out in creating a functionally graded Ti-50.8at%Ni shape memory alloy. The tasks can be divided into three stages. The first stage involved the isothermal ageing treatment of Ti-50.8at%Ni alloy at various combinations of ageing temperatures and durations. This provides a collection of isothermal ageing database in terms of thermal transformation behaviour and pseudoelastic behaviour, which are useful for designing functionally gradient psuedoelasticity. From the isothermal database, a continuous range of ageing temperature was selected as based on the largest change of transformation stress and smallest residual strain promoted. Over the selected temperature range, the transformation stress must continuously vary to promote linearity on the gradient stress plateau. Any overlapping value of transformation stress is undesirable, as this would contribute to constant stress plateau on the stress-strain curve.

The second stage involved in the fabrication of a gradient temperature furnace. The gradient temperature furnace was constructed for ageing NiTi specimens in the form of wire. The furnace design also incorporated the construction of jig and fixture for handling the wire upon the treatment process. The layout of the thermocouples for the gradient temperature furnace was designed to record the temperature profile along the interior of the furnace precisely.

The final stage dealt with the creation of functionally graded NiTi wire through the gradient ageing treatment using the gradient temperature furnace. The selected temperature range for each ageing duration was based on the isothermal database.

Throughout the heating process, the temperature along the wire length was carefully monitored and recorded.

3.2 Isothermal ageing treatment

Ni-rich Ti-50.8at%Ni alloy in the form of 0.1 cm diameter drawn wire was purchased from a commercial company. Two types of isothermal specimens were prepared; (i) 6.0cm length for tensile test and (ii) 0.2cm length for thermal transformation test using differential scanning calorimeter.

The isothermal specimens were solution treated using single zone MTI tube furnace model GSL-1100X at 900°C for 20 minutes in argon environment. The argon gas is used to flush out any oxygen gas inside the heating tube. The wire then quenched into cold water to avoid the effect oxidation.

The specimens were then aged at 36 different combinations of temperatures and durations. The ageing durations were fixed at 10, 20, 30 and 60 minutes, respectively. For each ageing duration, nine different temperatures were selected that include 310°C, 340°C, 370°C, 400°C, 430°C, 460°C, 490°C, 520°C and 550°C.

The ageing temperature range was chosen based on the active precipitation area in the NiTi phase diagram. The duration of ageing is limited to a maximum of 60 minutes to preserve the coherency of Ti_3Ni_4 precipitate [60, 84]. The ageing treatment is carried out in air, knowing that oxidation is nearly negligible at this range of temperature [111-113]. Nevertheless, the surface of the specimens was also cleaned mechanically by using a fine abrasive paper to remove any potential thin layer of oxide.

3.2.1 Thermal martensitic transformation analysis

The variations in thermal transformation temperatures of aged specimens were measured using DSC model TA-Q20. The differential scanning calorimeter was programmed to run at a constant heating and cooling rate of 10°C /min with data logging rate of 50 data/min.

In order to identify individual phase transformations owing to distinctive peaks on a DSC trace, partial heating and cooling cycles were performed with different starting and ending temperatures, as necessary. Later, the trace was analyzed to report the austenitic start (A_s) and austenite finish (A_f) plus the martensitic start (M_s) and martensitic finish (M_f) temperature in accordance to ASTM F2004, Standard Test Method for Transformation Temperature of Nickel-Titanium Alloys by Thermal Analysis.

3.2.2 Deformation behaviour analysis

The pseudoelastic behaviours of the aged specimens were evaluated from stress-strain curves obtained from tensile test. Tensile tests were done on Instron universal testing machine (UTM) model 3367 with 30kN load cell. The testing was conducted in an open air at room temperature of 25°C for 10 and 20 minutes specimen (since their A_f temperatures are below room temperature). Specimens aged for 30 and 60 minutes were tested in a thermal chamber at 49°C (since their A_f temperatures are above room temperature). The loading and unloading rate used is 0.0167s^{-1} . This loading rate is low enough for avoiding the effect of internal heat generation during the stress-induced martensitic phase transformation of the alloy [114].

The procedure of tensile test was based on ASTM E8, Standard Test Methods for Tension Testing of Metallic Materials. As specified by ASTM E8, the wire is mounted on a uniaxial screw driven load frame by wedge grips. The setup image for

the tensile test is shown in Figure 3.1. From the total length of the specimen, 1.5 cm from the wire each end was utilized for gripping, thus leaving 3.0 cm as the gauge length. Upon testing, the wire was strained until the end of the forward plateau before the unloading process takes place. The value of stress and strain was recorded by Bluehill 3.0 software installed on the universal testing machine's personal computer.

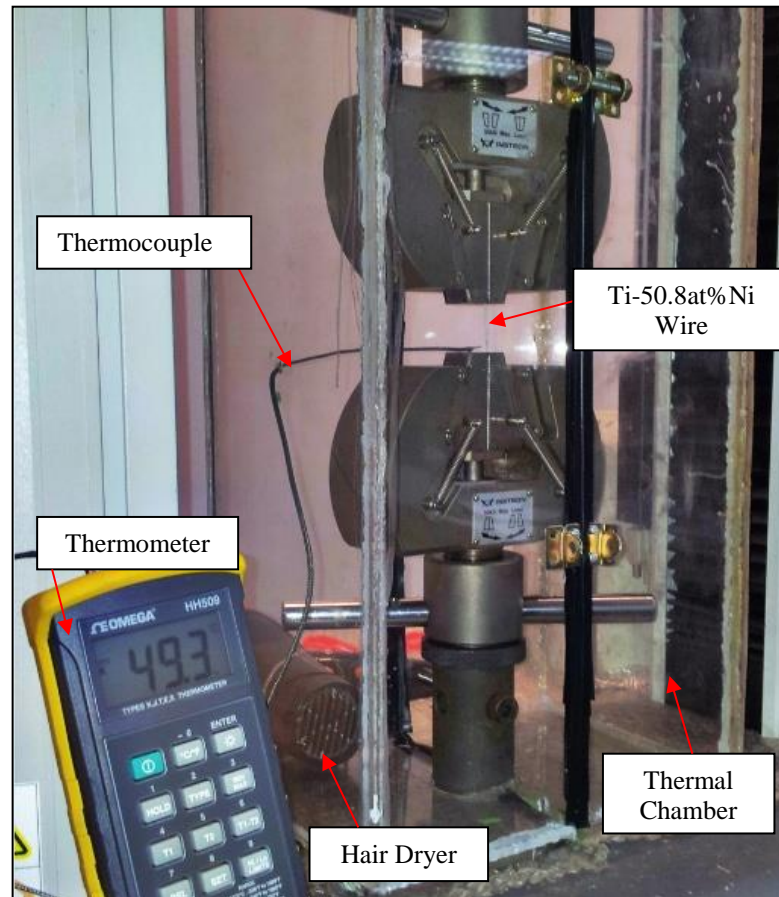


Figure 3.1. Tensile test setup with the thermal chamber

The pseudoelastic behaviour from each stress-strain curve was analysed along with the following properties: forward plateau, reverse plateau, plateau strain and residual strain. The measurement was made on each property by following the description included in ASTM-F2516, Standard Test Method for Tension Testing of

Nickel-Titanium Superelastic Materials. The details of measurements for all properties are listed in Table 3.1 and illustrated in Figure 3.2.

Table 3.1. Properties defined for pseudoelastic deformation behaviour

Property	Definition
Forward plateau	Stress at 3% strain during the initial loading of the specimen
Reverse plateau	Stress at 2.5% strain during unloading of the specimen
Plateau strain (ϵ_p)	Strain at the deviation of σ - ϵ line from stress plateau
Residual strain (ϵ_r)	Difference between the strain at a stress of 7.0MPa during loading and unloading of the specimen

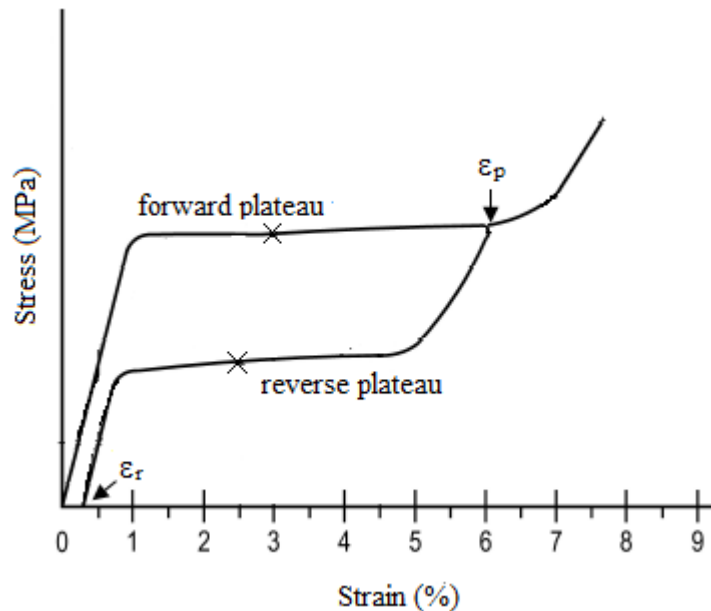


Figure 3.2. Illustration of properties defined for pseudoelastic stress-strain curve

3.3 Gradient temperature ageing

3.3.1 Furnace fabrication

The gradient temperature furnace used in this study was custom made as displayed in Figure 3.3. The heating of the furnace was achieved by using Kanthal heating element, which directly wound on the surface of the ceramic tube. The creation of gradient temperature profile inside the tube furnace was manipulated by the way the

heating element was installed. The gap between heating element loop was continuously increased from one end to the other end. In simple words, one end of the tube has many heating element loops per length compared to the other end as illustrated in Figure 3.4.

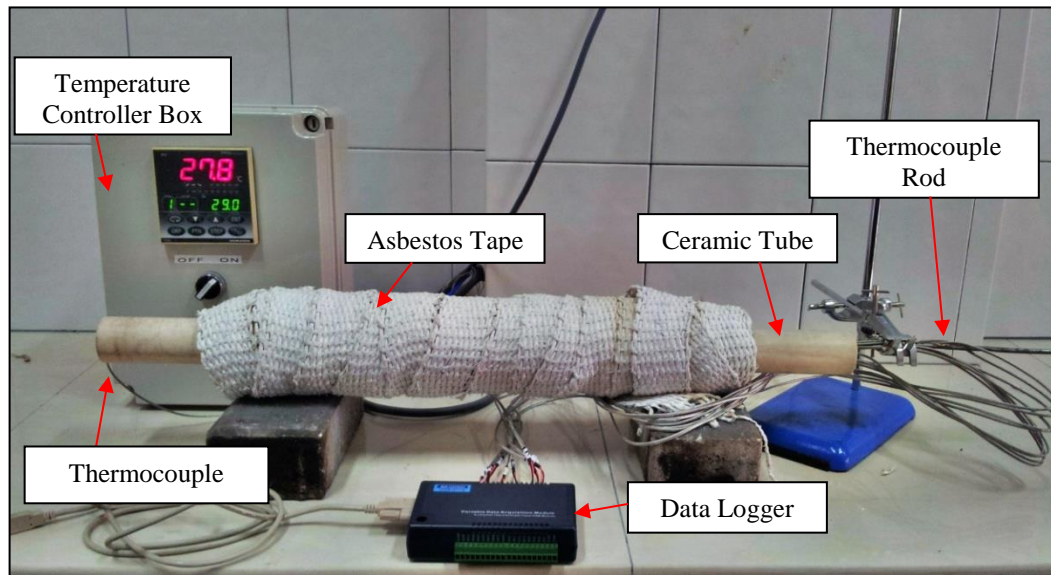


Figure 3.3. Gradient temperature furnace setup

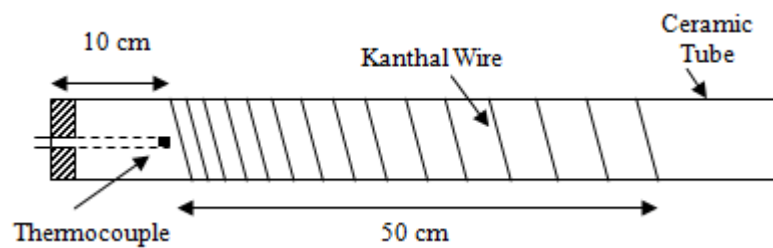


Figure 3.4. Schematic diagram of heating element loop on the ceramic tube

As the heating process started, the heat power from the heating element continuously transferred to the ceramic tube. The end with the large number of loops reached the specified temperature first, leaving the temperature of the remaining part of the tube be lower. At the moment, the temperature across the tube is reducing proportionally to the number of the heating loops, creating a linear gradient

temperature space. In order to assist efficient heat transfer along the tube length, the end with the lower number of heating loop was purposely open to ambient air.

For temperature monitoring, the high-temperature end of the furnace was attached with one thermocouple, which directly connected to the temperature controller. In addition, this end was purposely closed to avoid rapid fluctuation of the controlled temperature. Asbestos insulator tape was wrapped around the surface of the tube furnace to avoid heat loss to the environment, to improve the safety of the setup and to achieve good accuracy of temperature control.

The gradient temperature profile along the hearth of the furnace was measured with eight thermocouples set at 1.0 cm equal interval along the length of the furnace tube. The thermocouples were mounted on a metal rod for easy insertion into the tube. A retort stand was used to clamp one end of the metal rod and rigidly positioned it at the center of the furnace tube diameter. This fixture was made movable so that the rod position can be adjusted to locate the best linear gradient temperature profile across the furnace.

The schematic diagram of this thermocouple rod is illustrated in Figure 3.5. Each thermocouple is connected to the data logger channel and recorded by Wave 2.0 software. This software supports real-time graph plotting function, which makes temperature monitoring possible upon heating.

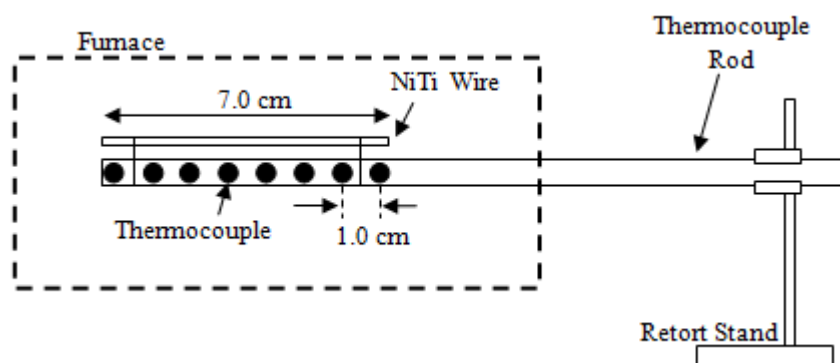


Figure 3.5. Schematic diagram of thermocouples and NiTi wire inside the gradient temperature tube furnace

3.3.2 Furnace parts

The gradient temperature furnace consisted of a ceramic tube, heating element wire, asbestos tape, temperature controller, data logger, thermocouple and thermocouple's rod. Brief descriptions of the individual items are listed as below;

a) Ceramic Tube

Ceramic tube with purity of $\text{Al}_2\text{O}_3 > 99.5\%$; $\text{Fe}_2\text{O}_3 < 0.01\%$ was selected as heating container for the gradient furnace owing to its good thermal insulator properties. The tube was purchased from MTI Corporation with 3.8 cm inner diameter, 4.2 cm outer diameter of and 70 cm in length.

b) Heating Element

Kanthal A-1 heat resistance wire was used as heating element for the gradient furnace. The wire was purchased in the coil form with 0.13 cm in diameter. This wire can be heated up to 1260°C owing to the resistance of 0.98 Ohms per meter length. A total of 15-meter heating element was used to wind along the tube length. This amount of length is known to supply power up to 4000 Watts upon heating. Both end of this heating element wire was directly

connected to the solid-state relay inside the temperature controller box. The power of the furnace was calculated as below;

Total resistant, R_t of 15 meters long heating element= $0.98 \Omega \times 15 \text{ m}$

$$R_t = 14.7 \Omega$$

Normal power supply from TNB station for domestic usage= 240V AC

Total current, I_t supplied through the heating element= V/R_t

$$I_t = 240/14.7$$

$$I_t = 16.32 \text{ Ampere}$$

Total power generates by heating element onto the furnace= $I_t(V)$

$$= 16.32 (240)$$

$$= 3918 \text{ Watt}$$

c) Temperature Controller

A Shimaden programmable controller model FP93-8P-90-0000 controlled the furnace temperature. This controller embedded with a proportional integral derivative (PID) tuning which tunes for the best temperature control. It calculates the difference between a measured temperature and a desired set point temperature and attempts to minimize the difference by adjusting the process current inputs.

In addition, this programmable controller also equipped with miniature circuit breaker (MCB) model: Hager CE240B and solid-state relay (SSR) Carlo Gavazzi RS1A23D25. This controller was powered up by 240V AC domestic power supply via the miniature circuit breaker. The output was connected to the solid-state relay drive in which the heating element wire was

connected. The whole setup of the temperature controller was shown in Figure 3.6.

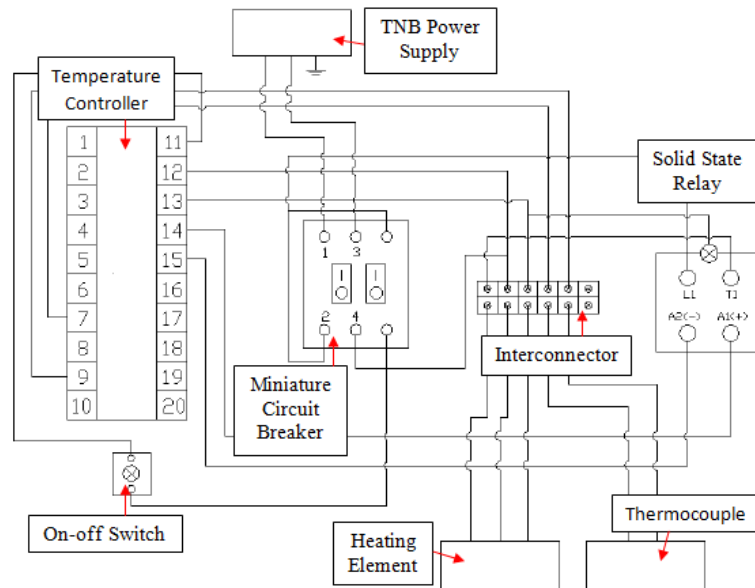


Figure 3.6. Circuit diagram of temperature controller

d) Data Logger

Eight input channels data logger powered up by universal serial bus (USB) power was used to collect the real-time furnace temperature.

e) Thermocouple

K-type thermocouple was fitted in the gradient temperature furnace setup. The thermocouple has an accuracy of $\pm 3.0^{\circ}\text{C}$ and can measure the temperature from 25°C to 600°C .

f) Asbestos Tape

Asbestos tape with 3.0 cm width was used to insulate the heating element, preventing significant heat loss to environment.

3.3.3 Gradient ageing

The gradient ageing specimens were cut into 7.0 cm length from the coil of Ti-50.8at%Ni alloy. The specimens were solution treated at 900°C for 20 minutes in argon environment followed by quenching. After quenching, the specimen was inserted through the tube furnace within the specified temperature range for ageing. The location of heating for the selected temperature range was based on the recorded thermocouple's reading. Figure 3.7 shows the real time plot of temperature recorded within the interior space of the furnace. The specimen was loaded into the gradient furnace once the temperature profile fully stabilized. The furnace took about 3 minutes to ramp from room temperature to the set value, and the temperatures stabilize at roughly $\pm 2^\circ\text{C}$

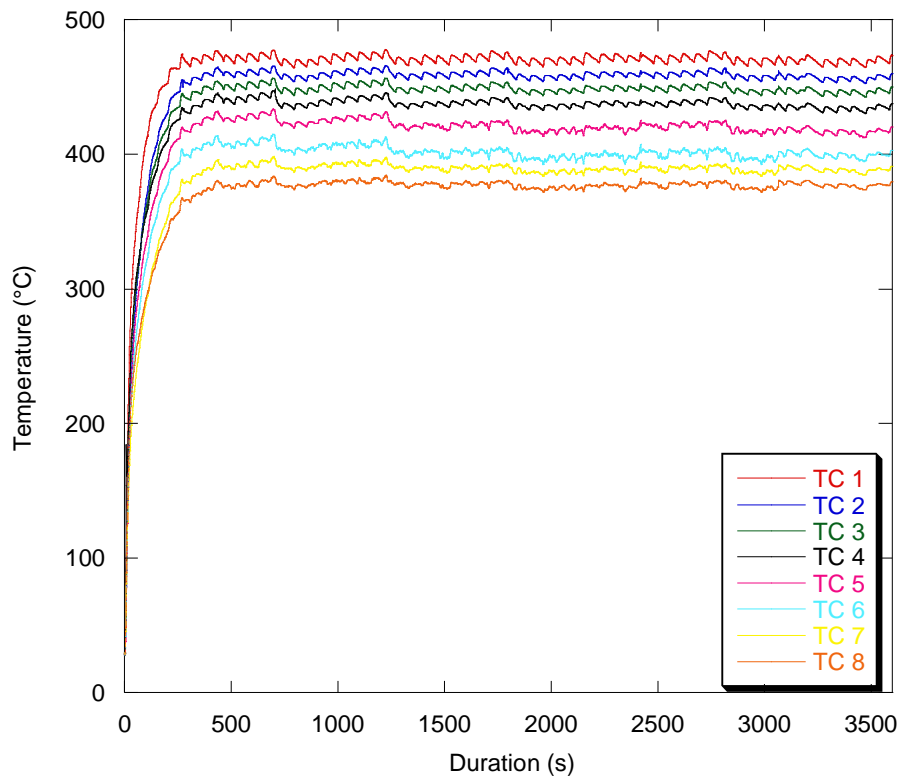


Figure 3.7. Real time plot of temperature recorded by eight thermocouples (TC) for 60 minutes of gradient ageing treatment

Figure 3.8 shows the local temperature recorded by the thermocouples along the length of gradient heating space. As seen, the profile showed a temperature interval of 100°C between both ends, with an average drop rate of 14°C per centimeter.

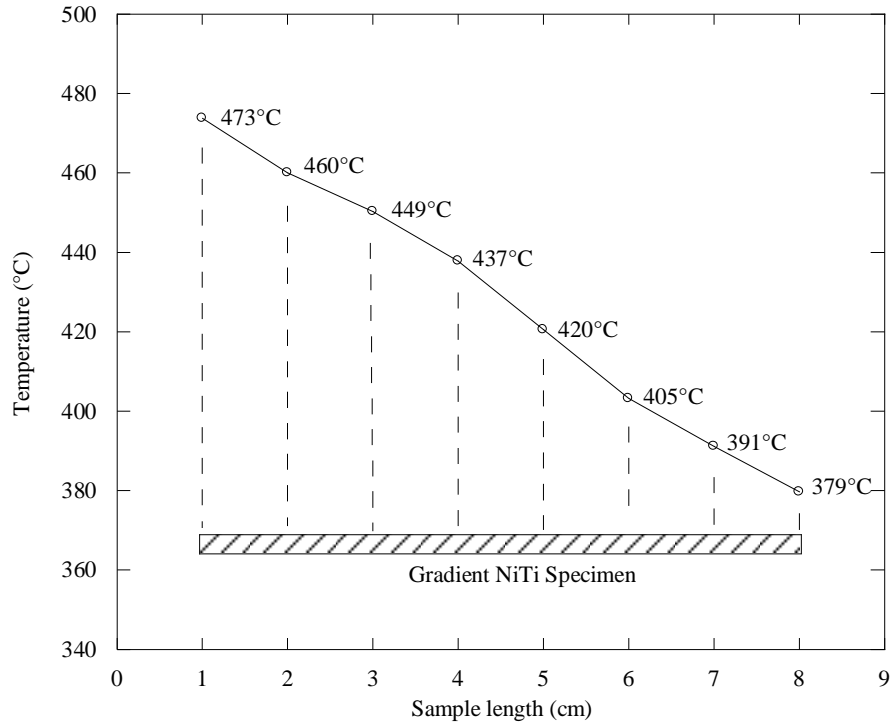


Figure 3.8. Temperature profile recorded by the thermocouples

3.3.4 Thermal and deformation analysis

The thermal and deformation behaviours were measured using the similar procedures as stated in isothermal ageing section (refer to section 3.2.1 and 3.2.2). Anyhow, the gauge length for each gradient tensile specimen varied according to the desired temperature range for each wire. The selection of wire length is listed in Table 3.2.

Table 3.2. Gauge length of gradient ageing specimen at different duration

Ageing duration (minutes)	Gauge length (cm)	Temp. Range (°C)
10	4.5	400–460
30	2.5	430–460
60	2.8	340–400
	2.5	430–460

For verification purpose, thermal transformation behaviours along the gradient tensile specimens were also measured. Four DSC specimens with each length of 0.2 cm were cut from the gauge length at specified position by using Brillant 210 diamond cutter. Figure 3.9 schematically shows the position of the cut for the DSC measurement.

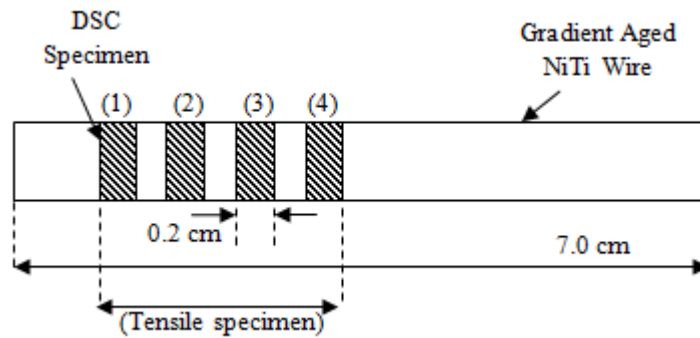


Figure 3.9. Sectioning of DSC and tensile specimen from the total length of gradient aged NiTi wire

CHAPTER 4

RESULT AND DISCUSSION

This chapter presents the experimental results obtained from isothermal and gradient ageing treatments done on Ti-50.8at%Ni wire. The first part of this chapter discusses the effect of temperature and duration on the thermal and deformation behaviour of isothermally aged specimens. Based on this finding, a range of ageing temperatures and duration are selected for gradient ageing. The last part of this chapter demonstrates the gradient deformation behaviour of functionally graded Ti-50.8at%Ni produced from the gradient ageing treatment.

4.1 Effect of ageing on thermal transformation behaviour

4.1.1 Complex multiple peak transformation

Figure 4.1 shows the trend of multiple peak transformation of Ti-50.8at%Ni alloy after aged at different set of temperature and duration. The solution treated specimen exhibited a common peak stage transformation of $M_0 \leftrightarrow A$ with a latent heat of 25.67J/g on both heating and cooling cycle. M_0 denotes the martensite formed from the solution-treated matrix. The peak is very sharp with small transformation temperature window of 14°C and peak hysteresis of 20°C.

When the specimen was aged at 460°C for as short as 10 minutes, the R-phase transformation begun to evolve yielding a three-peaks transformation. On cooling, a small intensity peak pointed by an arrow denotes the $A \rightarrow R$ transformation, followed by nearly combined peaks of $A \rightarrow M_2$ and $R \rightarrow M_1$ transformations. M_1 denotes the martensite formed along a grain boundary, which contained further developed precipitates and M_2 denotes the martensite formed in the nearly precipitate-free region of a grain interior. The $A \leftrightarrow R$ and $R \leftrightarrow M_1$ represent

the transformations occur at the grain boundary whereas the $A \leftrightarrow M_2$ transformation occurs near to the grain interior.

The transformation sequence remained the same when the specimen was further aged at a prolonged time of 60 minutes, but the transformations shifted to higher temperatures. However, when the specimen was aged at a higher temperature of 520°C for 60 minutes, the transformation temperatures of all phases shifted back to lower temperature range.

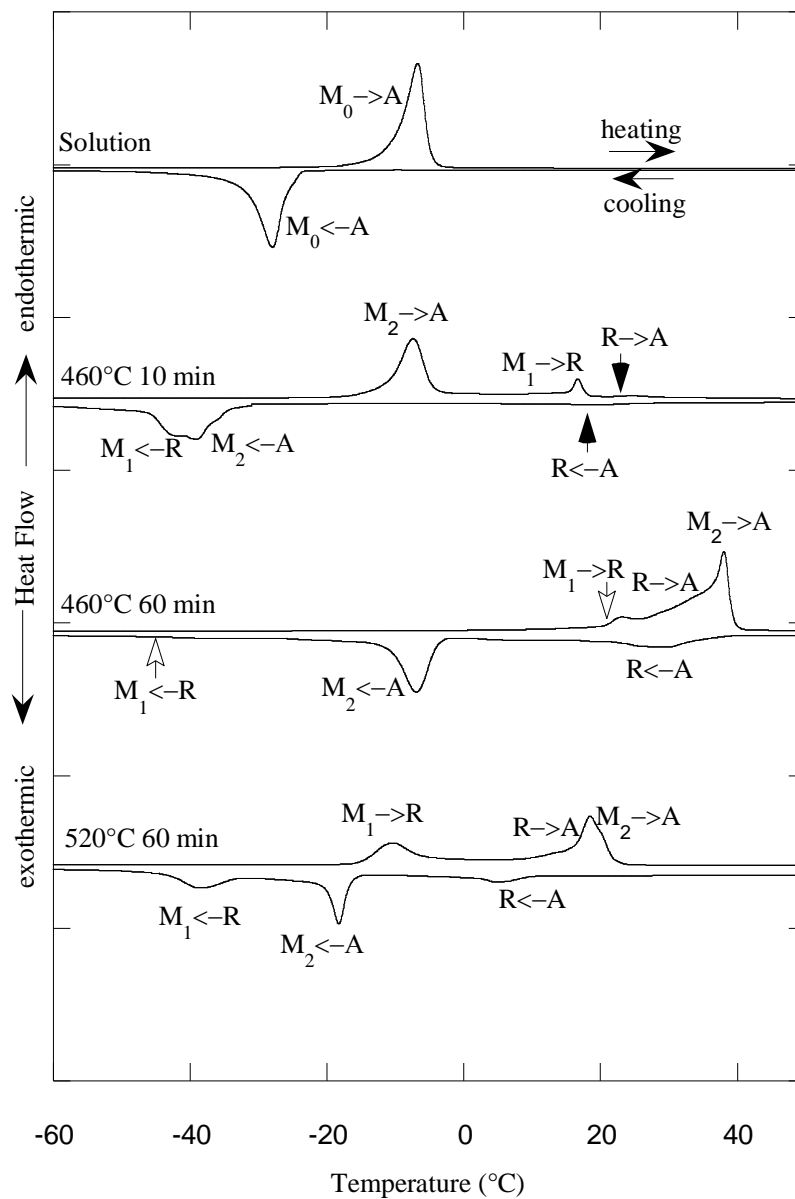


Figure 4.1. Complex multiple-peak transformation of aged Ti-50.8at%Ni alloy

The trend presented in Figure 4.1 illustrates that there is no linear correlation between temperature and duration of ageing on the transformation peak, as what is seen in partial annealing treatment [115]. With respect to low Ni of this Ni-rich Ti-50.8at%Ni alloy, the Ti_3Ni_4 precipitates are believed to distribute mainly along the grain boundary. The trend of those multiple peaks reflects the heterogeneous distribution of Ti_3Ni_4 precipitate developed inside the NiTi alloy during the ageing treatment. As explained in [45], the more Ti_3Ni_4 is formed at the grain boundary, the more Ni contents are consumed at this region as compared to the grain interior. This composition contrast leads to the introduction of the three different class of martensitic transformation of M_0 , M_1 and M_2 .

4.1.2 Effect of ageing duration towards transformation temperature

Figure 4.2 shows the effect of ageing duration on the temperature window of phase transformation. Ageing for 10 and 20 minutes exhibited a single peak of $M_0 \leftrightarrow A$ transformation, similar to solution treated specimen. Both 10 and 20 minutes specimen exhibited a normal temperature window (ΔT) at about 14°C. As ageing treatment prolonged to 60 minutes, the size of the temperature window of transformation peak increased. The DSC curve of 30 and 60 minutes is magnified by 2X to improve the peak intensity visibility. Thoroughly, the temperature window extended from 14°C (ΔT_B) to 50°C (ΔT_E) as the ageing treatment prolonged from 10 to 60 minutes.

The broadening of the temperature window of $A \leftrightarrow R$ and $R \leftrightarrow M_1$ is related to the overlapping of few transformation peaks over similar transformation temperature range. The classifications of transformation peaks were verified with partial cooling measurement as displayed in Figure 4.3. The $A \leftrightarrow R$ and $R \leftrightarrow M_1$ transformation exhibited over a broad transformation peak both on heating and

cooling whereas $A \leftrightarrow M_2$ transformation occurred on a single peak. The peaks of $R \leftrightarrow M_1$ transformations are pointed by the open arrow due to the low and broad peak intensity. This peak broadening phenomena supports well the work by Allafi *et al.* [49], who also observed similar thermal behavior upon ageing Ni-rich NiTi alloy.

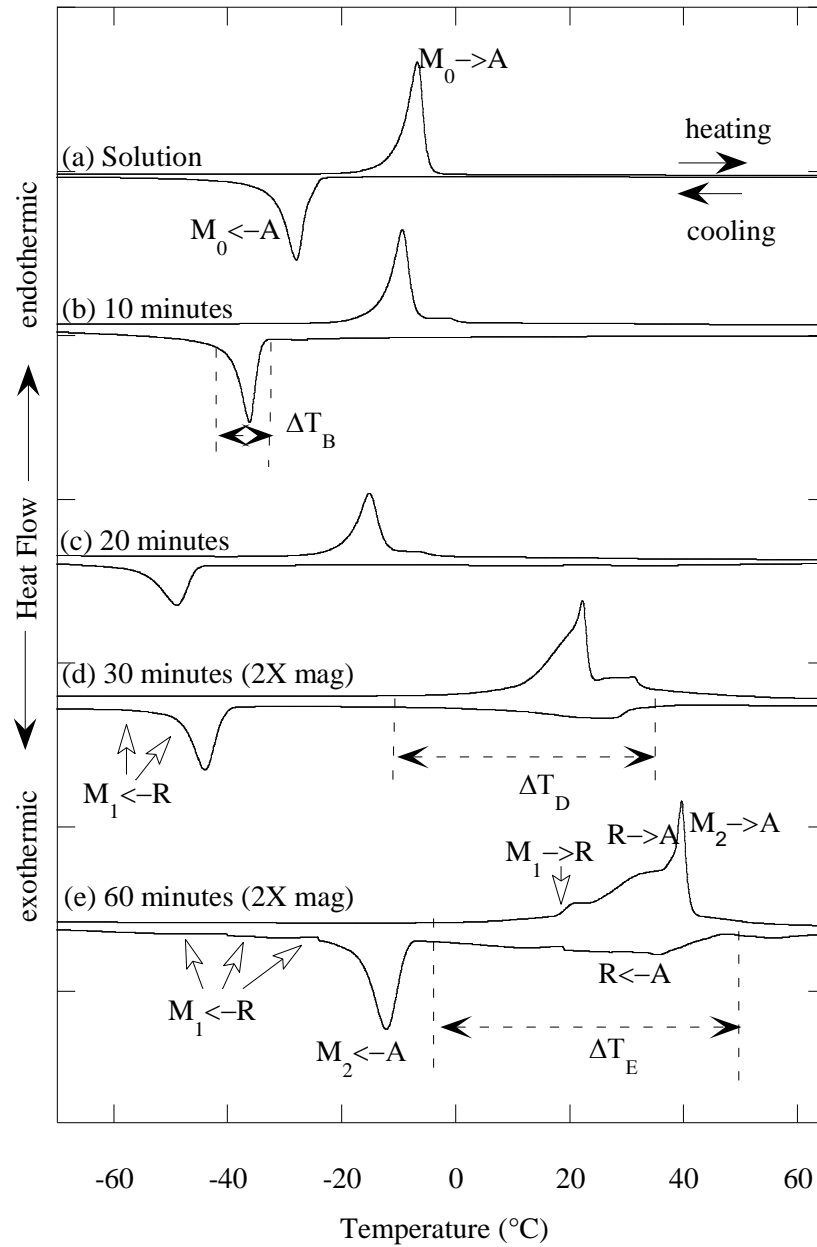


Figure 4.2. Thermal transformation behaviour of Ti-50.8at%Ni alloy after ageing at 430°C for different duration

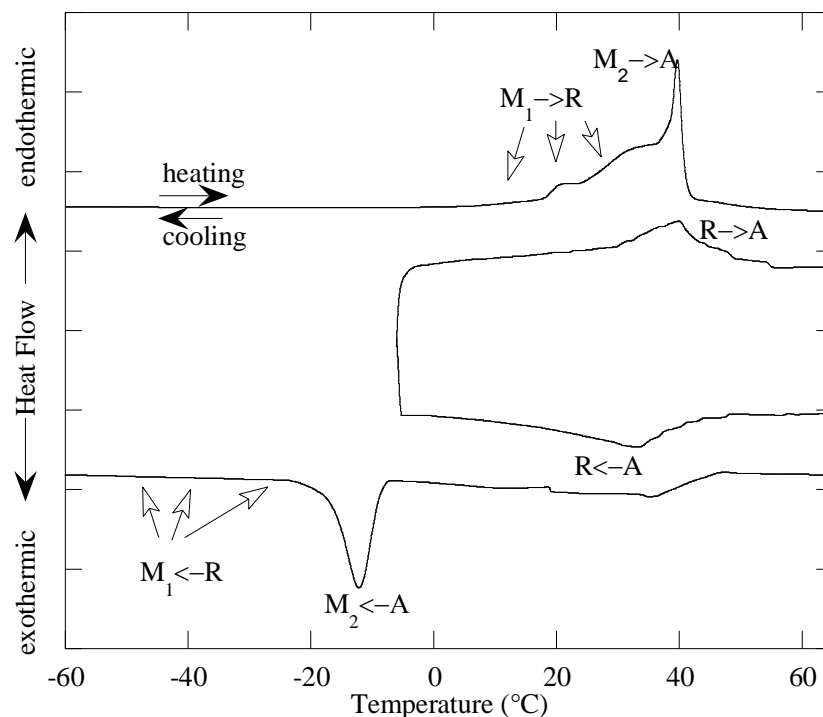


Figure 4.3. Partial cooling measurement of specimen aged at 430°C for 60 minutes

Figure 4.4 illustrates the possible explanation in microscopy scale on the peak broadening phenomena observed in Figure 4.2. Figure (a) and (b) illustrates the growth of precipitates density and size as the ageing time prolonged to 60 minutes as based on [83]. The increase in the size and density of Ti_3Ni_4 precipitate continuously depletes the Ni atom from the grain boundary matrix. Hence, the preferential precipitation process created a variation of Ni content between the grain boundary and grain interior, with the grain interior have the original amount of Ni composition.

The variation of M_s temperature is dependent on the growth of the Ti_3Ni_4 size. For the 10 minutes case, the small size and density of the precipitate lead to unnoticeable variation of Ni content across the grain matrix. At this moment, the amount of Ni content consumed during the formation of precipitates is too little and brings no apparent difference in the Ni composition between the two-grain vicinity (Figure 4.4a). Thus, under the DSC analysis, the transformation peak exhibited a

normal temperature window size (Figure 4.2b) representing a uniform temperature of M_s over the homogeneous specimen composition.

In contrast, as the ageing treatment extended to 60 minutes, more Ni elements were depleted from the grain boundary vicinity. The variation of Ni elements across the grain matrix started to be significant, leading to noticeable decrease of local M_s temperature (Figure 4.4b). Thus, this gradual decrease of M_s temperature is visualized by the overlapping of few $R \rightarrow M_1$ peaks on the same broad transformation peak (Figure 4.2d and Figure 4.2e).

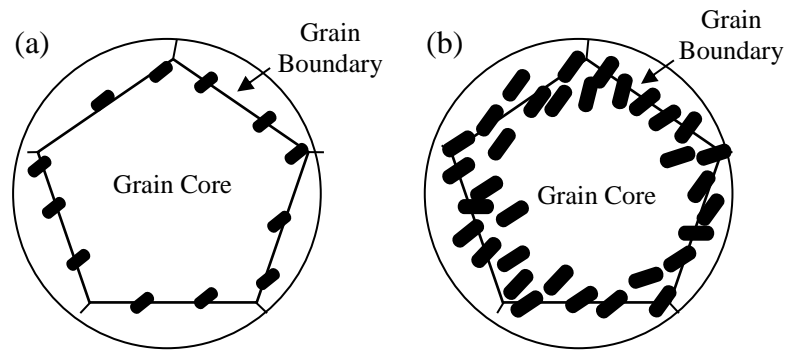


Figure 4.4. Schematic illustration to demonstrate the nucleation of Ti_3Ni_4 precipitate within NiTi specimen matrix: (a) after 10 minutes ageing, (b) after 60 minutes ageing

4.1.3 Effect of ageing temperature towards transformation temperature

Figure 4.5 and Figure 4.6, shows the variation of transformation peak upon ageing at different temperatures for short duration of ageing of 10 to 20 minutes. Ageing at 400°C and below produced a single peak of $M_0 \leftrightarrow A$ transformation on both heating and cooling cycle. The effect of ageing is only noticed on the specimen aged between 430°C – 550°C as the numbers of peak increased to correspond the occurrence of R -phase. Note that the transformation peaks temperature varied with respect to different ageing temperatures. This implies the dynamic growth of Ti_3Ni_4 induced at distinct ageing conditions.

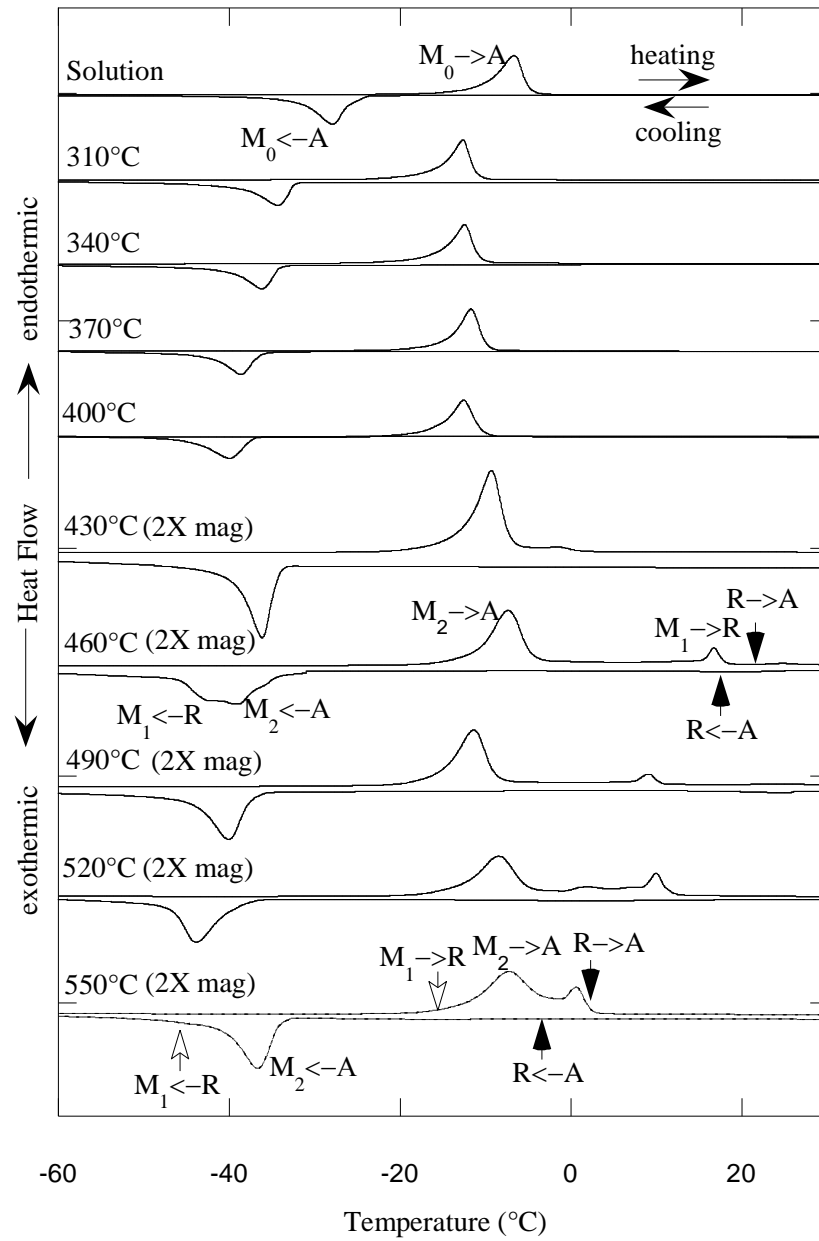


Figure 4.5. Thermal transformation behaviour of Ti-50.8at%Ni alloy after ageing at different temperature for 10 minutes

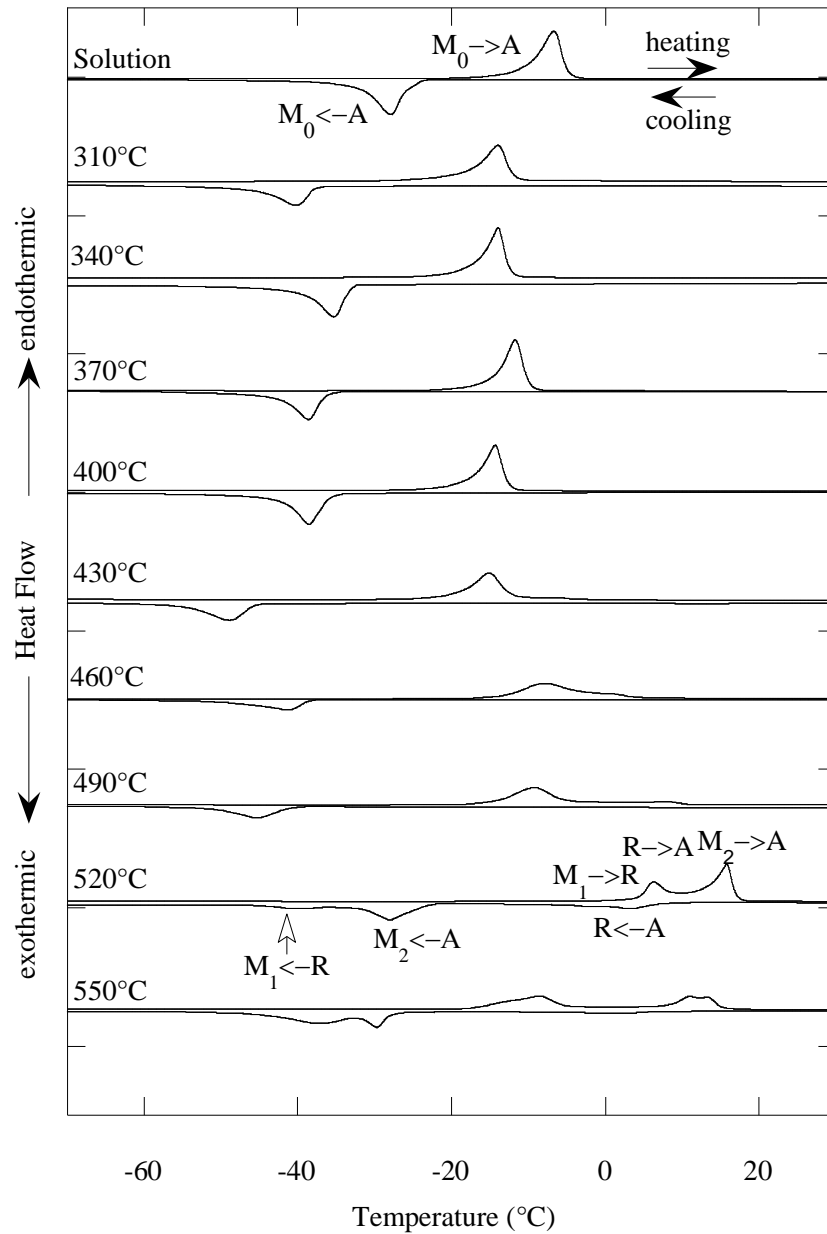


Figure 4.6. Thermal transformation behaviour of Ti-50.8at%Ni alloy after ageing at different temperature for 20 minutes

Figure 4.7 and Figure 4.8, shows the variation of transformation peak upon ageing at different temperatures for long duration of ageing of 30 and 60 minutes. The transformation remained at single peak of $M_0 \leftrightarrow A$ on heating and cooling for specimens aged at 310°C–340°C, indicating that ageing at these temperatures are not effective for the formation of Ti_3Ni_4 precipitate.

The second peak of $A \leftrightarrow R$ transformation started to occur as the specimen aged at 370°C onwards. This implies a significant presence of Ti_3Ni_4 precipitate in the alloy matrix. However, the heating and cooling cycle of the specimen aged at 550°C is transformed back to single-peak of $A \leftrightarrow M_2$ transformation with a decrease in the peak's temperature. This is due to the recovery of Ni content in the NiTi matrix as Ni atoms diffuse back upon disappearance of Ti_3Ni_4 at high ageing temperatures [60].

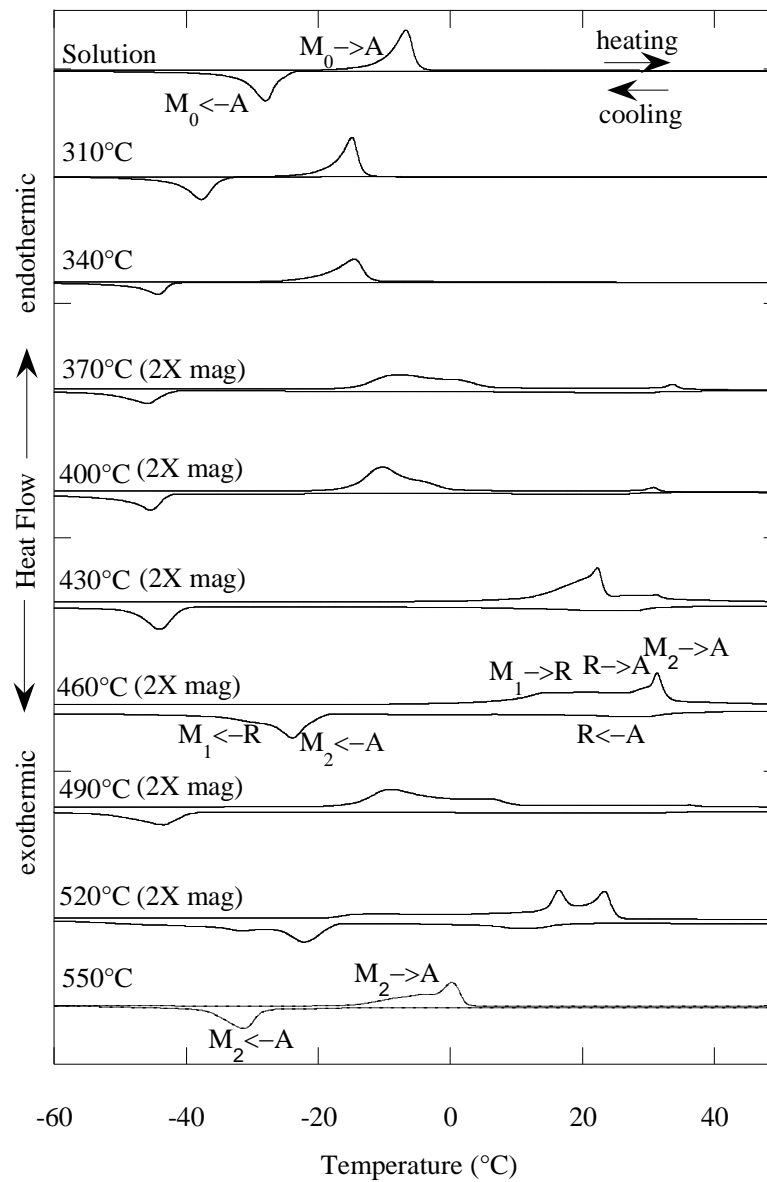


Figure 4.7. Thermal transformation behaviour of Ti-50.8at%Ni alloy after ageing at different temperature for 30 minutes

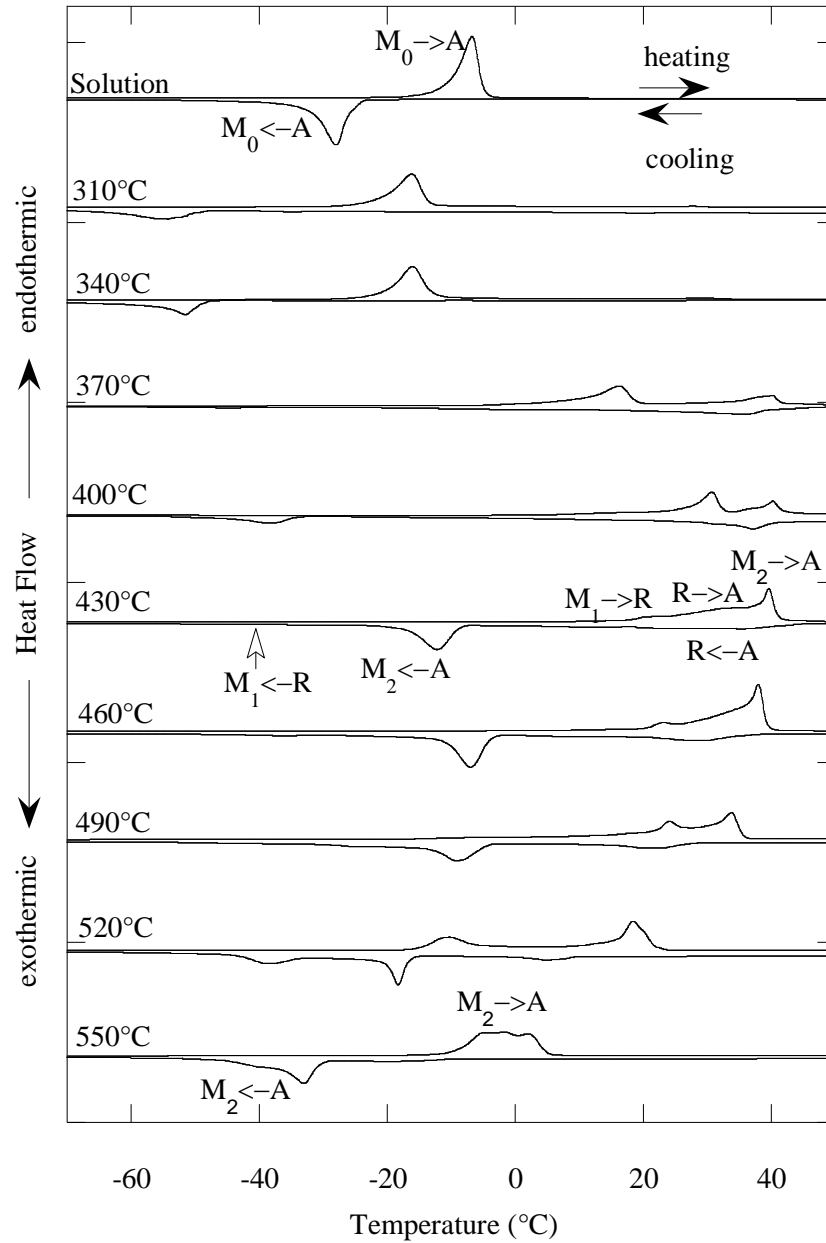


Figure 4.8. Thermal transformation behaviour of Ti-50.8at%Ni alloy after ageing at different temperature for 60 minutes

Regardless of the multiple stage transformation, the variation of A_f temperature is the main interest in this study as it determines the minimum operating temperature to obtain the pseudoelastic behaviour on each aged specimen. Figure 4.9 illustrates the effect of ageing temperature for each duration towards A_f temperature.

In general, all specimens showed an initial A_f temperature at -4°C prior to solution treatment. The A_f of specimen aged at 460°C and above shifted to higher

temperature as the ageing prolonged. However, specimens aged at 430°C and below exhibited a gradual decrease of A_f temperature as the ageing duration prolonged from 10 minutes to 20 minutes. Eventually, as the ageing time was further prolonged to 60 minutes, the A_f increased marginally by at least 40°C, as compared with the solution treated specimen. It is also seen that ageing at 430°C and below requires at least 20 minutes for a significance effect of precipitation in shifting the A_f temperature.

Ageing within 460°C–490°C produced maximum increment of A_f temperature. It is seen that only 20 minutes of ageing duration was needed to raise the A_f temperature from -4°C to 35°C. This temperature set are claimed to induce maximum precipitation rate where the right amount and size of precipitates needed to alter the transformation temperature can be formed during a short period of ageing [60].

On the other hand, it is obvious that prolonging the ageing duration to 60 minutes for specimens aged at 370°C and above produced a very minimal effect in shifting up the A_f temperature. Prolonged ageing to 60 minutes may cause the precipitate to grow larger and start to lose its coherency with the main matrix of the alloy. As this is the case, further growth of Ti_3Ni_4 precipitates with ageing duration no longer affect the thermal transformation behaviour [84].

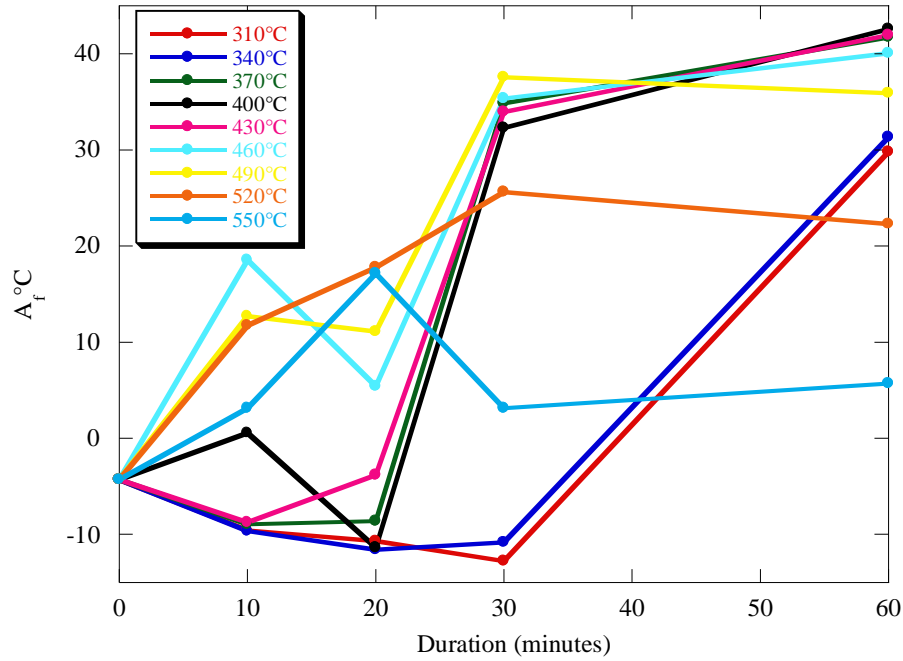


Figure 4.9. Effect of ageing temperature and duration on A_f temperature of Ti-50.8at%Ni alloy

4.2 Effect of ageing temperature on deformation behaviour

4.2.1 Isothermal ageing for 10 minutes

Figure 4.10 shows the pseudoelastic behaviour of specimens aged between 310°C–550°C for 10 minutes. The tensile test was conducted at room temperature of 23°C. All specimens exhibited the stress-induced martensitic transformation at a constant stress plateau. There are nearly zero stress intervals between the critical stress needed to start, σ_{Ms} and finish, σ_{Mf} the martensitic transformation. This constant stress plateau specified that the specimen has homogeneous microstructure properties across its length.

In general, the specimens exhibited two different behaviours. Specimens aged at 400°C and below transformed at nearly stress level of 500MPa and ~8% plateau strain on the forward. Their deformation behaviour is very much similar with the solution treated specimen. On the other hand, specimens aged at 430°C–520°C stress

induced to forward transformation at lower stress levels by at least 100MPa, as compared to the solution treated specimen, and their plateau strain is only ~5%.

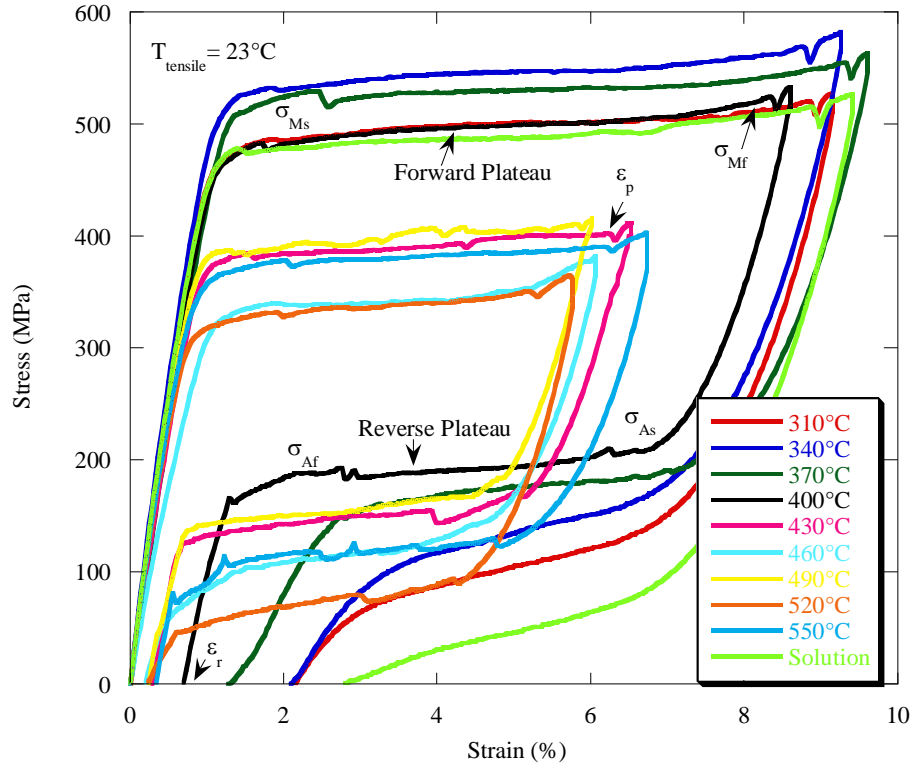


Figure 4.10. Pseudoelastic behaviour of Ti-50.8at%Ni alloy after ageing at different temperature for 10 minutes

Figure 4.11 summarizes the forward and reverse transformation plateau at each temperature of ageing. The forward plateau reduced continuously as ageing temperature increases from 340°C to 460°C. The reverse plateau continuously reduced upon ageing within 400°C–460°C. Meanwhile, no reverse plateau is recorded for ageing within 310°C–340°C.

The effect of ageing temperature towards plateau strain and residual strain is illustrated in Figure 4.12. Both plateau and residual strain continuously drop after the increase of ageing temperature. Rapid drop in the value of strain is observed as the ageing temperature rise from 370°C to 460°C. The continuous drop of the deformation characteristics upon ageing between 340°C–460°C highlights the

effectiveness of this temperature range in altering the alloy microstructure through precipitating different size of Ti_3Ni_4 .

For this set of ageing duration, ageing between 400°C – 460°C is selected to be carried out on the gradient ageing treatment. This temperature range promoted the largest continuous change of transformation stress both on the forward and reverse plateau with a stress interval of 150MPa and 70MPa. Besides, this temperature range also promoted small residual strain, which is less than 1%.

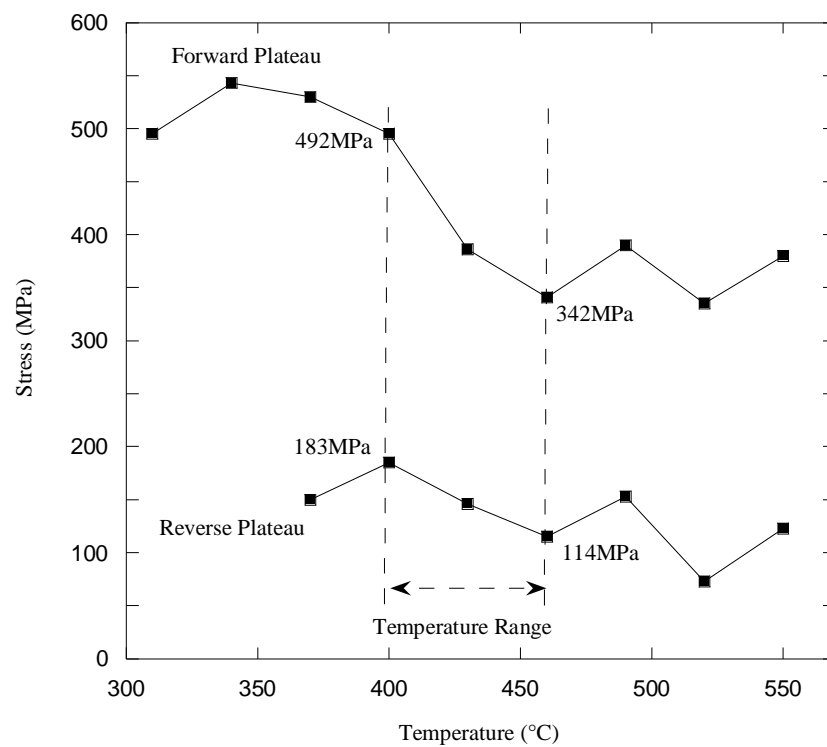


Figure 4.11. Effect of ageing temperature on stress-induced deformation behaviour of Ti-50.8at%Ni alloy aged for 10 minutes

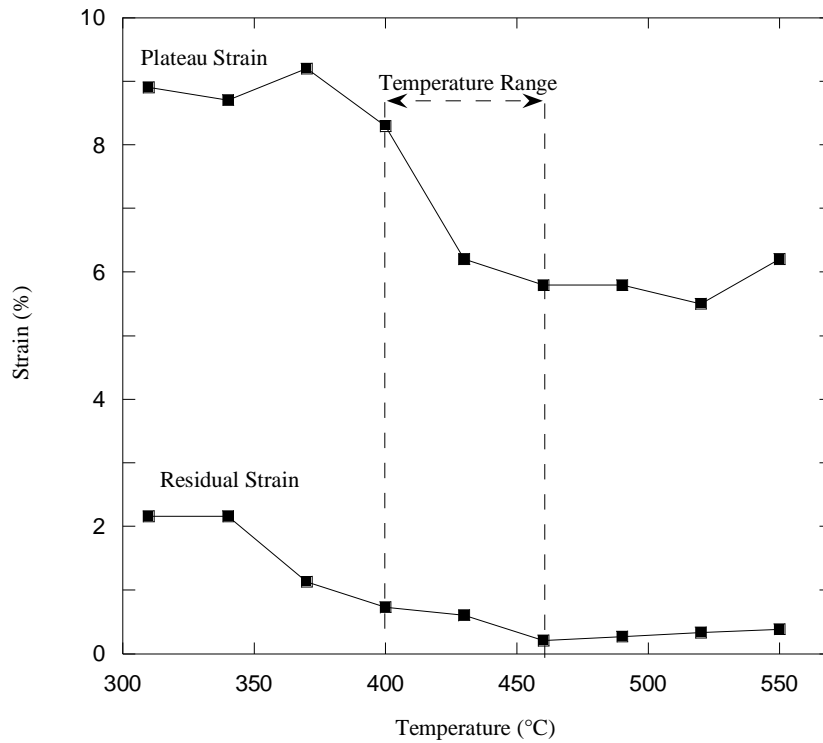


Figure 4.12. Effect of ageing temperature on plateau and residual strain of Ti-50.8at%Ni alloy aged for 10 minutes

4.2.2 Isothermal ageing for 20 minutes

The forward and reverse plateau of specimens aged for 20 minutes are shown in Figure 4.13. The tensile test was conducted in a thermal chamber at temperature of 23°C. Similar to 10 minutes cases, the forward plateau continuously dropped as ageing temperature increased from 340°C to 460°C. There is no reverse stress plateau observed for ageing between 430°C–520°C as this temperatures range yielded large residual strain of 3% as illustrated in Figure 4.14. There is no temperature range which promoted continuous change in the forward and reverse transformation stress. Thus, no temperature range is suggested to be carried out for 20 minutes gradient ageing treatment.

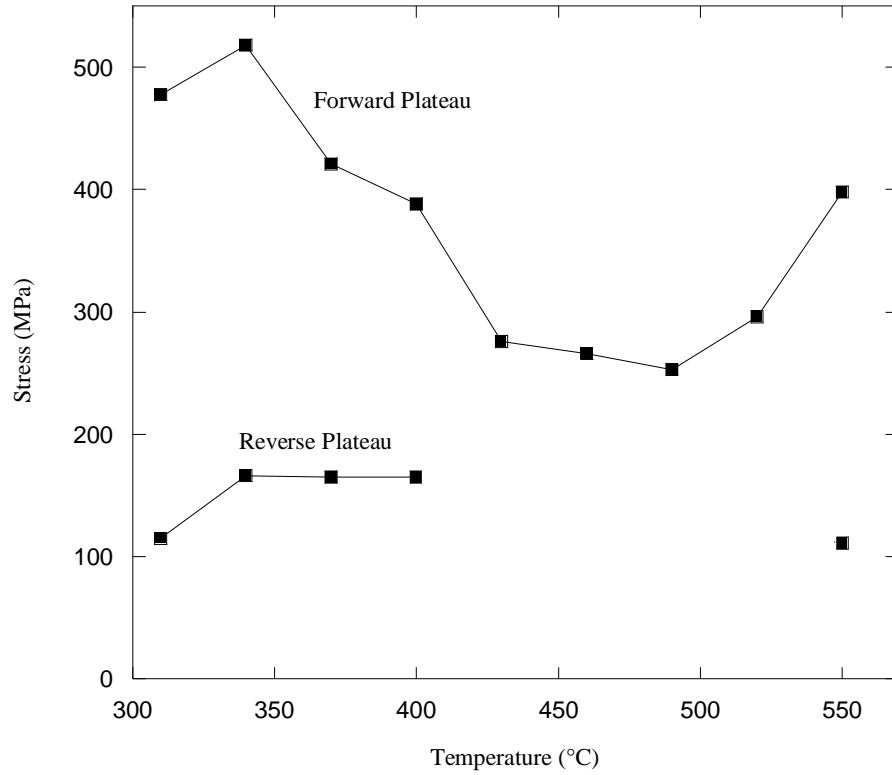


Figure 4.13. Effect of ageing temperature on stress-induced deformation behaviour of Ti-50.8at%Ni alloy aged for 20 minutes

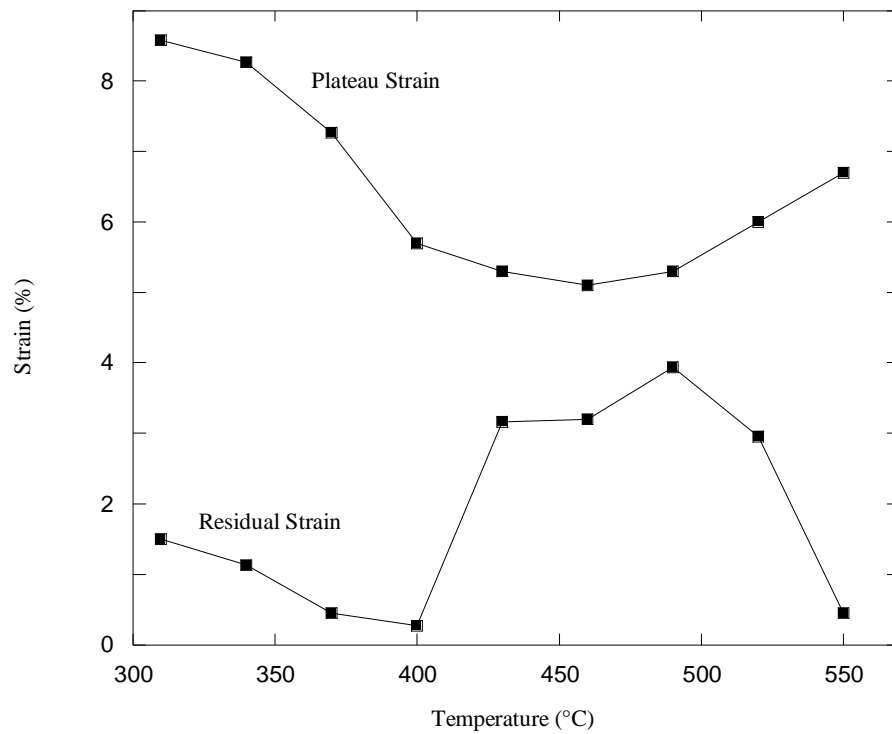


Figure 4.14. Effect of ageing temperature on plateau and residual strain of Ti-50.8at%Ni alloy aged for 20 minutes

4.2.3 Isothermal ageing for 30 minutes

The pseudoelastic behaviour of specimens aged for 30 minutes is displayed in Figure 4.15. As compared to the solution curve, all ageing temperature demonstrated the forward and reverse plateau on a gradient stress plateau. There is a stress gap existed in between the $\sigma_{Ms}-\sigma_{Mf}$ and $\sigma_{As}-\sigma_{Af}$ transformation. The gradient stress plateau highlighted that the accommodation of martensitic transformation is proceeded through a gradual increment in the transformation stress. This gradient stress plateau also observed in the specimen aged for 60 minutes. To update, there is no such gradient stress plateau is reported in literature on the case of isothermal ageing. Possible explanation on this unexpected deformation behaviour is discussed in details later in section 4.3.

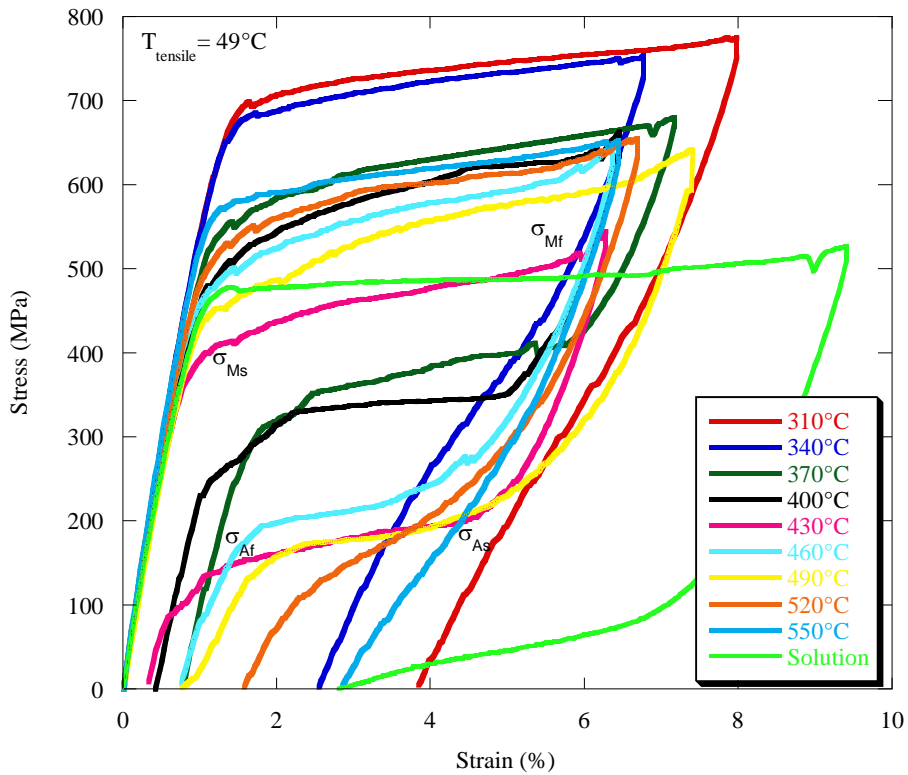


Figure 4.15. Pseudoelastic behaviour of Ti-50.8at%Ni alloy after ageing at different temperature for 30 minutes

Since the 30 and 60 minutes of the isothermal aged specimens already deformed through a gradient stress plateau, the evaluation in selecting the temperature range for gradient ageing treatment is quite different. For this longer ageing duration case, the gradient ageing treatment is conducted with an intention to increase the slope of the gradient stress plateau. This is promising by selecting the temperature range, which offering the largest summation of stress interval upon forward and reverse transformation.

Figure 4.16 shows the effect of ageing temperature on the transformation stress of specimens aged for 30 minutes. Since the specimen was deformed in a gradient manner, σ_{Ms} and σ_{Mf} are used to specify the start and finish of forward plateau and σ_{As} and σ_{Af} are used to specify the start and finish of the reverse plateau.

The forward and reverse plateau gradually decreased as ageing temperature increased from 310°C to 430°C. Eventually, both transformation plateaus gradually rise back to higher level as ageing conducted at 460°C and above. There is no σ_{As} and σ_{Af} are recorded upon ageing at 310°C, 340°C, 520°C and 550°C correspond to their higher residual strain value as shown in Figure 4.17.

For this case, ageing between 430°C–460°C has been selected as the temperature range for the used in gradient ageing treatment. This temperature range endorsed the largest continuous change of transformation stress of 187MPa and 140MPa on forward and reverse plateau, respectively. The predicted gradient stress plateau of the gradient aged specimen is labeled as dotted line in Figure 4.16.

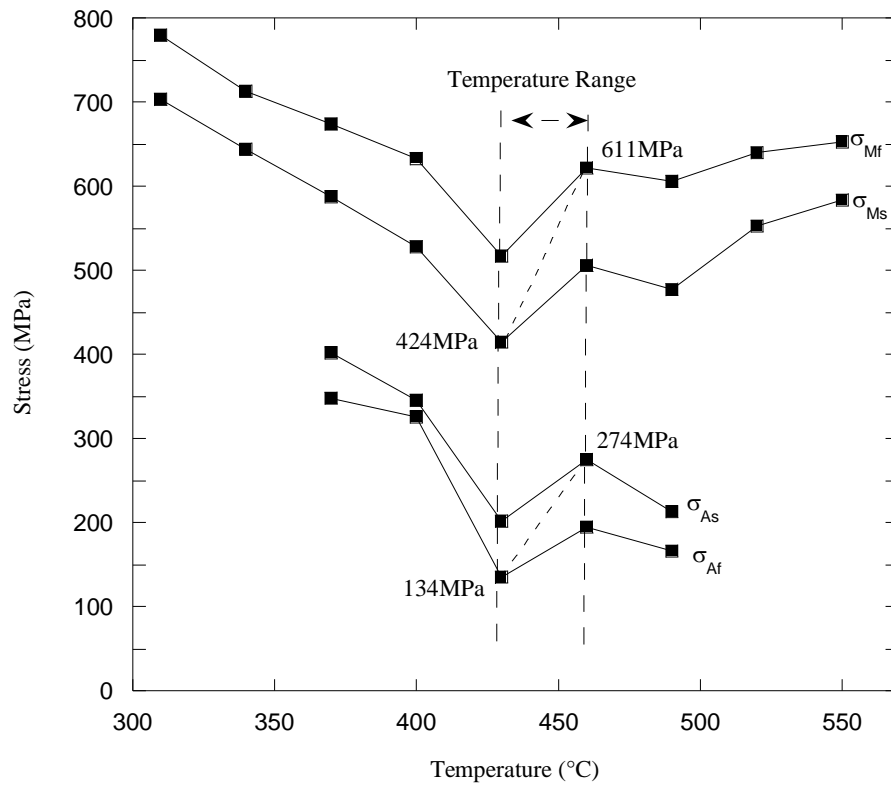


Figure 4.16. Effect of ageing temperature on stress-induced deformation behaviour of Ti-50.8at%Ni alloy aged for 30 minutes

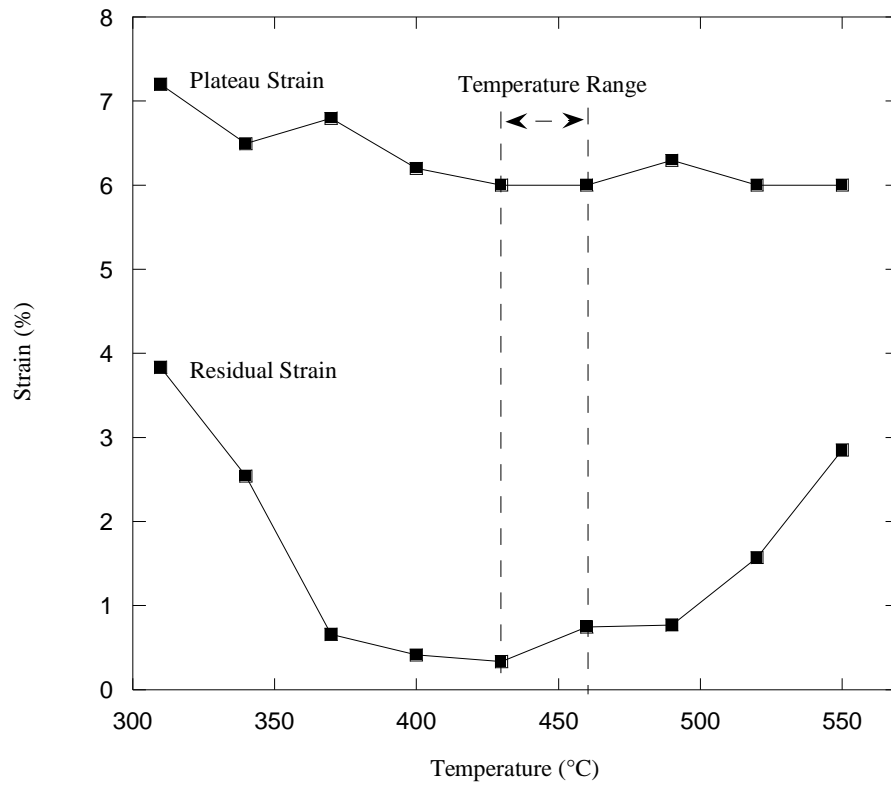


Figure 4.17. Effect of ageing temperature on plateau and residual strain of Ti-50.8at%Ni alloy aged for 30 minutes

4.2.4 Isothermal ageing for 60 minutes

The deformation criteria of specimens aged for 60 minutes are tabulated in Figure 4.18. Similar to 30 minutes cases, the forward and reverse plateau shows a positive hyperbolic pattern against the ageing temperature. Ageing at 310°C, 520°C and 550°C produced no plateau on the σ_{As} and σ_{Af} . In average, most of the ageing temperature yielded the plateau strain to 6% as shown in Figure 4.19. It is only ageing between 340°C–460°C, which promoted residual strain less than 1% upon the completion of the tensile test.

Two set of temperature range has been chosen for 60 minutes of gradient ageing treatment, in particular 340°C–400°C and 430°C–460°C. As labeled by the dotted line on Figure 4.18, gradient ageing within 340°C–400°C expressed the stress interval of 247MPa and 233MPa both on the forward and reverse plateau. In contrary, the second set of temperature range (430°C–460°C) demonstrated the forward and reverse transformation stress interval at 254MPa and 141MPa.

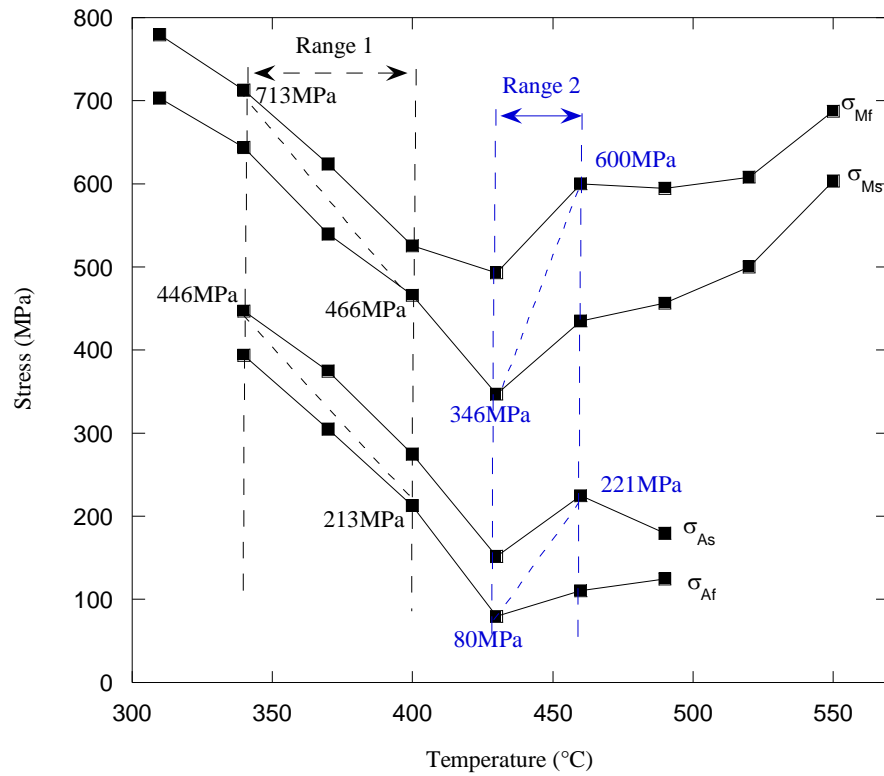


Figure 4.18. Effect of ageing temperature on stress-induced deformation behaviour of Ti-50.8at%Ni alloy aged for 60 minutes

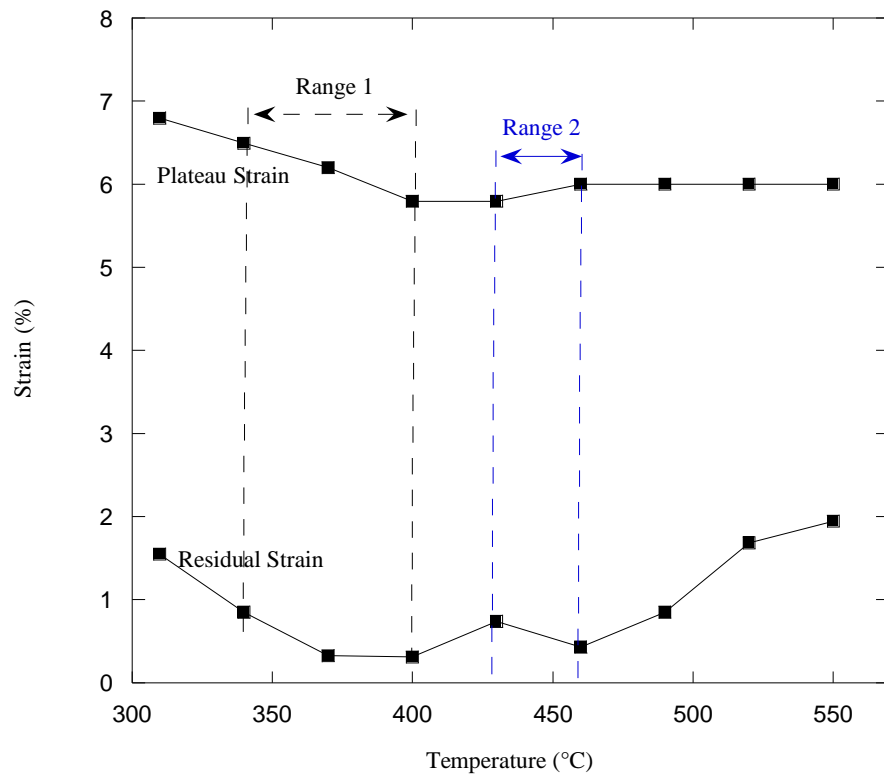


Figure 4.19. Effect of ageing temperature on plateau and residual strain of Ti-50.8at%Ni alloy aged for 60 minutes

The forward and reverse transformation stress intervals of the selected temperature range are compiled in Table 4.1. The bold transformation stress belongs to the respective bold ageing temperature. Upon tensile test, the end of the specimen that aged at the bold temperature will be deformed first with regard to the lower transformation stress.

Table 4.1. Forward and reverse stress interval of isothermal ageing specimen

Ageing duration (minutes)	Temperature range (°C)	Forward Stress Interval(MPa)	Reverse Stress Interval(MPa)
10	400– 460	342 –492	183– 114
30	430 –460	424 –611	274– 134
60	340– 400 430 –460	466 –713 346 –600	446– 213 221– 80

4.3 Effect of ageing duration on deformation behaviour

Figure 4.20 shows the effect of ageing duration on the stress-induced martensitic transformation behaviour of Ti-50.8at%Ni alloy. Specimen aged for 10 minutes produced a flat stress plateau on both forward and reverse transformation. In contrary, specimens aged for 30 and 60 minutes deformed through a gradient stress plateau. The 30 minutes specimen exhibited 2.5 GPa positive stress gradient on the forward transformation as the 113MPa stress interval yielded over 4.5% plateau strain. The 60 minutes specimen exhibited larger stress gradient of 3.4 GPa as the loading process yielded the same transformation strain over a stress interval of 154MPa.

The gradual increase in the transformation stress may be linked to the continuous variation of stress field created by the Ni-rich precipitates along the individual grain matrix. Based on [87], Gall *et al.* claimed that the existence of precipitate inside the NiTi matrix created a stress field which assist in the stress-

induced martensitic transformation. In this respect, it is believed that the 30 minutes specimen started to experience the stress-induced martensitic transformation from the grain boundary (3) and finished at the core (4). This phenomenon is amplified on the specimen aged for 60 minutes as the stress gradient presented steeper slope with larger stress interval. Notice that the start of transformation (5) is at lower stress than (3) and the finish for both (4) and (6) is nearly similar, implying the similarity of the matrix at the core.

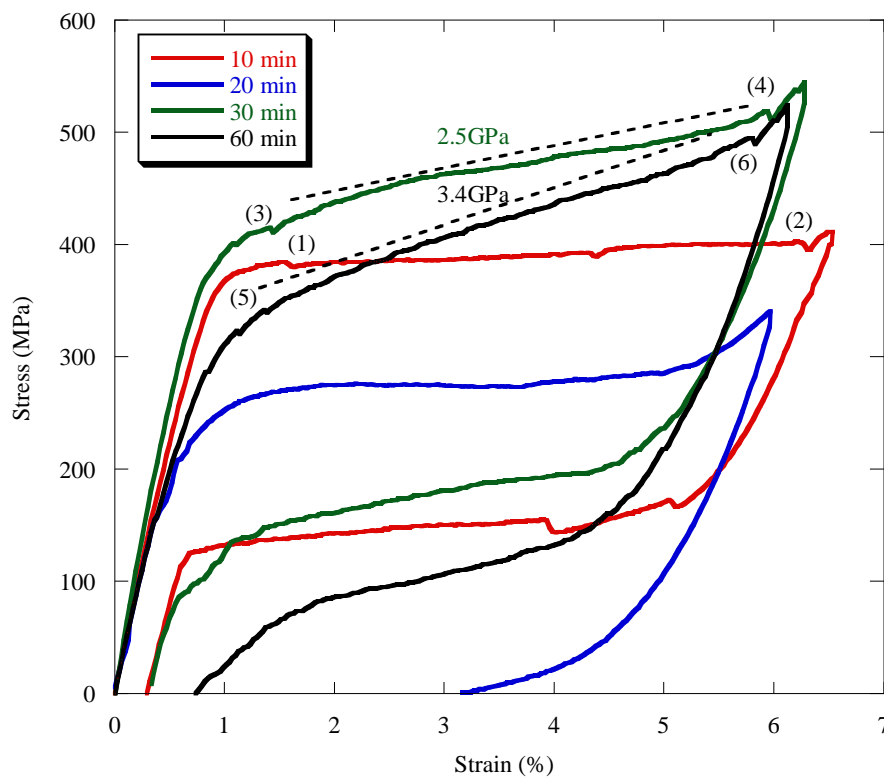


Figure 4.20. Effect of ageing duration on pseudoelastic behaviour of Ti-50.8at%Ni alloy ageing at 430°C

4.4 Gradient ageing treatment

4.4.1 Gradient deformation behaviour

Figure 4.21 shows the gradient deformation behaviour of specimens underwent gradient ageing treatment. The 10 minutes specimen was deformed at 23°C whereas

the 30 and 60 minutes was deformed at 49°C. All specimens exhibited stress-induced forward transformation and reverse transformation along a linear positive stress gradient. In average, the forward transformation yielded the plateau strain nearly up to 6%.

It is only specimen aged within 340°C–460°C for 60 minutes failed to present recovery at ~0.6% upon unloading due to the buckling process. As labeled, the buckling phenomena occurred at the end of the test, at the stage where the austenite phase recovering its elastic deformation. The buckling process occurred as the down movement of the wire gripper upon recovery no longer recovers the elastic strain of the austenite structure. Instead recovering the remaining 10MPa stress, the force caused the wire to bend. The buckling takes place as the wires experienced permanent strain, as the transformation stress needed for martensitic transformation exceeding the yield stress.

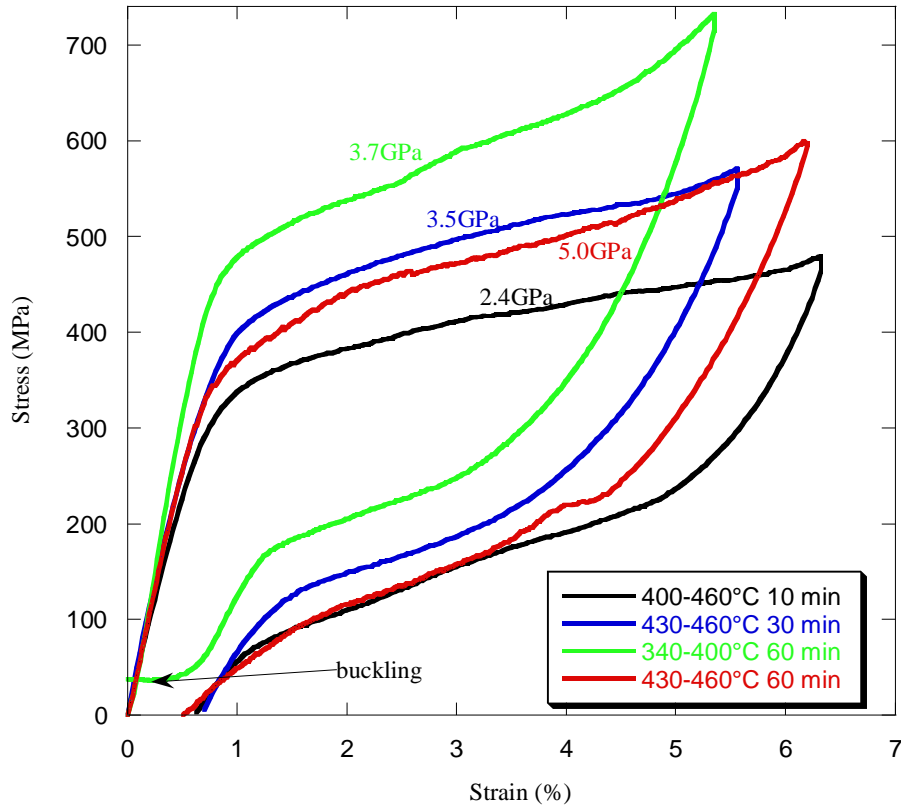


Figure 4.21. Gradient deformation behaviour of specimen ageing within gradient temperature furnace

Table 4.2 summarizes the deformation characteristic of gradient ageing specimens. The value in the bracket denotes the strain accommodated during the martensitic transformation. The specimen ageing within 400°C–460°C for 10 minutes presented the lowest stress gradient of 2.4 GPa on the forward transformation. Meanwhile, ageing between 430°C–460°C for 60 minutes demonstrated the highest stress gradient on the forward transformation with a value of 5.0 GPa. This high value of stress gradient highlighted that the gradient ageing treatment has enhanced the stress gradient from 3.4 GPa in isothermal ageing to 5.0 GPa. Thus, the gradient deformation behaviour is attributed to be the effect of heterogeneous precipitate formation across the grain matrix plus the effect of gradient microstructure properties created along the specimen length.

In addition, both specimens aged within 400°C–460°C for 10 minutes and 430°C–460°C for 60 minutes exhibited the stress gradient of forward transformation over similar transformation stress interval recorded in Table 4.1. This figures out that the gradient ageing treatment has produced nearly the same microstructure properties as in the isothermal ageing on the gradient aged specimen. As this is the case, the gradient deformation of specimen aged within 400°C–460°C for 10 minutes is highly believed to start from the end aged at 460°C and finish at the end aged at 400°C. The same goes for specimen aged within 430°C–460°C for 60 minutes, where the deformation starts from the end aged 430°C with respected to the low level of transformation stress.

Table 4.2. Forward and reverse stress interval of gradient ageing specimen

Ageing duration (minutes)	Optimal temperature range (°C)	Forward Stress Interval (MPa)	Reverse Stress Interval (MPa)	Residual Strain (%)
10	400– 460	350 –480 (5%)	220– 90 (3.4%)	0.6
30	430 –460	420 –570 (4.2%)	203– 131 (1.7%)	0.6
60	340– 400	486 –686 (5.3%)	262– 173 (1.9%)	Buckle
	430 –460	353 –597 (4.9%)	220– 84 (2.6%))	0.5

Among the gradient ageing works, ageing within 430°C–460°C for 60 minutes has been selected as the optimal ageing condition in creating a functionally graded behaviour on Ti-50.8at%Ni alloy. This selection was made based on the large transformation stress interval obtained on both forward and reverse plateaus, and the residual strain produced on the reverse is only ~0.5%.

The wide transformation stress ranges demonstrates continuous shape change of NiTi specimens against the external stress stimulus. This type of deformation behavior can improve the controllability issues of shape memory alloy in sensor and actuation application. For example, the gradient deformation behavior may be utilized on a spring so that we can have a step control on the spring length as the length changes against the variations of the external input signals of stress.

4.4.2 Gradient transformation behaviour

Figure 4.22 illustrates the DSC curve collected along the length of the 10 minutes gradient aged specimen. The DSC curves are nearly identical to the curve of isothermal ageing as in Figure 4.5. However, due to the gradient heating, the three peak of $A \leftrightarrow M_2$, $A \leftrightarrow R$ and $R \leftrightarrow M_1$ transformation already observed on the portion aged at 400°C. Since the duration of ageing is too short, the small density of Ti_3Ni_4 lessens the intensity of $A \leftrightarrow R$ and $R \leftrightarrow M_1$ peak on the DSC curve. Note that the DSC curve progressively changed with respect to ageing temperature correspond to the different reduction rate of Ni content along the specimen length.

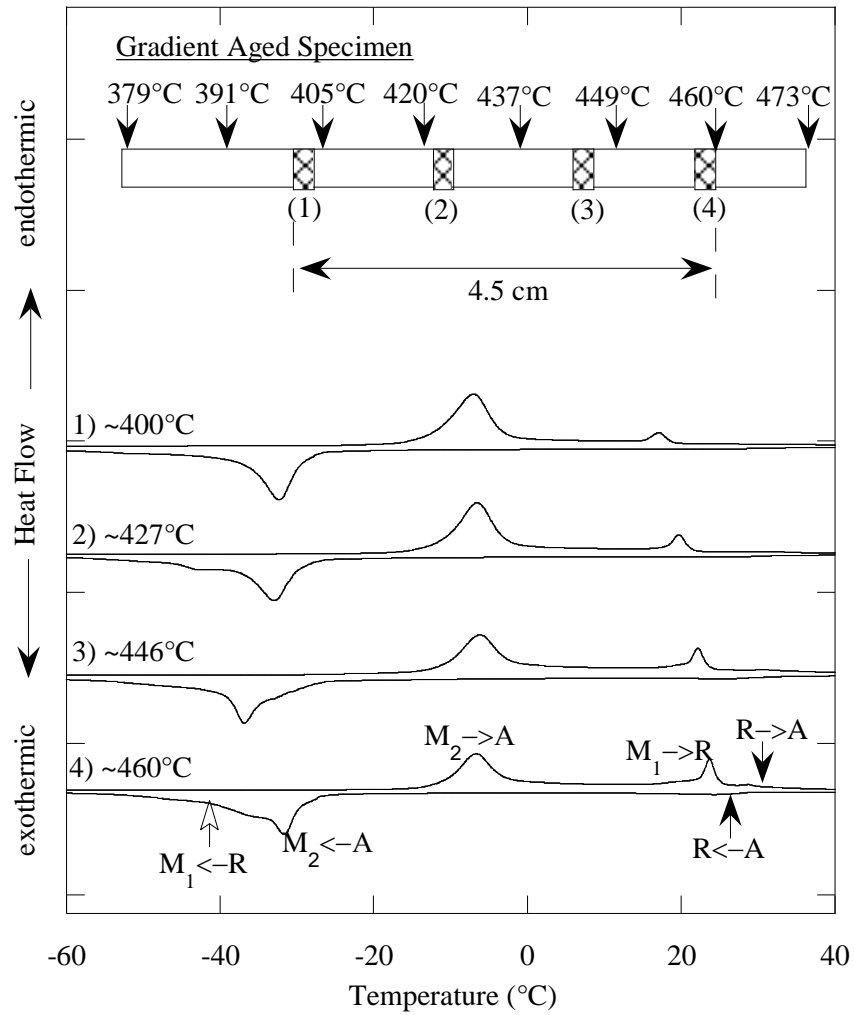


Figure 4.22. Thermal transformation behaviour along the length of 10 minutes gradient ageing specimen

Figure 4.23 shows the DSC curve measured along the length of the 30 minutes gradient aged specimen. The pattern of the DSC curve obtained from both specimen ends is quite contrasted from the isothermal curve as in Figure 4.7. The peak of transformation tends to occur separately instead of overlapping on the same transformation window as in isothermal ageing. Even though the peak pattern is different between the isothermal and gradient ageing, both treatments exhibited the transformation peak of $R \rightarrow A$ at $\sim 35^\circ\text{C}$.

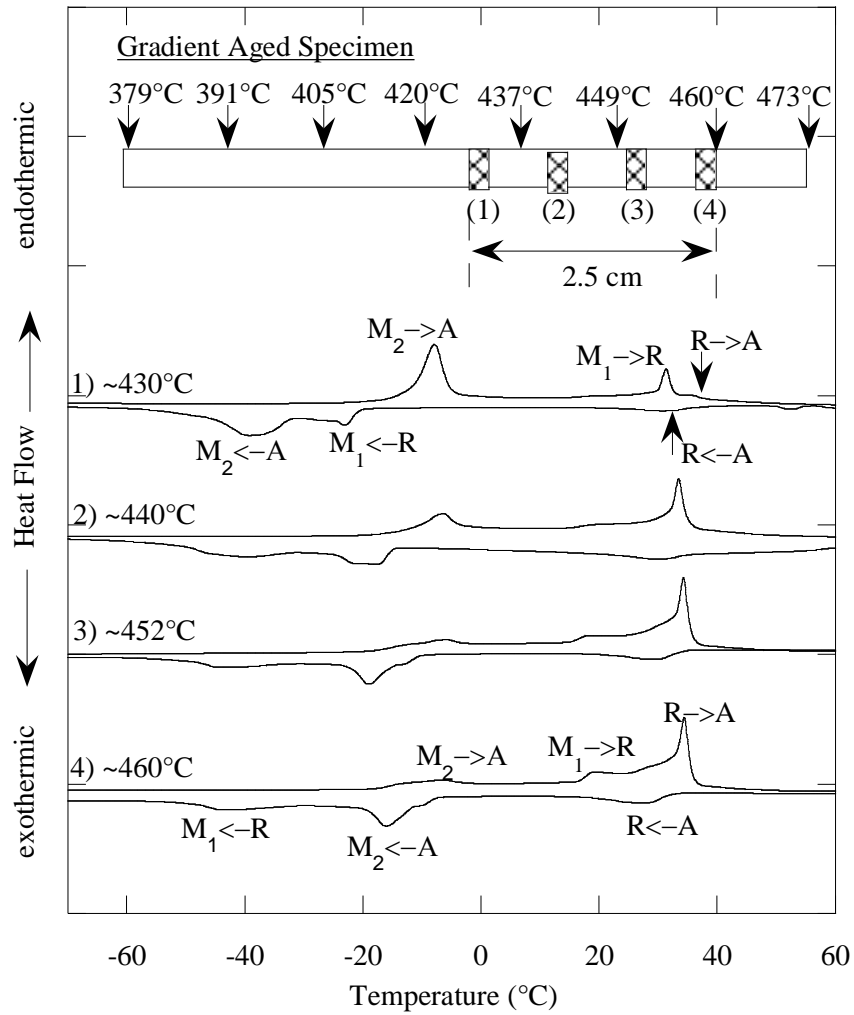


Figure 4.23. Thermal transformation behaviour along the length of 30 minutes gradient ageing specimen

Figure 4.24 shows the DSC curve measured along the 60 minutes gradient aged specimen. The transformation peaks exhibited similar transformation temperature as seen in isothermal DSC curve. Subsequent to gradient ageing treatment, the A_f reduced gradually from 45°C to 41°C as the ageing temperature increased from one end to the other. The reduction of the A_f temperature reflected the variation of Ni content across the specimen length. Even though the A_f difference is too little ~4°C, this behaviour may promote great advantages in the field of shape memory application as the recovery of the wire can be triggered at different heating

temperature. It might be very useful for application, which requires recovery in sequence over a small temperature variation.

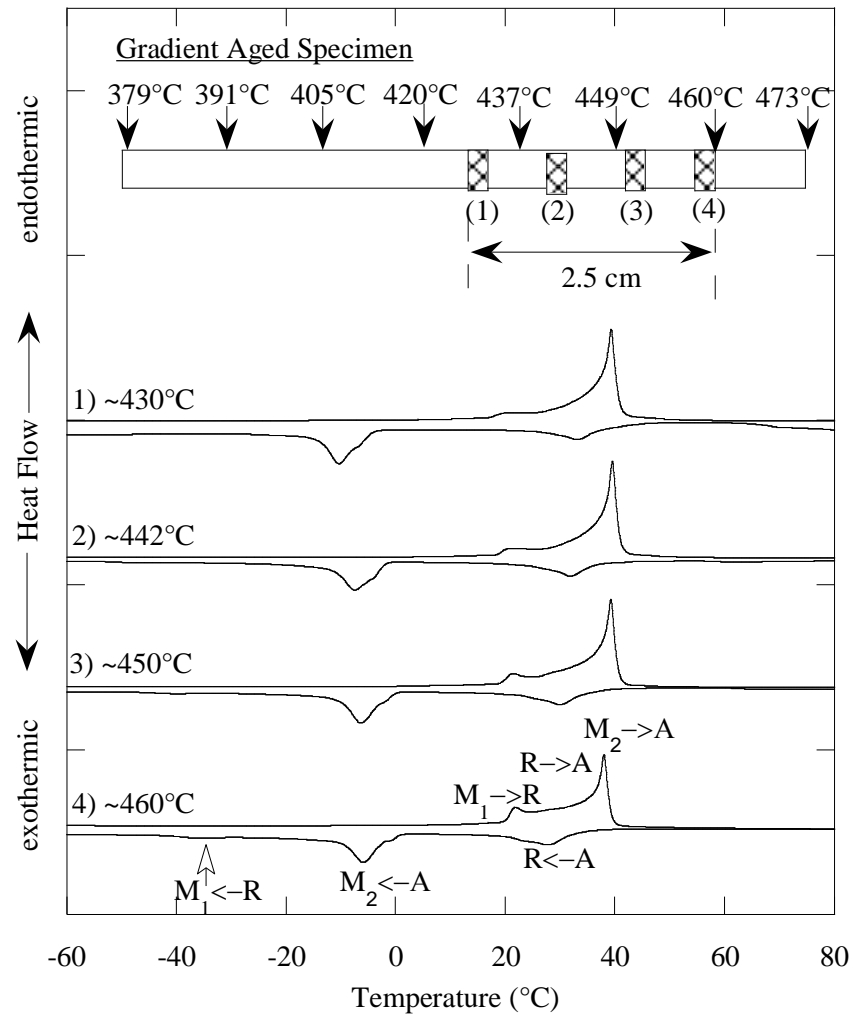


Figure 4.24. Thermal transformation behaviour along the length of 60 minutes gradient ageing specimen

CHAPTER 5

CONCLUSION AND FUTURE WORKS

5.1 Isothermal ageing treatment

This study was done on Ti-50.8at%Ni shape memory alloy in the form of wire. The main agenda of the work is to produce a maximum positive gradient of the stress plateau of martensite phase transformation. This is done by modifying the alloy microstructure via ageing treatment. Comprehensive isothermal ageing treatment was carried out to map the optimum treatment conditions in achieving the stress gradient purpose. The main conclusions of this study may be summarized as the following.

5.1.1 Effect of ageing on thermal behaviour

Ageing treatment within the range of 370°C–550°C introduces complex multiple peak transformation on the DSC curve. As ageing introduces Ti_3Ni_4 precipitates in the alloy matrix, the number of transformation peak increases up to three peaks of $A \leftrightarrow R$, $R \leftrightarrow M_1$ and $R \leftrightarrow M_2$ transformation. Ageing at 460°C and 490°C promoted maximum precipitation rate of Ti_3Ni_4 . It took only 20 minutes of ageing to elevate the A_f temperature from -4°C to 35°C. Additionally, prolonged ageing of low Ni-rich alloy led to the broadening of transformation peak.

5.1.2 Effect of ageing on deformation behaviour

The deformation behaviour of this alloy varies with ageing condition. Ageing within 430°C–460°C at any duration always produce lower stress level of forward transformation plateau as compared to the other temperature. This deformation behaviour does not affected by the geometrical parameter of NiTi shape memory

alloy. Moreover, prolonged ageing led to the gradient deformation on the isothermal aged specimen.

5.2 Gradient ageing treatment

The gradient ageing treatment carried out in this study managed to create gradient pseudoelastic behaviour on the Ti-50.8at%Ni wire. It is concluded that ageing at 430°C–460°C for 60 minutes is the optimal ageing condition for the creation of functionally graded Ti-50.8at%Ni alloy. This ageing condition promoted linear gradient deformation with large stress interval of 244MPa on forward and 136MPa on reverse transformation complies and a small residual strain of 0.5%.

5.3 Future development

The recommendations for future work related to the present study are listed as below:

- i. It is suggested to analyze the gradient deformation behaviour developed by gradient ageing treatment under different load conditions, e.g. compression, torsion and bending. The information will be useful in expanding the functionality of this alloy in the sensor-actuator field.
- ii. It is recommended to evaluate the gradient deformation behaviour of the functionally graded NiTi alloy under cycling deformation. For this, the effect of gradient ageing can be coupled with cold work effect, which is known well for improving deformation cycle.
- iii. It is suggested to discover the range of gradient deformation behaviour from different alloy compositions, from 50.9at%Ni to 52.0at%Ni. This provides wider range of operating temperatures of the functionally graded microstructure for various types of applications.

REFERENCES

- [1] Z. L. Wang and Z. C. Kang, *Functional and smart materials: structural evolution and structure analysis*: Springer, 1998.
- [2] J. Dong, J. Xie, J. Lu, C. Adelman, C. Palmstrøm, J. Cui, Q. Pan, T. Shield, R. James, and S. McKernan, "Shape memory and ferromagnetic shape memory effects in single-crystal Ni₂MnGa thin films," *Journal of applied physics*, vol. 95, pp. 2593-2600, 2004.
- [3] M. Wuttig, J. Li, and C. Craciunescu, "A new ferromagnetic shape memory alloy system," *Scripta materialia*, vol. 44, pp. 2393-2397, 2001.
- [4] N. Ma, G. Song, and H. Lee, "Position control of shape memory alloy actuators with internal electrical resistance feedback using neural networks," *Smart Materials and Structures*, vol. 13, p. 777, 2004.
- [5] K. Ikuta, M. Tsukamoto, and S. Hirose, "Shape memory alloy servo actuator system with electric resistance feedback and application for active endoscope," in *Robotics and Automation, 1988. Proceedings., 1988 IEEE International Conference on*, 1988, pp. 427-430.
- [6] J. Feuchtwanger, E. Asua, A. García-Arribas, V. Etxebarria, and J. M. Barandiaran, "Ferromagnetic shape memory alloys for positioning with nanometric resolution," *Applied Physics Letters*, vol. 95, p. 054102, 2009.
- [7] T. Yoneyama and S. Miyazaki, *Shape memory alloys for biomedical applications*: CRC Press, 2009.
- [8] S. Saadat, J. Salichs, M. Noori, Z. Hou, H. Davoodi, I. Bar-On, Y. Suzuki, and A. Masuda, "An overview of vibration and seismic applications of NiTi shape memory alloy," *Smart Materials and Structures*, vol. 11, p. 218, 2002.
- [9] D. E. Hodgson, W. Ming, and R. J. Biermann, "Shape memory alloys," *ASM International, Metals Handbook, Tenth Edition.*, vol. 2, pp. 897-902, 1990.
- [10] L. M. Schetky, "Shape-Memory Alloys," *Kirk-Othmer Encyclopedia of Chemical Technology*, 1982.
- [11] K. Otsuka and K. Shimizu, "Pseudoelasticity and shape memory effects in alloys," *International Metals Reviews*, vol. 31, pp. 93-114, 1986.
- [12] T. Borden, "Forming Tight Fit," *Mechanical Engineering*, vol. 113, 1991.
- [13] T. Duerig, "Applications of shape memory," in *Materials Science Forum*, 1991, pp. 679-691.
- [14] T. Duerig, "Present and future applications of shape memory and superelastic materials," in *Materials Research Society Symposium Proceedings*, 1995, pp. 497-497.
- [15] T. Duerig and K. Melton, "Applications of shape memory in the USA," *New Materials and Processes for the Future*, pp. 195-200, 1989.
- [16] T. Duerig, A. Pelton, and D. Stöckel, "An overview of nitinol medical applications," *Materials Science and Engineering: A*, vol. 273, pp. 149-160, 1999.
- [17] G. K. Otsuka, "Shape memory alloy heat engine," ed: Google Patents, 1995.
- [18] A. Ölander, "An electrochemical investigation of solid Cadmium-Gold alloy," *J. Am. Chem. Soc.*, vol. 54, pp. 3819-3833, 1932a.
- [19] A. Ölander, "The crystal structure of AuCd," *Zeit. Für Kristol*, vol. 83, p. 145, 1932b.
- [20] L. C. Chang and T. A. Read, *Trans. AIME*, vol. Vol 191, p. 47, 1951.

- [21] K. Bhattacharya, *Microstructure and Martensite: Why it Forms and how it Gives Rise to the Shape-memory Effect* vol. 2: Oxford University Press, 2003.
- [22] G. Kauffman and I. Mayo, "Memory Metal," *Chem Matters*, vol. 11, p. 4, 1993.
- [23] A. S. Mahmud, "Thermomechanical Treatment of NiTi Shape Memory Alloy," Degree of Doctor of Philosophy, School of Mechanical Engineering, The University of Western Australia, Australia, 2009.
- [24] A. S. Mahmud, Y. Liu, and T.-h. Nam, "Gradient anneal of functionally graded NiTi," *Smart Materials and Structures*, vol. 17, p. 015031, 2008.
- [25] D. A. Miller and D. C. Lagoudas, "Influence of cold work and heat treatment on the shape memory effect and plastic strain development of NiTi," *Materials Science and Engineering: A*, vol. 308, pp. 161-175, 2001.
- [26] J. A. Shaw and S. Kyriakides, "Thermomechanical aspects of NiTi," *Journal of the Mechanics and Physics of Solids*, vol. 43, pp. 1243-1281, 1995.
- [27] K. Otsuka and C. Wayman, "Shape memory materials," in *Cambridge University Press*, Cambridge, 1998.
- [28] K. Otsuka and T. Kakeshita, "Science and technology of shape-memory alloys: new developments," *MRS Bulletin*, vol. 27, pp. 91-100, 2002.
- [29] A. Falvo, "Thermomechanical characterization of Nickel-Titanium Shape Memory Alloys," Doctor of Philosophy, Mechanical Engineering, University Della Calabria, 2004.
- [30] P. Wollants, M. D. Bonte, and J. R. Roos, "A thermodynamic analysis of the stress induced martensitic transformation in a single crystal," *Zeitschrift fur Metallkunde*, vol. 70, p. 113, 1979.
- [31] D. Favier, Y. Liu, L. Org  as, A. Sandel, L. Debove, and P. Comte-Gaz, "Influence of thermomechanical processing on the superelastic properties of a Ni-rich Nitinol shape memory alloy," *Materials Science and Engineering: A*, vol. 429, pp. 130-136, 2006.
- [32] S. W. Robertson, "On the Mechanical Properties and Microstructure of Nitinol for Biomedical Stent Applications," Doctor of Philosophy, Engineering-Materials Science and Engineering, University of California, Berkeley, 2006.
- [33] W. Huang and W. Toh, "Training two-way shape memory alloy by reheat treatment," *Journal of materials science letters*, vol. 19, pp. 1549-1550, 2000.
- [34] Z. Bo and D. C. Lagoudas, "Thermomechanical modeling of polycrystalline SMAs under cyclic loading, Part III: evolution of plastic strains and two-way shape memory effect," *International Journal of Engineering Science*, vol. 37, pp. 1175-1203, 1999.
- [35] D. C. Lagoudas and Z. Bo, "Thermomechanical modeling of polycrystalline SMAs under cyclic loading, Part II: Material characterization and experimental results for a stable transformation cycle," *International Journal of Engineering Science*, vol. 37, pp. 1141-1173, 1999.
- [36] S. Miyazaki, K. Otsuka, and Y. Suzuki, "Transformation Pseudoelasticity and Deformation Behavior in a Ti-- 50. 6 At.-% Ni Alloy," *Scr. Metall.*, vol. 15, pp. 287-292, 1981.
- [37] J. Shaw and S. Kyriakides, "On the nucleation and propagation of phase transformation fronts in a NiTi alloy," *Acta Materialia*, vol. 45, pp. 683-700, 1997.

- [38] J. Shaw and S. Kyriakides, "Initiation and propagation of localized deformation in elasto-plastic strips under uniaxial tension," *International journal of plasticity*, vol. 13, pp. 837-871, 1997.
- [39] C. M. Jackson, H. Wagner, and R. J. Wasilewski, "55-Nitinol-The Alloy with a Memory: It's Physical Metallurgy Properties, and Applications. NASA SP-5110," *NASA Special Publication*, vol. 5110, 1972.
- [40] S. A. Shabalovskaya, "On the nature of the biocompatibility and on medical applications of NiTi shape memory and superelastic alloys," *Bio-medical materials and engineering*, vol. 6, pp. 267-289, 1996.
- [41] L. Machado and M. Savi, "Medical applications of shape memory alloys," *Brazilian Journal of Medical and Biological Research*, vol. 36, pp. 683-691, 2003.
- [42] T. B. Massalski, H. Okamoto, P. R. Subramanian, and L. Kacprzak, "Binary alloy phase diagrams," ASM International, Materials Park, OH1990.
- [43] M.-X. Wagner, S. Dey, H. Gugel, J. Frenzel, C. Somsen, and G. Eggeler, "Effect of low-temperature precipitation on the transformation characteristics of Ni-rich NiTi shape memory alloys during thermal cycling," *Intermetallics*, vol. 18, pp. 1172-1179, 2010.
- [44] X. Huang and Y. Liu, "Effect of annealing on the transformation behavior and superelasticity of NiTi shape memory alloy," *Scripta materialia*, vol. 45, pp. 153-160, 2001.
- [45] Y. Zheng, F. Jiang, L. Li, H. Yang, and Y. Liu, "Effect of ageing treatment on the transformation behaviour of Ti-50.9at.% Ni alloy," *Acta Materialia*, vol. 56, pp. 736-745, 2008.
- [46] D. Chrobak, D. Stróż, and H. Morawiec, "Effect of early stages of precipitation and recovery on the multi-step transformation in deformed and annealed near-equiatomic NiTi alloy," *Scripta materialia*, vol. 48, pp. 571-576, 2003.
- [47] M. Carroll, C. Somsen, and G. Eggeler, "Multiple-step martensitic transformations in Ni-rich NiTi shape memory alloys," *Scripta materialia*, vol. 50, pp. 187-192, 2004.
- [48] G. Fan, W. Chen, S. Yang, J. Zhu, X. Ren, and K. Otsuka, "Origin of abnormal multi-stage martensitic transformation behavior in aged Ni-rich Ti-Ni shape memory alloys," *Acta Materialia*, vol. 52, pp. 4351-4362, 2004.
- [49] J. Khalil-Allafi, G. Eggeler, A. Dlouhy, W. Schmahl, and C. Somsen, "On the influence of heterogeneous precipitation on martensitic transformations in a Ni-rich NiTi shape memory alloy," *Materials Science and Engineering: A*, vol. 378, pp. 148-151, 2004.
- [50] J. Khalil-Allafi, G. Eggeler, W. W. Schmahl, and D. Sheptyakov, "Quantitative phase analysis in microstructures which display multiple step martensitic transformations in Ni-rich NiTi shape memory alloys," *Materials Science and Engineering: A*, vol. 438, pp. 593-596, 2006.
- [51] M. Nishida, C. Wayman, R. Kainuma, and T. Honma, "Further electron microscopy studies of the Ti₁₁ Ni₁₄ phase in an aged Ti-52at%Ni shape memory alloy," *Scripta Metall*, vol. 20, pp. 899-906, 1986.
- [52] Y. Zhou, G. Fan, J. Zhang, X. Ding, X. Ren, J. Sun, and K. Otsuka, "Understanding of multi-stage R-phase transformation in aged Ni-rich Ti-Ni shape memory alloys," *Materials Science and Engineering: A*, vol. 438, pp. 602-607, 2006.

- [53] K. Otsuka and X. Ren, "Physical metallurgy of Ti–Ni-based shape memory alloys," *Progress in materials science*, vol. 50, pp. 511-678, 2005.
- [54] F. Jiang, Y. Liu, H. Yang, L. Li, and Y. Zheng, "Effect of ageing treatment on the deformation behaviour of Ti–50.9 at.% Ni," *Acta Materialia*, vol. 57, pp. 4773-4781, 2009.
- [55] T. W. Duerig, *Engineering aspects of shape memory alloys*. London; Boston: Butterworth-Heinemann, 1990.
- [56] P. Marshall, "Filter delivery device," ed: Google Patents, 2001.
- [57] L. M. Schetky, "Shape memory alloys," *Scientific American*, vol. 241, pp. 74–82, 1979.
- [58] B. V. Finander and Y. Liu, "Characterization of the unloading forces of Ni–Ti orthodontic archwires," *The first international conference on shape memory and superelastic technologies*, pp. 151–156, 1994.
- [59] Q. Meng, H. Yang, Y. Liu, and T. Nam, "Transformation intervals and elastic strain energies of B2-B19' martensitic transformation of NiTi," *Intermetallics*, vol. 18, pp. 2431-2434, 2010.
- [60] A. R. Pelton, J. DiCello, and S. Miyazaki, "Optimisation of processing and properties of medical grade Nitinol wire," *Minim Invasive Ther Allied Technol*, vol. 9, pp. 107–18, 2009.
- [61] C. Churchill, J. Shaw, and M. Iadicola, "Tips and tricks for characterizing shape memory alloy wire: Part 4–thermomechanical coupling," *Experimental Techniques*, vol. 34, pp. 63-80, 2010.
- [62] S. Miyazaki, T. Imai, Y. Igo, and K. Otsuka, "Effect of cyclic deformation on the pseudoelasticity characteristics of Ti-Ni alloys," *Metallurgical Transactions A*, vol. 17, pp. 115-120, 1986.
- [63] K. Gall and H. J. Maier, "Cyclic deformation mechanisms in precipitated NiTi shape memory alloys," *Acta Materialia*, vol. 50, pp. 4643-4657, 2002.
- [64] Y. Liu, Z. Xie, and J. Van Humbeeck, "Cyclic deformation of NiTi shape memory alloys," *Materials Science and Engineering: A*, vol. 273, pp. 673-678, 1999.
- [65] Y. Liu, A. Mahmud, F. Kursawe, and T.-H. Nam, "Effect of pseudoelastic cycling on the Clausius–Clapeyron relation for stress-induced martensitic transformation in NiTi," *Journal of Alloys and Compounds*, vol. 449, pp. 82-87, 2008.
- [66] S. Miyazaki, Y. Ohmi, K. Otsuka, and Y. Suzuki, "Characteristics of deformation and transformation pseudoelasticity in Ti-Ni Alloys," *J. Phys. Colloques*, vol. 43, pp. C4-255-C4-260, 1982.
- [67] M. Nishida, C. Wayman, and T. Honma, "Precipitation processes in near-equiatomic TiNi shape memory alloys," *Metallurgical and Materials Transactions A*, vol. 17, pp. 1505-1515, 1986.
- [68] C. P. Frick, A. M. Ortega, J. Tyber, A. E. M. Maksoud, H. J. Maier, Y. Liu, and K. Gall, "Thermal processing of polycrystalline NiTi shape memory alloys," *Materials Science and Engineering: A*, vol. 405, pp. 34-49, 2005.
- [69] M. Doyama and M. Yabe, "Data Handbook of Intermetallic Compounds," in *Science Forum, Tokyo*, 1989, p. 375.
- [70] J. I. Kim and S. Miyazaki, "Effect of nano-scaled precipitates on shape memory behavior of Ti-50.9at.%Ni alloy," *Acta Materialia*, vol. 53, pp. 4545-4554, 2005.
- [71] T. Saburi, K. Otsuka, and C. Wayman, "Shape memory materials," in *Cambridge University Press*, 1988.

- [72] T. Saburi, S. Nenno, and T. Fukuda, "Further electron microscopy studies of the $\text{Ti}_{11}\text{Ni}_{14}$ phase in an aged Ti – 52 at %Ni shape memory alloy," *J Less-Comm Metals*, vol. 125, pp. 157- 163.
- [73] M. Nishida, C. Wayman, and T. Honma, "Precipitation processes in near-equiatomic TiNi shape memory alloys," *Metallurgical Transactions A*, vol. 17, pp. 1505-1515, 1986.
- [74] J. Zhang, X. Ren, K. Otsuka, and M. Asai, "Reversible change in transformation temperatures of a Ti-51at% Ni alloy associated with alternating aging," *Scripta materialia*, vol. 41, 1999.
- [75] F. Jiang, L. Li, Y. Zheng, H. Yang, and Y. Liu, "Cyclic ageing of Ti–50.8at.% Ni alloy," *Intermetallics*, vol. 16, pp. 394-398, 2008.
- [76] S. Miyazaki and K. Otsuka, "Deformation and transition behavior associated with the R-phase in titanium-nickel alloys," *Metallurgical Transactions A: Physical Metallurgy and Materials Science*, vol. 17, pp. 53-63, 1986.
- [77] M. Nishida and T. Honma, "All-round shape memory effect in Ni-rich TiNi alloys generated by constrained aging," *Scripta Metallurgica*, vol. 18, 1984.
- [78] R. Kainuma, M. Matsumoto, and T. Honma, in *Int. Conf. on Martensitic Transformation (ICOMAT-86)*, Sendai: Japan Institute of Metals, 1987.
- [79] T. Fukuda, A. Deguchi, T. Kakeshita, and T. Saburi, "Two-way shape memory properties of a Ni-Rich Ti-Ni alloy aged under tensile-stress," *Materials Transactions, JIM(Japan)*, vol. 38, pp. 514-520, 1997.
- [80] J.I. Kim, Yinong Liu, and S. Miyazaki, "Ageing-induced two-stage R-phase transformation in Ti–50.9at.%Ni," *Acta Materialia*, vol. 52, pp. 487- 499, 2004.
- [81] C. Y. Xie, L. C. Zhao, and T. C. Lei, "Effect of Ti_3Ni_4 precipitates on the phase transitions in an aged Ti-51.8% Ni shape memory alloy.," *Scripta Metallurgica et Materialia*, vol. 24, pp. 1753-1758, 1990.
- [82] Q. Chen, X. F. Wu, and T. Ko, "The effects of Ti_3Ni_4 precipitates on the R phase transformation," *Scripta Metallurgica et Materialia*, vol. 29, pp. 49-53, 1993.
- [83] J. Khalil-Allafi, A. Dlouhy, and G. Eggeler, " Ni_4Ti_3 -precipitation during aging of NiTi shape memory alloys and its influence on martensitic phase transformations," *Acta Materialia*, vol. 50, pp. 4255-4274, 2002.
- [84] X. Liu, Y. Wang, D. Yang, and M. Qi, "The effect of ageing treatment on shape-setting and superelasticity of a nitinol stent," *Materials Characterization*, vol. 59, pp. 402-406, 2008.
- [85] S. M. Russell and A. R. Pelton, "International conference on shape memory superelastic technologies " in *SMST-2000 proceedings of the International Conference on Shape Memory and Superelastic Technologies*, Asilomar Conference Center, Pacific Grove, California, USA, 2001.
- [86] A. Pelton, S. Russell, and J. DiCello, "The physical metallurgy of nitinol for medical applications," *Journal of the Minerals, Metals and Materials Society*, vol. 55, pp. 33-37, 2003.
- [87] K. Gall, J. Tyber, V. Brice, C. P. Frick, H. J. Maier, and N. Morgan, "Tensile deformation of NiTi wires," *Journal of Biomedical Materials Research Part A*, vol. 75A, pp. 810-823, 2005.
- [88] L. Bataillard and R. Gotthardt, "Influence of thermal treatment on the appearance of a three step martensitic transformation in NiTi," *Journal de physique. IV*, vol. 5, pp. C8. 647-C8. 652, 1995.

- [89] H. Morawiec, D. Stroz, T. Goryczka, and D. Chrobak, "Two-stage martensitic transformation in a deformed and annealed NiTi alloy," *Scripta materialia*, vol. 35, 1996.
- [90] H. Morawiec, J. Ilczuk, D. Stróz, T. Goryczka, and D. Chrobak, "Two-stage martensitic transformation in NiTi alloys caused by stress fields," *Le Journal de Physique IV*, vol. 7, pp. C5-155-C5-159, 1997.
- [91] J. Khalil Allafi, X. Ren, and G. Eggeler, "The mechanism of multistage martensitic transformations in aged Ni-rich NiTi shape memory alloys," *Acta Materialia*, vol. 50, pp. 793-803, 2002.
- [92] J. Michutta, M. Carroll, A. Yawny, C. Somsen, K. Neuking, and G. Eggeler, "Martensitic phase transformation in Ni-rich NiTi single crystals with one family of Ni₄Ti₃ precipitates," *Materials Science and Engineering: A*, vol. 378, pp. 152-156, 2004.
- [93] A. W. Johnson, H. Sehitoglu, R. Hamilton, G. Biallas, H. Maier, Y. Chumlyakov, and H. Woo, "Analysis of multistep transformations in single-crystal NiTi," *Metallurgical and Materials Transactions A*, vol. 36, pp. 919-928, 2005.
- [94] Z. Wang, X. Zu, and Y. Fu, "Study of incomplete transformations of near equiatomic TiNi shape memory alloys by DSC methods," *Materials Science and Engineering: A*, vol. 390, pp. 400-403, 2005.
- [95] L. Chiang, C. Li, Y. Hsu, and W. Wang, "Age-induced four-stage transformation in Ni-rich NiTi shape memory alloys," *Journal of Alloys and Compounds*, vol. 458, pp. 231-237, 2008.
- [96] D. Stróz, "TEM studies of the R-phase transformation in a NiTi shape memory alloy after thermo-mechanical treatment," *Materials chemistry and physics*, vol. 81, pp. 460-462, 2003.
- [97] D. Holec, O. Bojda, and A. Dlouhý, "Ni₄Ti₃ precipitate structures in Ni-rich NiTi shape memory alloys," *Materials Science and Engineering: A*, vol. 481, pp. 462-465, 2008.
- [98] Y. Liu, X. Chen, and P. McCormick, "Effect of low temperature ageing on the transformation behaviour of near-equiatomic NiTi," *Journal of Materials Science*, vol. 32, pp. 5979-5984, 1997.
- [99] J. Michutta, C. Somsen, A. Yawny, A. Dlouhy, and G. Eggeler, "Elementary martensitic transformation processes in Ni-rich NiTi single crystals with Ni₄Ti₃ precipitates," *Acta Materialia*, vol. 54, pp. 3525-3542, 2006.
- [100] Y. Liu, H. Yang, and A. Voigt, "Thermal analysis of the effect of aging on the transformation behaviour of Ti-50.9at.% Ni," *Materials Science and Engineering: A*, vol. 360, pp. 350-355, 2003.
- [101] Y. Zhou, G. Fan, J. Zhang, X. Ding, X. Ren, J. Suna, and K. Otsuka, "Understanding of multi-stage R-phase transformation in aged Ni-rich Ti-Ni shape memory alloys," *Material Science and Engineering*, vol. A, pp. 602-607, 2006.
- [102] K. Gall, H. Sehitoglu, Y. I. Chumlyakov, I. V. Kireeva, and H. J. Maier, "The Influence of Aging on Critical Transformation Stress Levels and Martensite Start Temperatures in NiTi: Part I---Aged Microstructure and Micro-Mechanical Modeling," *Journal of Engineering Materials and Technology*, vol. 121, pp. 19-27, 1999.
- [103] X. J. Yan, D. Z. Yang, and X. P. Liu, "Influence of heat treatment on the fatigue life of a laser-welded NiTi alloy wire," *Materials Characterization*, vol. 58, pp. 262-266, 2007.

- [104] K. Gall, H. Sehitoglu, Y. I. Chumlyakov, Y. L. Zuev, and I. Karaman, "The role of coherent precipitates in martensitic transformations in single crystal and polycrystalline Ti-50.8at%Ni," *Scripta Materialia*, vol. 39, pp. 699-705, 1998.
- [105] N. Yang, "Fracture mechanisms in B2 NiTi shape memory alloys," in *ICF10, Honolulu (USA) 2001*, 2013.
- [106] K. Gall, K. Juntunen, H. J. Maier, H. Sehitoglu, and Y. I. Chumlyakov, "Instrumented micro-indentation of NiTi shape-memory alloys," *Acta Materialia*, vol. 49, pp. 3205-3217, 2001.
- [107] Q. Meng, Y. Liu, H. Yang, and T.-h. Nam, "Laser annealing of functionally graded NiTi thin plate," *Scripta Materialia*, vol. 65, pp. 1109-1112, 2011.
- [108] Q. Meng, Y. Liu, H. Yang, B. S. Shariat, and T.-h. Nam, "Functionally graded NiTi strips prepared by laser surface anneal," *Acta Materialia*, vol. 60, pp. 1658-1668, 2012.
- [109] A. S. Mahmud, Y. Liu, and T. Nam, "Design of functionally graded NiTi by heat treatment," *Physica Scripta*, vol. 2007, p. 222, 2007.
- [110] A. S. Mahmud, Y. Liu, and T. Nam, "Gradient anneal of functionally graded NiTi," *Smart Materials and Structures*, vol. 17, p. 015031, 2008.
- [111] C. Xu, X. Ma, S. Shi, and C. Woo, "Oxidation behavior of TiNi shape memory alloy at 450–750° C," *Materials Science and Engineering: A*, vol. 371, pp. 45-50, 2004.
- [112] L. Zhu, J. M. Fino, and A. R. Pelton, "Oxidation of nitinol," in *SMST-2003 Proceedings of the International Conference on Shape memory and Superelastic Technologies, SMST Society, Inc., (California, 2004)*, 2004, pp. 357-366.
- [113] C. Chu, S. Wu, and Y. Yen, "Oxidation behavior of equiatomic TiNi alloy in high temperature air environment," *Materials Science and Engineering: A*, vol. 216, pp. 193-200, 1996.
- [114] C. Churchill, J. Shaw, and M. Iadicola, "Tips And Tricks For Characterizing Shape Memory Alloy Wire: Part 4—Thermo-Mechanical Coupling," *Experimental Techniques*, vol. 34, pp. 63-80, 2010.
- [115] A. S. Mahmud, H. Yang, S. Tee, G. Rio, and Y. Liu, "Effect of annealing on deformation-induced martensite stabilisation of NiTi," *Intermetallics*, vol. 16, pp. 209-214, 2008.

LIST OF PUBLICATIONS

1. A. S. Mahmud, M. F. Razali, and N. Nawawi, "Ageing effects on NiTi shape memory behavior: A review," in *CAN'2012 Eleventh AES-ATEMA International Conference*, Toronto, Canada, 2012, pp. 277-284.[indexed by Scopus]
2. A. S. Mahmud, N. Nawawi, M. F. Razali, and K. Mohamed, "The oxide sequential layers formation and mechanism in NiTi shape memory alloy thermal oxidation," in *CAN'2012 Eleventh AES-ATEMA International Conference*, Toronto, Canada, 2012, pp. 285-294.[indexed by Scopus]
3. M. F. Razali, and A. S. Mahmud, "Gradient Deformation Behavior of NiTi Shape Memory Alloy from Heterogeneous Precipitation of Ti_3Ni_4 ," in *2013 IEEE Symposium on Business, Engineering & Industrial Applications*, Kuching, Sarawak, 2013, In Press.[indexed by IEEE]
4. A. S. Mahmud and M. F. Razali, "Gradient Thermomechanical Behavior Shape Memory Alloy for Linear Actuation," in *1st International Conference of Global Network for Innovation Technology*, Penang, 2013, pp. 76.In Press [indexed by IEEE]